The effects of a high fat diet on musculoskeletal health in aged male C57BL/6J mice

Kirsten Nicole Bott, BSc. (Kin)

Submitted in partial fulfillment of the requirements for the degree of
Master of Science in Applied Health Sciences
(Kinesiology)

Faculty of Applied Health Sciences
Brock University
1812 Sir Isaacs Way
St. Catharines, ON
L2S 3A1

Abstract

Aging and obesity are two major aspects that can negatively impact musculoskeletal structure and function. It is important to study these aspects because of current high rates of obesity and the increasing proportion of seniors in North America. This study investigated the effects of a long-term high fat and sucrose diet (HFS) superimposed with aging on bone and muscle structure and function. Male C57BL/6J mice were randomized 1 of 2 diets: control (AGE, AIN93M, 10.3% kcal fat, 100 g/kg sucrose) or HFS (HFS-AGE, 45.3% kcal fat 200 g/kg sucrose) for 13 weeks starting at 20 weeks of age to represent middle age. Trabecular bone structure and volumetric bone mineral density (vBMD), body composition, and grip strength were measured longitudinally at 20, 24, 28, and 32 weeks of age. *In vitro* contractile measures were performed on isolated soleus and extensor digitorum longus (EDL) muscles at baseline (BSL, 20 weeks of age, n=11) and at the end of the 13-week intervention when AGE (n=12) and HFS-AGE (n=12) mice were 33 weeks of age. Both the AGE and HFS-AGE groups had similar declines in trabecular bone (bone structure and vBMD). For muscle contractile function, HFS+AGE resulted in increased soleus cross-sectional area (CSA) compared AGE (p=0.0008), but this did not translate to greater twitch or tetanus peak force. The ratio of outcomes of bone to muscle declined in both the AGE and HFS-AGE groups as a result of a greater decline in key measures of bone structure (BV/TV) than muscle function (soleus and EDL peak tetanus and CSA) and was not altered by feeding HFS. In conclusion, beginning a HFS diet during middle age did not exacerbate age-related declines in bone or muscle, but these tissues do not decline in a coordinate manner with aging as bone structure declined at a greater rate than muscle function.

Acknowledgments

Dr. Peters

Thank you for being an outstanding mentor and providing me with so many incredible opportunities. You allowed me to follow my own research interests and passions and granted me the freedom to work independently. I look forward to continuing my doctoral studies under your supervision and guidance along with Dr. Ward.

Dr. Ward & Dr. LeBlanc

Thank you for your hard work and dedication in working with me to complete my thesis project. I appreciate all your time and effort and the expertise you provided that allowed me to complete the project I was passionate about.

Mackenzie Hunter

Thanks for being an awesome lab mate, you made coming into lab enjoyable. I appreciate all your help throughout my study, except for that time you got hit by a truck to get out of helping me with my final surgeries.

My Family

Thank you to my family for continuing to encourage me to follow my dreams. Your love and support have been integral to my success.

To my Mom I would like to specially thank you for all the home cooked meals that were on the table when I came home from a long day at school in lab.

Table of Contents

List of Tables

List of Figures

List of Appendices

List of Abbreviations

BMD	bone mineral density
vBMD	volumetric bone mineral density
BV/TV	bone volume/total volume
CSA	cross-sectional area
EDL	extensor digitorum longus
HFD	high fat diet
HFS	high fat and sucrose diet
kcal	kilocalorie
L_0	optimal length
MHC	myosin heavy chain
ROI	region of interest
Tb.N	trabecular number
Tb.Sp	trabecular separation
Tb.Th	trabecular thickness
+df/dt	rate of force development
-df/dt	rate of relaxation
µCT	microcomputed tomography

Chapter 1: Introduction

The musculoskeletal system is comprised mainly of bone and skeletal muscle. In combination, this is what protects the vital organs and supports and moves the body. When this system becomes compromised it can potentially impact an individuals' mobility, quality of life, daily living, and work [1]. Musculoskeletal diseases, which include osteoporosis, osteoarthritis, rheumatoid arthritis and spinal disorders, are the most common cause of chronic disability worldwide. The prevalence of these diseases increase with age [2]. With aging, bone is weakened and is increasingly prone to fragility fractures [3] and there is also concomitant loss in muscle mass and function [4]. Thus, both tissues are compromised with aging, albeit some individuals are more susceptible than others due to risk factors that include genetic predisposition as well as a variety of lifestyle factors. In Canada, as of the year 2000, musculoskeletal diseases cost taxpayers $22.3 billion, making it the most expensive of any group of diseases [5].

In addition to aging, obesity and its associated diseases such as type II diabetes, cardiovascular disease, and bone degeneration are becoming more prevalent, making studying the effects of diet-induced obesity of great interest. The combination of inactivity and the typical Western diet, which is high in saturated fat and refined sugars [6], are the main contributors to obesity [7]. Currently, it is well established that obesity is detrimental to health, however the mechanisms behind the effects of inactivity and a high fat and sugar diet (HFS) on the musculoskeletal system, more specifically how a HFS affects bone and muscle structure and function, remains poorly understood.

The relationship between bone and muscle is a developing area of research, with an increasing interest in muscle-bone "crosstalk" [8, 9]. This muscle-bone "crosstalk" is a new term used to describe the interaction of bone and muscle and the how each affects

the other's ability to function optimally. This interaction has more recently been suggested to have a biochemical component with muscle acting as an endocrine organ releasing growth factors and cytokines that target bone, however the biochemical influence of bone on muscle is less well established [8, 10, 11]. This interaction also includes an established physical relationship with muscle acting as a primary mechanical force on bone [12], which will be the focus of this thesis. For example, bone and muscle tissue mass are closely associated throughout the lifetime, with aging, chronic exercise, and disuse [8]. Since Canada has an aging population [13], in combination with increasing obesity rates [7], the combined effects of diet induced obesity with aging on the musculoskeletal system is an important area of research. The superimposition of these two factors has not been well studied, even though the effects of diet-induced obesity or aging on bone or muscle have been studied separately using animal models [3, 14-20]. This thesis examines the effects of aging and aging superimposed with a HFS, on bone and muscle structure and function. More specifically, body composition, volumetric bone mineral density (vBMD), bone structure, and grip strength were measured longitudinally, and muscle contractile function and muscle fibre typing, were analyzed as endpoint measures. To analyze alterations in the ratio of bone to muscle structure and function, both proximal tibia bone structure (bone volume/total volume, BV/TV) and bone mineral density (BMD) were used, while peak tetanus force and cross-sectional area (CSA) for the soleus and EDL served as measures for muscle function and size.

Chapter 2: Literature Review

Bone

Structure and Function

Bone functions to support the body, enable movement, and protect various organs. To carry out these functions bone presents an interesting dichotomy. It must be stiff to resist deformation to allow for loading, but flexible to absorb force and light to allow for ease of movement yet strong to allow for loading without fracture [21]. The composition of bone allows for this dichotomy, which includes mainly type I collagen for elasticity and calcium hydroxyapatite ($[Ca_{10}(PO_4)_6(OH)_2]$) for stiffness [21, 22].

There are two main structural types of bone, known as cortical and trabecular bone. Cortical bone is very dense with a low turnover rate and contains osteocytes, canaliculi, and blood vessels. Trabecular bone is porous, and typically described as a network of boney struts, and it is known to have a high turnover rate for remodeling [22]. Trabecular thickness (Tb.Th), trabecular number (Tb.N), and trabecular separation (Tb.Sp) are used to measure and quantify trabecular bone. These measures of trabecular bone characterize the overall percentage of bone volume to total volume within a region of interest (BV/TV) [23]. For example, decreased Tb.Th and Tb.N and increased Tb.Sp would result in an overall decrease in BV/TV; it is the combination of these measures that contributes to overall percent bone volume. Therefore, it is the bone geometry (size and shape) and structure (trabecular architecture and cortical thickness) that play a role in the structural properties associated with the strength of bone [24]. It is the combination of bone quantity measured as the amount of BMD, and quality, measured as bone geometry and structure that determines overall bone strength [25].

In addition to their structural properties, bones are classified into three main groups: flat (i.e., bones of the skull), short (i.e., carpal bones and vertebral bodies), and long (i.e., tibia, femur, and humerus) [25]. Unique to long bones is the medullary cavity which houses bone marrow [21]. Aside from erythrocyte production, bone marrow is important as the site where both osteoblast (responsible bone formation) and osteoclast (responsible for bone resorption) cells originate. Osteoblasts and osteoclasts are involved in bone turnover and remodeling and the ratio of their activities determines whether there is overall bone formation or resorption.

The maximum quantity of bone over the lifespan, achieved following the growth period in early adulthood, is known as the peak bone mass [26]. Maximizing peak bone mass is considered important as it is believed to set a trajectory for a skeleton that is less prone to fragility fractures as a consequence of the loss of BMD and structure that often occurs during aging [26]. Male C57BL/6J mice were selected for this thesis research since they do not have the loss of estrogen with aging like females, which accounts for a decline in bone [27] and could confound the effects of aging and diet-induced obesity. In addition, the C57BL/6J mouse strain is vulnerable to diet-induced obesity and is a good model of the human metabolic syndrome [28]. The proximal tibia was analyzed since it is a skeletal site that contains a high proportion of trabecular bone, known to be responsive to modifiable lifestyle factors, such as diet [29]. Depending on the composition, diet during early life can have positive or negative effects on bone development and, ultimately, the attainment of peak bone mass [29]. The focus of this study is examining if an obesogenic diet (HFS) exacerbates the negative effect of aging alone on bone structure and function.

Dietary Considerations for Bone Health

Nutrition is an important factor in the development, remodeling, and maintenance of bone. Essential nutrients for bone include a variety of micronutrients (calcium, phosphorus, vitamin D) and macronutrients (protein, essential fatty acids) [30-35].

Micronutrients: Calcium, Phosphate, Vitamin D

Calcium and phosphate are important since these minerals compose 80-90% of bone mineral content mainly in the form of hydroxyapatite [30]. Bones contain approximately 99% and 80% of the calcium and phosphate in the body, respectively [36]. Adequate calcium intake is important during growth for normal bone development in both rodents [37] and humans [38, 39] and remains an important nutrient with aging for the maintenance of bone in both rodents [40] and humans [41, 42]. Calcium and phosphate not only play a structural role in bone, but also influence bone formation and resorption through direct influences on osteoblasts and osteoclasts. Phosphate inhibits the differentiation of osteoclasts and stimulates mature osteoclast apoptosis [43, 44], while, calcium stimulates the proliferation and differentiation of osteoblasts and inhibits osteoclastogenesis [45]. But calcium and phosphate intake must be in the presence of adequate levels of vitamin D.

Vitamin D influences calcium and phosphate metabolism at the intestine (absorption), kidneys (resorption), and bone (indirect and direct affects). Specifically, it is the active metabolite of vitamin D, 1,25-dihydroxyvitamin D, which has an effect on these target organs [30]. There are two ways of obtaining vitamin D, which include skin exposure to sunlight and through the diet, consumption of vitamin D_2 and D_3 - differing only in their side chains [46]. Vitamin D status can be compromised during aging through

several mechanisms: less sun exposure; attenuated de novo synthesis of vitamin D; lower intake of vitamin D; and sequestration in fat tissue due to higher fat mass that accompanies aging [47], [48]. Thus, bioavailability of vitamin D decreases with obesity [49-52]. Since lard was the fat source in the experimental diets used in this thesis, it was important to test for vitamin D content to ensure the experimental group was not receiving excess vitamin D. Aside from vitamin D, other vitamins that play a role in bone health include vitamins A, C, E, K and B vitamins and other essential micronutrients for bone health include magnesium, phosphorus, potassium, fluoride, copper, iron, zinc, and manganese [30, 32, 33]. Therefore, to be able to study the effects of dietary fat content on the rate of bone decline with aging, nutrients (especially calcium, phosphate, and vitamin D) were kept consistent in the experimental diet (HFS) compared to the control diet on the basis of energy so that only the effects of the high fat diet were studied.

Macronutrients: Protein and Fat

Protein is an important macronutrient for BMD, structure, and strength, as reviewed by [34, 35]. Deficient dietary protein results in the development of osteoporosis in aged male rats (8 months of age, 1 or 7 month diet) with thinning of trabecular and cortical bone and decreased bone strength [53]. Adequate dietary protein is essential for maintaining bone health, especially since low protein intake is associated with an increased risk of hip fractures in the elderly men and women [34].

In addition to protein, dietary fats are also an important macronutrient for bone health. However, dietary fats are not all equal, some fats are essential for optimal bone health while others can be considered detrimental. Since the body cannot produce unsaturated fatty acids with a double bond in the first nine carbons, these are known as

essential fats that must be consumed in the diet, which include n-3, α-linolenic acid, which can be converted to eicosapentaenoic acid and docosahexaenoic acid and n-6, linolenic acid, which can be converted to arachidonic acid, as reviewed by [54]. Other fats, such as trans and saturated fats, are considered unhealthy for bone development [55]. The effects of a high fat will be further discussed in the following sections.

Bone Remodeling

Bone is a dynamic tissue that is constantly being turned over, with the ability to adapt its shape and size in response to mechanical loads. The process of adding and removing bone is known as bone remodeling, which is mediated by osteoblasts and osteoclasts (responsible for bone formation and resorption, respectively), and osteocytes (responsible for sensing bone deformation), and is modulated by hormones, cytokines, and mechanical stimuli [56]. Bone remodeling is a continuous process throughout the lifespan with greater bone formation during growth and development, followed by a maintenance period during middle age, and bone resorption with aging [3]. It is the balance between the osteoblast and osteoclast activity that determine the rate of remodeling and whether there is overall bone formation or resorption at any given time. Control of osteoblast and osteoclast activity is a result of multiple factors including hormones, growth factors, and cytokines [57]. These bone cells are derived from different progenitor cells, and differ in their molecular control mechanisms.

Osteoblasts are derived from mesenchymal stem cells, which can also differentiate into adipocytes, chondrocytes, or myoblasts [56]. In the presence of runt-related transcription factor 2 (Runx2), mesenchymal stem cells will become preosteoblasts and further differentiate to functional osteoblasts in the presence of the

transcription factor osterix [58, 59]. Some osteoblasts become encased in the bone matrix and become osteocytes, which play a role in regulating both osteoblast and osteoclasts activity and sense bone deformation with mechanical stimuli, sending the signal for bone remodeling [60, 61]. However, certain transcription factors, such as leptin can shift the differentiation of mesenchymal stem cells to osteoblastogenesis [62] and in contrast peroxisome proliferator-activated receptor gamma (PPARγ), can shift the mesenchymal differentiation to adipogenesis, creating fat cells rather than osteoblasts [63, 64].

In contrast to osteoblasts, the osteoclasts are derived from granulocyte-macrophage lineage of hematopoietic stem cells, and can also differentiate into monocytes or macrophages [57]. To differentiate into osteoclasts, the hematopoietic stem cells must first be exposed to macrophage colony-stimulating factor, secreted by osteoblasts, to become preosteoclasts. Following which, receptor activator of nuclear factor- κB (RANK) receptor on the preosteoclasts either directly associates with RANK-ligand (RANKL) found on the osteoblast membrane or is activated by soluble RANKL secreted from osteoblasts. It is this binding between RANK and RANKL that activates osteoclasts and further promotes osteoclastogenesis and inhibits osteoclast apoptosis [65]. Therefore, osteoblasts and osteoclasts are integrally linked for bone remodeling. The differentiation of osteoblasts, osteoclasts, and bone remodeling is directly and indirectly affected by both nutrition and aging.

Bone and Obesity

There is an association between body mass and BMD based on the established relationship between mechanical loading and bone formation, as explained by the mechanostat theory [19]. The mechanostat theory states that mechanical usage is

translated into signals that determine bone remodeling to fit bone mass to the load placed on the bone [12]. Since the body cannot distinguish the gravitational forces exerted from lean mass or fat mass, obesity has traditionally been considered to have a positive effect on bone [66, 67]. However, fractures in obese postmenopausal women and older men make up a significant proportion of overall fragility fractures and it is suggested that obese individuals are at a greater risk for certain types of fractures. Specifically, postmenopausal women are at a greater risk of ankle, upper leg, proximal humerus, and vertebral fractures, while men are at a greater risk of rib, nonvertebral, and hip fractures, as reviewed by [18]. This may be due to metabolic disturbances, such as impaired glucose tolerance, as well as differences in how obese versus non-obese individuals fall and fat distribution acting as padding around certain sites [18].

A higher body mass index (BMI), calculated by expressing body mass (kg) per body height (m^2), is associated with a greater BMD [68]. This is considered protective against fragility fractures in humans, but studies remain inconclusive with evidence suggesting beneficial, detrimental, or no effect of a greater BMI on fracture risk [68-70]. The relationship between BMI and fracture risk is complex with discrepancies based on skeletal sites measured and assessment of fracture risk with or without a correction for body weight. A large proportion of research examining the relationship between obesity and osteoporosis has not accounted for mechanical loading caused by greater body weight. When bone mass is adjusted for body weight, the mechanical loading effect on bone is removed and in Chinese and Caucasian subjects it is suggested that the correlation between fat mass and bone mass becomes negative [71]. Whereas, body composition goes beyond calculated BMI by distinguishing alteration in relative lean, fat,

and bone mass. Diet induced-obesity increases relative fat mass and decreases lean mass [72]. This relationship between a greater BMD and fractures within an obese population presents a potentially interesting dichotomy.

It has become increasingly apparent that this is not a simple relationship and there are mechanisms beyond just mechanical loading [73]. Aside from the direct mechanical load from body weight, obesity may affect bone metabolism through multiple different mechanisms and pathways. Thus, it is suggested that there are competing effects of mechanical loading inferred from body weight and adiposity negatively altering bone metabolism in the cumulative effects on bone structure and function.

Effects of Diet-Induced Obesity on Bone Structure and Strength

Although dietary fat is essential for life, the effects of a high fat diet on bone quality and composition vary based on the source of fat. Bone is highly responsive to dietary fats with the source of the fatty acids reflected in the bone lipid composition [74-76]. However, the role of altered bone lipid composition on bone strength and/or structure remains unclear [75-77]. Diet interventions that use polyunsaturated fatty acids, specifically long chain n-3 fatty acids, appear to have beneficial effects on bone (reviewed in [31, 78-80]). While high-saturated fat diets, present in a typical Western diet, have shown detrimental effects [81-88], no effect [89], or even positive effects [72] on bone using mice and rats.

Before discussing the specifics of the effects of diet-induced obesity on bone structure and strength, it is important to discuss differences in diet composition and reporting of diet composition. In particular, incomplete reporting of diet composition makes it particularly challenging to compare findings among studies. A high fat diet

(HFD) is generally defined as a diet with a 40% or greater kilocalories (kcal) from fat [72, 81-89]. While we know diet-induced obesity with a HFD can effectively be achieved by adding sucrose to the diet, many studies refer to a HFD and fail to include details of the diet composition, including whether sucrose was incorporated. Also, few studies report whether micronutrient composition was adjusted for the higher energy level present in a HFD or HFS. This has created confusion on the effects of diet-induced obesity on the musculoskeletal system. Some but not all rodent studies that feed a diet containing higher saturated fat without altering sucrose report heavier body weight as well as a higher fat mass. Therefore, this thesis defined diet-induced obesity as an increase in weight gain and/or fat mass with feeding a HFD or HFS.

Studies that adequately report the details of the diet composition have found detrimental effects of high saturated fat and sucrose diets in mice (6 weeks of age) [81, 82] and rats (4 weeks of age) [90], no effect in mice (10 weeks of age) [89], or even a positive effect in mice (12 weeks of age) [72]. However, other studies with limited information on diet composition without specification of the source of fat or addition of sucrose have also found detrimental effects of a HFD in mice (5-20 weeks of age) [85, 86] and rats (4 weeks of age) [87]. As previously mentioned, saturated fats during early growth and development negatively affect bone growth by reducing the peak bone mass [55]. A majority of studies investigating the effects of diet-induced obesity on bone in mice and rat models have either begun during growth and development [76, 81, 82, 84-87, 90], and/or the diets have been short term [86, 87]. It is suggested that diet-induced obesity is more detrimental in developing rodent models than adult rodent models [85]. However, there are limited studies investigating effects of diet induced obesity at middle

age through aging, a life stage when structure and function of bone is declining [3].

Bone is considered a less metabolically active tissue than muscle; nevertheless, some studies using only a short duration (4 weeks) high fat diet (66% or 94.5% kcal fat) can elicit negative changes in young rats (4 weeks of age) on bone outcomes (BMD, structure, and strength), partially explained by reductions in bone formation markers [87]. Feeding HFS more adversely affect trabecular bone than cortical bone in male mice (6 weeks of age), measured using μCT [81, 82]. The detrimental structural changes with diet-induced obesity have been associated with a decrease in bone formation (osteocalcin) and increase in bone resorption (tartrate resistant acid phosphatase), measured by blood serum markers [82].

In addition to the greater mechanical stimuli due to an increase body weight gain, there are changes in hormones and cytokines associated with an obesogenic diet. It appears that diet-induced obesity works in two opposing phases in bone in young adult mice (12 weeks of age) [72]. Chronic obesogenic diets lead to an increase in body weight and therefore greater mechanical loading on the bone, which is suggested to have a protective effect. However, there is also an increase in inflammatory cytokines, which have detrimental effects on bone remodeling rates. It has recently been hypothesized that diet-induced obesity may have mediated effects in an inverted 'U' shape, acting in two opposing phases. The initial phase characterized as beneficial effects on bone with increased mechanical load and a second phase that is detrimental with lower bone formation rates (Figure 2.1) [72]. This theory stemmed from a study using young adult (12 weeks old) male C57BL/6J mice on an 11-week HFS (45% kcal lard and 173g/kg sucrose). This two-phase hypothesis was suggested due to the positive effects on

trabecular bone structure between baseline and endpoint measures, but lower mineral apposition rates (i.e., lower bone formation) with the HFS suggesting potential detriments. To better understand this two-phase hypothesis a longer duration diet intervention or older animals should be studied.

Building off this hypothesis using this proposed model the literature suggests that diet-induced obesity would be detrimental to bone health during development in young animals and in old age during bone decline, but in young adult animals would result in positive effects on bone through the mechanostat theory. This age-related model would help explain some of the discrepancies seen between studies based on the age of animals examined during diet interventions. Although this dichotomy between high BMD and the increased incidence of fracture at certain skeletal sites in obese postmenopausal and older men has been documented [18], the effects on bone structure, geometry, and function in middle aged adults remains an active area of research.

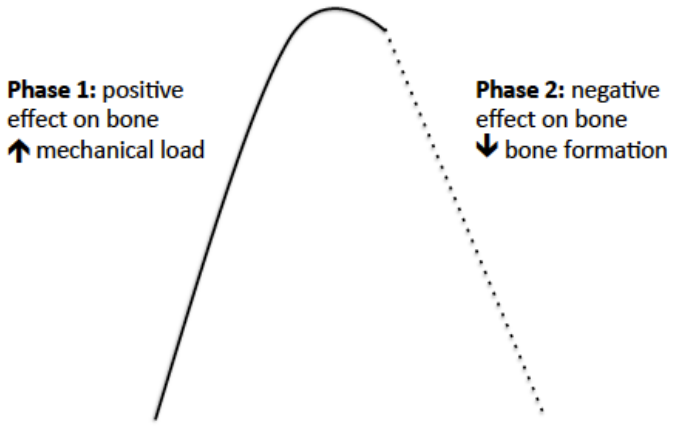

Figure 2.1. Hypothesized inverted 'U' shaped curve model for describing the effects of diet-induced obesity on bone. The solid line represents the improved trabecular bone structure, while the dotted line represents the suggested detriments of diet-induced obesity on bone structure based on a decrease in bone formation [72].

Using this hypothesized inverted 'U' shaped curve model, we can examine how diet-induced obesity affects bone and muscle differently throughout the lifespan. Differential results may be due to different phases in the life span, diet composition, and the duration of nutritional interventions. Young mice and rat models (3 to 7 weeks of age) are adversely affected by diet-induced obesity regardless of the diet duration (1 to 24 months) [81, 82, 84-88, 90], while in young adult mice appears to have a positive effect (11 week diet) [72], and diet-induced obesity over the lifespan has a negative affect [88, 90]. However, studies examining the effects of diet-induced obesity on bone have not included muscle measures and muscle-generated loads play a key role in bone size and structure [12]. Since bone and muscle are integrally linked and both are affected by diet-induced obesity it is important to study these tissues in conjunction to better understand their relationship and how these tissues may affect one another.

Effects of Diet-Induced Obesity on Negative Regulation of Bone Remodeling

There are a number of possible mechanisms for negative changes in bone structure and function associated with diet-induced obesity. One suggested mechanism is the inverse relationship between adipocytes and osteoblasts, since they are both derived from mesenchymal stem cells. This competitive relationship between the differentiations of precursor cells to osteoblasts versus adipocytes translates into less osteoblast activity and bone formation [91].

Another potential mechanism is related to changes in hormonal and cytokine signaling. Diet-induced obesity is associated with an increase in fat mass and a resultant increase in adipokines, chronic low-grade inflammation and resultant increase in proinflammatory cytokines, such as TNF-α and IL-6. Although bone remodeling may be

positively influenced by adipokines such as leptin [62], proinflammatory cytokines stimulate osteoclast differentiation, survival, and as a result bone resorption [92, 93].

Bone and Aging

Maintaining bone health throughout the lifespan is important because of the inevitable decline in bone and increased risk of fragility fracture with aging [3]. Modifiable lifestyle factors, such as nutrition, are important for bone health to slow the loss of BMD and strength, which increases the risk of a fragility fracture [27, 29]. Although osteoporosis is considered a disease associated with aging, it is a lifelong disease with geriatric consequences. This has earned the disease the name of "the silent thief" since significant losses in mineral and structure often occur with no symptoms. This increased bone loss is a not necessarily a result of aging alone, but a combination of factors, including 1) genetics, a strong predictor of bone health that cannot be altered, and 2) lifestyle and nutrition choices throughout the life span, which are modifiable and can have both a positive or negative impact [27].

Effects of Aging on Bone Structure and Function

There is a natural decline in BMD and bone structure with aging. However, the extent of this decline varies among individuals and understanding the mechanisms and factors that contribute to these alterations is an active area of research [3]. It is the decline in both bone quantity and quality that contributes to bone strength and thus overall risk of a fragility fracture [3]. Therefore, it is important to not only analyze bone quantity but also bone structure to have a better understanding of alterations in bone strength.

In general, cortical bone becomes thinner, more brittle, and weaker with aging [94, 95], while trabecular bone struts also weaken [96]. This alteration in bone brittleness

with aging is due to changes in bone composition. Bones become more brittle as a result of a decrease in collagen content, resulting in a shift towards a higher bone mineral content and reduced elasticity [3]. The two other contributors to bone strength in addition to bone composition are bone quantity and structure. A comparison between young (5 months) and aged (23 months) male rats highlights this decline in BMD, bone volume, and trabecular number with age at the proximal tibia [97]. Similarly, this has been demonstrated in separate studies using aged male C57BL/6J mice (20 and 24 months of age) with significant decreases in bone volume, as a result of decreased trabecular number and increase in trabecular separation with little change or even an increase in trabecular thickness. This decline in trabecular bone was observed to continuously decrease from approximately 1.5 to 24 months of age and from 1 to 20 months of age with an initial rapid decline in trabecular bone from 2 to 6 months of age in male mice [94, 98].

The structural changes that occur in the trabecular and cortical bone, as well as the bone marrow are a result of alterations in osteoblast and osteoclast activity [14]. Bones are repetitively loaded, which causes micro-damage to the bone tissue. Normally this micro-damage allows for bone remodeling, however with aging there is an exponential increase in this micro-damage as seen in human bones [99]. It is suggested that there is an inability to repair these cracks [100], propagating this micro-damage and resulting in a decrease in trabecular and cortical bone strength [101]. This decrease in bone repair is a result of the relatively higher rates of bone resorption that exceed bone formation that also causes this decline in bone tissue. These alterations in bone remodeling with aging that result in structural changes are controlled by a number of signaling factors. Since

diet-induced obesity may further compromise bone with aging and given Canada's aging population [13] and rising obesity rates [7], this makes for an important research area.

Aging also highlights sex-related differences in bone loss. In trabecular bone, for men, bone loss is mainly a result of thinning of trabecular struts, while with women it is a decrease in trabecular connectivity [102]. Since osteoporosis is considered more of a women's disease with 1 in 3 women compared to 1 and 5 men suffering an osteoporotic fracture in their lifetime [103], research examining aging and bone health is often female-orientated. However, compromised bone is still a major health concern for men and sex-related differences in aging make it important to understand how aging affects males differently from females.

Effects of Aging on Negative Bone Remodeling

There is a decrease in osteoblast activity and increase in osteoclast activity resulting in this age-associated bone loss. With aging the cellular activity of the bone marrow is altered [57], with mesenchymal stem cells differentiating more into adipocytes instead of osteoblasts, since osteoblast differentiation becomes suppressed with aging [64]. There is an overall decrease in the amount of bone deposition with each bone remodeling cycle [104]. Aging is also associated with the progressive inability to sense and respond to forces as a result of dysfunctional osteocytes [105]. In addition to this dysfunction, osteocyte apoptosis increases with aging, which contributes to bone weakness separate from BMD by filling in lacunae with mineralization causing a disruption in the lacunae system and increasing micro cracks [3]. Changes in bone structure and strength is a result of a combination of increased osteoclast activity, decreased osteoblast activity and differentiation, and apoptosis of osteocytes. Although

age-related decline in bone has been well characterized and diet induced obesity appears to be detrimental to young mice and rats this is only part of the equation since muscle forces play a key role in bone structure and strength.

Skeletal Muscle

Structure and Function

Skeletal muscle allows for voluntary movement and exerts forces on bones. In terms of function, skeletal muscle can be viewed from both a mechanical and metabolic context. From a mechanical perspective, skeletal muscle generates forces to maintain posture and produce movement, while from a metabolic view it contributes to basal energy metabolism, heat production, and storage for substrates (e.g. amino acids, carbohydrates, and fat) [106]. It contributes approximately 40% to total body weight and is composed of mainly water (75%), protein (20%), and other substances including inorganic salts, minerals, fats, and carbohydrates (5%). Similar to bone metabolism, muscle mass depends on a balance between protein synthesis and degradation, both of which are sensitive to a variety of factors including nutrition, hormones, physical activity/exercise, and injury or disease [106]. The sensitivity of skeletal muscle to these factors and its dynamic nature make it one of the most plastic or adaptable tissues in the body.

Structurally, muscle is organized into multiple compartments separated by layers of connective tissue with an organized arrangement of muscle fibres. The epimysium connective tissue encases the whole muscle, the perimysium encases bundles of muscle fibres, and the endomysium encases single muscle fibres. These single muscle fibres are composed of thousands of myofibrils that consist of a repeating unit known as the sarcomere, which is the basic contractile unit of skeletal muscle. It is the arrangement of

myofilaments that form the sarcomere, with the two most abundant myofilaments being actin and myosin [107].

There are three main fibre types each with their own set of characteristics. These include type I slow twitch fibres, which rely heavily on oxidative energy production, have a relatively slow contraction and relaxation speed, and are fatigue resistant. Type II fibres can be subdivided into type IIa, type IIx, and type IIb, all of which are considered fast twitch and rely more on glycolytic energy production. Type IIa fibres rely on both oxidative and glycolytic energy production with a faster relative contraction and relaxation speed than type I fibres. While type IIx and IIb rely on glycolytic energy production with type IIx having a faster relative speed of contraction than type IIa. Type IIb is considered the fastest and most extreme fibre type, and is found almost exclusively in animal populations and not normally expressed to any great degree in human skeletal muscle [107]. It is the expression of isoforms of the myosin heavy chain (MHC) protein, the 'motor' of the thick filament, that in part determines the relative speed of contraction of a fibre [108]. The basic muscle fibre type characteristics have been summarized in Table 1.1.

Table 1.1 Skeletal muscle fibre type characteristics.

Fibre Type	Contraction Speed	Power Produced	Resistance to Fatigue	Energy production
Type I	slow	low	high	aerobic
Type IIa	moderately fast	medium	intermediate	aerobic/ anaerobic
Type IIx	fast	high	low	anaerobic
Type IIb	very fast	very high	very low	anaerobic

Note. Type IIb fibres exclusively in animal populations.

Muscle fibre type is commonly determined by staining muscle sections for the different MHC isoforms (also named MHC I, IIa, IIx and IIb). Studying these different

types of muscle fibres in murine models is beneficial since some of their muscles are homogenous, such as the soleus, which is predominantly composed of type I and type IIa fibres, and the EDL, which is predominantly composed of type II fibres [109]. Despite characterizing muscle fibres as distinct fibre types, recent immunohistochemical staining of both rodent and human muscle has indicated that muscle fibres can express two MHC isoforms, classifying these fibres as hybrids [110-113]. However, human skeletal muscle is more heterogeneous in nature, therefore there is not a direct comparison between rodents and humans [106]. But, rodent research provides valuable information on these individual fibre types because muscles such as the soleus and EDL can be chosen to represent the different contractile fibre types, since rodent muscles are more specialized and can contain high percentages of individual fibre types. The male C57BL/6J mouse model was selected for this thesis since the C57BL/6J mouse model is commonly used for muscle contractile function [114-117] and males do not have a loss of estrogen with aging like females, which could affect muscle function. Specifically the soleus and EDL were used to represent slow twitch and fast twitch muscles respectively, since these hind limb muscle are commonly isolated and incubated for contractile studies [114-117], and the fibre type composition of these muscles has been characterized (summarized in Table 1.2) [110].

Table 1.2. Soleus and EDL fibre type composition in C57BL/6J mice.

	Type I	Type I/IIa	Type IIa	Type IIa/IIx	Type IIx	Type IIa/IIb	Type IIb
Soleus	30.6%	0.6%	49.1%	4.4%	11.8%	0.5%	3.1%
EDL	0%	0%	10.2%	3.6%	23.7%	6.8%	55.7%

Skeletal Muscle and Obesity

Obesity leads to an increase in ectopic fat accumulation in tissues such as liver and skeletal muscle, and this associated with the metabolic syndrome, a whole body disease. Because skeletal muscle, by virtue of its size, is an important player in whole body glucose homeostasis, the accumulation of ectopic fat in skeletal muscle is thought to play an important role in this disease. The metabolic syndrome is characterized by a reduced muscle glucose uptake and insulin sensitivity, mitochondrial dysfunction and lipotoxicity [118]. The accumulation of intramyocellular lipids, specifically toxic intermediates (e.g., ceramides and diglycerides) rather than intramuscular triglyceride storage, is thought to be associated with the development of muscle insulin resistance by interfering with normal intramyocellular signaling at several levels [20, 119]. Through this mechanism, diet-induced obesity also interferes with muscle protein synthesis resulting in reduced muscle mass [118]. However, the effects of ectopic fat infiltration in response to a long duration HFD differentially effects the slow and fast twitch muscle fibres, with predominantly fast twitch muscles (e.g., tibialis anterior, EDL) accumulating ectopic lipids, while predominantly slow twitch muscles (e.g., soleus) demonstrating no significant change in lipid accumulation [118]. This suggests that slow twitch muscles are protected from the detrimental effects of a HFD, while fast twitch muscles are not. This differential effect of a HFD on lipid accumulation is also associated with differential responses for muscle contractile function in response to HFS. These changes will be discussed more fully in the following sections.

Effects of Diet-Induced Obesity on Skeletal Muscle

It has been well documented that diet-induced obesity leads to an increase in intramuscular fat in both a high saturated fat (lard) and sucrose diet (31.5% kcal from fat)

similar to the Westernized diet [118] and an extremely high fat diet (60% kcal from fat) [117]. Current theory suggests that it is not the accumulation of neutral lipids, such as triglycerides in the muscle that are problematic, but rather the accumulation lipotoxic intermediates (e.g., ceramides and diacylglycerols) that often accompany muscle lipid uptake that negatively affect muscle signaling and function and this has been well studied (reviewed in [20, 119]). The effect of this ectopic fat accumulation on muscle contractile properties in different muscle types, fast twitch (e.g., EDL) versus slow twitch (e.g., soleus) is a newer area of research [116, 117, 120]. The effects of diet-induced obesity on contractile properties appear to be sex-specific, such that pre-menopausal females appear to be protected from diet-induced obesity decreases in muscle function. This is possibly because female mice have a greater number of type I fibres, compared to males [121]. Type I fibres rely more heavily on fat oxidation for energy, potentially protecting females from intramuscular lipotoxic fat accumulation and subsequent muscle dysfunction. In addition, male mice show a strong inverse relationship between the proportions of type I fibres and relative fatness, which is not seen in female mice. This indicates that as adiposity increases in male mice there is a decrease in the number of type I fibres (a process that is yet to be explained) [121]. However, in this study, the male and female mice began the HFD (60% kcal fat, lard) when they were very young (21 days) and remained on the diet for approximately one year, and therefore reflects a very long exposure to a HFD from an early age, relative to most of the literature [121].

The data from other studies give mixed results – largely based on the muscle performance measures that are used and the ages of the animals that are studied. Male middle age mouse models have been examined, but instead of looking at the effects of

diet-induced obesity over the lifespan, the diet interventions normally begin at middle age (9 months of age) for duration of 5 months. Since these are middle age mice, this model can be used to examine muscle wasting, or sarcopenia, in conjunction with the effects of diet-induced obesity, which is known as "sarcopenic obesity". In this model, *in vivo* functional muscle tests, including grip strength and sensorimotor coordination, were decreased with a HFD (60% kcal fat, lard) [120]. These authors attributed decreases in muscle function to the decrease in muscle cross sectional area of gastrocnemius and decrease in satellite cells and myonuclei that are associated with muscle repair. Unlike plantaris, a mixed but relatively fast twitch muscle, slow twitch soleus muscle weight decreased, indicating age-related sarcopenia. In these middle aged male mice, this appeared to be due primarily to a loss of type I fibres. Because of their advanced age, both control and HFD mice lost muscle mass, but there was a greater effect of sarcopenia in the HFD group. In addition, soleus did not appear to take up any more total lipid on the HFD, while fast twitch plantaris did increase lipid accumulation [120]. At first glance, this appears to disconnect muscle fat overload from muscle fibre loss, but it may be that soleus is already loaded with lipids (lipid content of the soleus is almost 2 times higher than the plantaris in lean mice) and HFD could not increase the soleus muscle lipid content any further. In addition, these authors only measured total muscle lipid and did not delineate the different lipid species in muscle (i.e., inert triglycerides, or lipotoxic diglycerides and ceramides) making it difficult to ascertain any link between muscle function and specific lipid accumulation.

However, shorter duration (10 weeks) HFD interventions (60% kcal fat, lard) in young male mice elicit muscle fibre type specific adaptations. Contrary to the more long

term (5 months) study in which a selective loss of type I fibres was observed [120], there was a shift towards oxidative type I fibres accompanied by increases in total muscle lipid content, in a muscle-specific manner. These changes were observed in the relatively fast twitch gastrocnemius and plantaris muscles but not in slow twitch soleus muscle. However, muscle contractile function (as measured by *ex vivo* whole muscle stimulation) remained relatively similar in these fast twitch muscles, with only a decrease in relative force post fatigue with a HFD [117].

These fibre type specific changes have also been reported in HFD interventions using a lower amount of fat (45% kcal fat, lard or palm oil), but with added sucrose [116]. In this very recent study, even using a short duration diet intervention (5 weeks) in young mice (12 weeks old), fibre type specific changes were elicited. As expected, the HFS had little effect on soleus muscle lipid content, but there was a significant increase in EDL total muscle lipid content. Muscle-specific contractile changes were also observed. Only fast twitch EDL had a slower relaxation time, while soleus had a decrease in peak twitch force, twitch force time integral, peak tetanic contraction, tetanic force time integral and faster relaxation time. However, in the case of this study the source of fat, lard or palm oil, played a role in altering muscle contractile force, with more detrimental effects elicited by palm oil compared to lard [116].

Taken together, these results suggest that slow twitch muscles, such as soleus, do not further increase their normally high intramuscular total lipids with diet-induced obesity, while fast twitch muscles, such as EDL and plantaris, are more adversely affected by increased muscle lipid content. However, there is a gap in the literature comparing *in vivo* (e.g. sensorimotor coordination and grip strength) and *ex vivo* (e.g.

stimulated muscle contractions) muscle functions. The effects of diet-induced obesity are not just isolated to muscle, but affect the entire body. As previously discussed, bone and muscle work in conjunction for body support and movement, and therefore there is a need to study the effects of aging and a high fat lifestyle in both tissues simultaneously.

Skeletal Muscle and Aging

With aging there is an inevitable decline in muscle strength and muscle mass, which is termed as sarcopenia. In addition to this decline, there is a decrease in muscle force production per unit of muscle mass meaning there is deterioration in muscle function and efficiency [122]. This suggests a greater decline in the function of the muscle than the quantity. This phenomenon of a disproportionate loss in muscle strength compared to muscle mass has been observed in humans with an approximate a 3-fold greater loss in muscle strength compared to muscle mass, in both men and women [4]. Although this relationship between muscle and aging is well established, the mechanism contributing to alterations in skeletal muscle mass, strength, and function with aging remains less understood.

Effects of Aging on Skeletal Muscle

Specific age-related changes have been established, which include decreases in muscle protein turnover and synthesis, remodeling of motor units, and alteration in fibre type [122]. Similar to bone, muscle is remodeled to meet its functional demands, however, with aging this become dysregulated and there is less protein synthesis resulting in this age-related decline in muscle mass [122], with a specific decline in the synthesis of myosin heavy chains, a key protein in muscle contraction [123]. In addition to this decline in protein turnover and synthesis, there is a remodeling of motor units, mainly a

result of denervation of some muscle fibres with re-innervation by surrounding motor nerves, or overall loss of motor units as a whole [16]. This alteration in muscle fibre innervation contributes to the co-expression of myosin heavy chains in muscle fibres, which determines muscle fibre type [124]. Alterations in muscle fibre type with aging are contradictory with some studies suggesting a shift towards type I fibres, others suggesting a shift towards type II, and many with inconclusive results [15].

This unresolved research question could be in part due to the difficulties in muscle fibre typing with aging since many muscle fibres co-express two myosin heavy chains simultaneously as previously mentioned. If denervated muscle fibres are not re-innervated they die, resulting in a greater atrophy of fast fibre types compared to slow fibre types since fast fibre types are more likely to become denervated [16]. Therefore some fast-twitch dominant muscles atrophy while other do not, making the effects on aging muscle fibre type specific [125]. Weight bearing muscles, specifically those with a high proportion of type IIb fibres, atrophy more than non-weight bearing muscles [125]. These alterations in muscle fibre type and atrophy alter muscle contractile properties of any given muscle.

Both maximum isometric force production and maximum power have been found to decline with age [114, 115, 126, 127]. It has previously been reported that soleus and EDL muscles of aged mice (26-27 months of age) produce significantly less maximum tetanic force than their middle aged counter parts (9-10 months of age) [114]. In addition, half relaxation time in soleus but not EDL for aged mice was increased compared to young mice (2-3 months of age), but force-velocity relationship between soleus and EDL remained unchanged with age [114]. In contrast, there are age-related declines in velocity

when concentrically contracting against heavy loads comparing male mice from adult (6-7 months), old (~24 months), and elderly (~28 months) [115]. In terms of time to reach maximum force, there was only an increase in contraction time with elderly mice compared to old and adult mice in EDL but not soleus [115]. In another study, comparing EDL of young (2-3 months), middle aged (12-13 months), and old (26-27 months) mice also found lower absolute power and normalized power to muscle mass, as well as an increase in fatigability with a lower tolerance to sustain power with repeated contractions [127].

The loss in muscle force generating capacity with aging can be partly attributed to this reduction in muscle mass, and the differential atrophy and innervation of the fibre types explains some of the fibre dependent alterations with aging. This progressive muscle wasting with aging plays a major role in frailty and functional ability to complete tasks of daily living, making it an important area of study [122]. By combining muscle contractile function experiments with changes in muscle mass in the present study, both the quality and quantity of muscle will be measured for a more comprehensive understanding of the changes in muscle with a HFD and aging.

Bone and Muscle Relationship

It is clear that bone and muscle are physically inter-dependent. Bone and muscle are integrally linked throughout the lifespan, with both tissues undergoing age-related declines in structure and function (Figure 2.2) [3, 122]. However, it remains unknown how diet induced obesity alters this age-related decline in bone and muscle. There is growing evidence of a link between osteoporosis and sarcopenia, with individuals with sarcopenia at a greater risk of osteoporosis and vice versa, which is hypothesized to be

connected by the mechanostat theory [128]. It is suggested that muscle force has a greater influence on bone than body weight alone [129, 130]. However, there are limited studies examining how muscle influences bone, even though muscle-generated loads play a key role in bone size and structure.

The majority of research investigating the ratio of outcomes of bone and muscle and how these ratios are altered with aging has been in humans (reviewed in [9]). A ratio between outcomes of bone (e.g., BMD, bone CSA) and muscle (e.g., muscle force, muscle CSA, lean mass) exists since bone and muscle are inter-dependent, however the alteration in this ratio with aging is controversial with general findings of no change or an increase, suggesting that these two tissues either change in a coordinate manner or muscle declines at a greater rate than bone [9]. A lack of continuity between findings may be due to different outcomes that are measured, sites measured, and age of humans being studied. BMD or bone CSA only captures alterations in bone quantity and not bone structure and human models limit the measures that can be used to assess bone and muscle, while rodent models allow for more detailed measures. Age related declines in bone and muscle in mice follow the same pattern as in humans making it an accelerated model for studying the effects of aging [15, 131]. Similar to human studies, using a mouse model comparing the ratio bone (mid-diaphysis tibia ultimate load) to muscle (EDL peak tetanus normalized to CSA) outcomes using male C57BL/10 mice at 7 and 24 months of age also found no alteration in this relationship [132]. In addition to the limitations using a human model, there have also been advances in technology that allow for more accurate measures such as bone structure using μCT.

Previous human literature mainly assessed bone health by measuring BMD and bone CSA – which provide insight in the quantity of mineral and bone size but no information about bone structure. Therefore, the present study measured both BMD and bone structure throughout the study duration providing more detailed measures of bone, while muscle function testing allowed muscle forces to be measured in addition to muscle CSA. This allowed for a comparison between previously calculated ratios (e.g., BMD to muscle CSA) to newer ratios (e.g., bone structure to muscle force). Since both osteoporosis and sarcopenia have a high prevalence and serious consequences with aging, it is important to study the effects of a HFS superimposed with aging to understand musculoskeletal health as a unit. Studying the influence of a HFS is especially important, since many Canadians exceed the upper limit for fat, which is suggest to 20-35% caloric intake for individuals 19 and older [133].

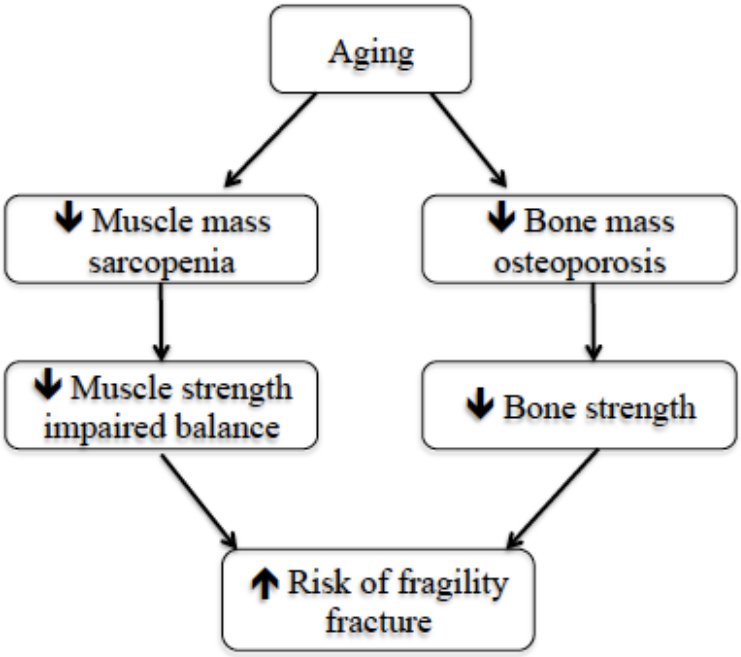

Figure 2.2. Effects of aging on muscle and bone structure and function. Aspects of how a HFS modulate these pathways was studied in this thesis.

Chapter 3: Statement of the Problem and Study Objectives

The effect of a HFS over the lifespan is a relevant area of research with rising obesity rates and our aging population. The suggested inverted 'U' shaped curve associated with a HFS on bone health creates an interesting dichotomy and suggests that while the increased adiposity induced by an obesogenic diet in young adult mice (12 weeks old) can positively affect bone health, there are decreasing bone apposition rates and increased fragility and fractures in later life. In addition, the changes in muscle contractile properties with diet-induced obesity remain poorly understood. While there are a few studies that have investigated the response of young adult animals to diet-induced obesity, fewer have investigated the combination of a diet-induced obesity and aging, which is important since bone and muscle both decline with age and nutrition plays an integral role or musculoskeletal health. Furthermore, bone and muscle tissue has traditionally been studied separately and not simultaneously. Since bone and muscle are integrally linked it is important to study both tissues together to have a comprehensive understanding of changes in the musculoskeletal system. The objectives of this study are to determine if and how a 13-week obesogenic diet, high in fat and sucrose, fed to 20-week old (middle aged) C57BL/6J male mice modulates bone and muscle structure and function, compared to aging alone. In addition, how aging on aging superimposed with an obesogenic diet alters the ratio of bone and muscle outcomes. A 13-week diet intervention was selected since it is a long-term diet intervention and similar diet durations have previously been used [72, 81, 82, 85]. To better understand the inverted 'U' shape curve model, middle aged (20 weeks old) C57BL/6J mice were used instead of using young adult mice (12 weeks old) and extending the HFS (from 11 weeks to 15

weeks) due to the logistics and time constraints of extending the diet versus using older mice.

Hypotheses

1. The aging group will have a steady decline in bone structure and BMD throughout the 13-week study, while the group fed obesogenic diet (HFS-AGE) will initially be protected from the age-related bone loss due to increased body weight, but would have an exacerbated decline in bone structure and BMD at older ages.
2. The aging group would have a decline in muscle function compared to the baseline group, while the HFS superimposed with aging group would have an exacerbated decline in muscle function associated with aging as a result of disruptions in muscle signaling. Specifically, the soleus force production and EDL relaxation time would be negatively impacted by the HFS.
3. The ratio of bone to muscle will be constant in the aging group, indicating that these two tissues decline in a coordinate manner. Although the ratio of bone to muscle will also remain constant in the high fat diet superimposed on aging group, this would be a result of both the bone and muscle structure and function being negatively affected to a similar extent by a high fat diet in aging animals.

Chapter 4: Methods

Animals

All procedures that involved animals were in compliance with the Canadian Council on Animal Care and approved by the Brock University Animal Care Committee (AUP #06-01). Middle aged wild-type male C57BL/6J mice (26.9 ± 1.9 g, 19 weeks old, n = 36) were ordered from Jackson Laboratories (Bar Harbor, Maine, USA) and were allowed to acclimatize for 5 days in the Comparative Biosciences Facility. All mice were kept on a standard 12-hour light: 12-hour dark cycle and had *ad libitum* access to food and water throughout the study. Mice were randomized to baseline (BSL, n = 12), control aging (AGE, n = 12), or high fat diet in combination with aging (HFS-AGE, n = 12) groups (refer to Figure 2 for experimental design flow chart). Unfortunately, during the BSL measures a mouse from the high fat diet group severely injured its cage mate resulting in euthanasia. As a result, a weight-matched mouse from the BSL group was moved to the high fat diet experimental group and all mice were separated and individually housed as a precaution against the male C57BL/6J aggressive tendencies towards other males. During acclimatization and BSL measures all mice were fed standard chow (2014 Teklad global 14% protein rodent maintenance diet, Harlan Tekland, Mississauga, ON).

Experimental Design

The *in vivo* BSL measures conducted at 20 weeks of age for all mice (n= 36) included grip strength testing, *in vivo* scans of the lower right hind limb by μCT, and *in vivo* body μCT scans. Following *in vivo* measures, the BSL group (n= 11) were euthanized at 22 weeks of age, while the control (AGE, n = 12, diet TD.94048, Harlan Teklad, Mississauga, ON) and high fat and sucrose diet (HFS-AGE, n = 12, diet

TD.150448, Harlan Teklad, Mississauga, ON) groups were switched to their respective diets for the 13-week diet intervention (Table 4.1). Throughout the diet intervention the control and HFS groups underwent grip strength testing, *in vivo* body scans, and *in* vivo leg scans, at 20, 24, 28, and 32-weeks of age to measure longitudinal changes due to aging and the obesogenic diet. In addition, body weight and food intake were measured three times a week throughout the study. The AGE and HFS-AGE groups were euthanized when the mice were middle aged at 33-weeks of age for further measures.

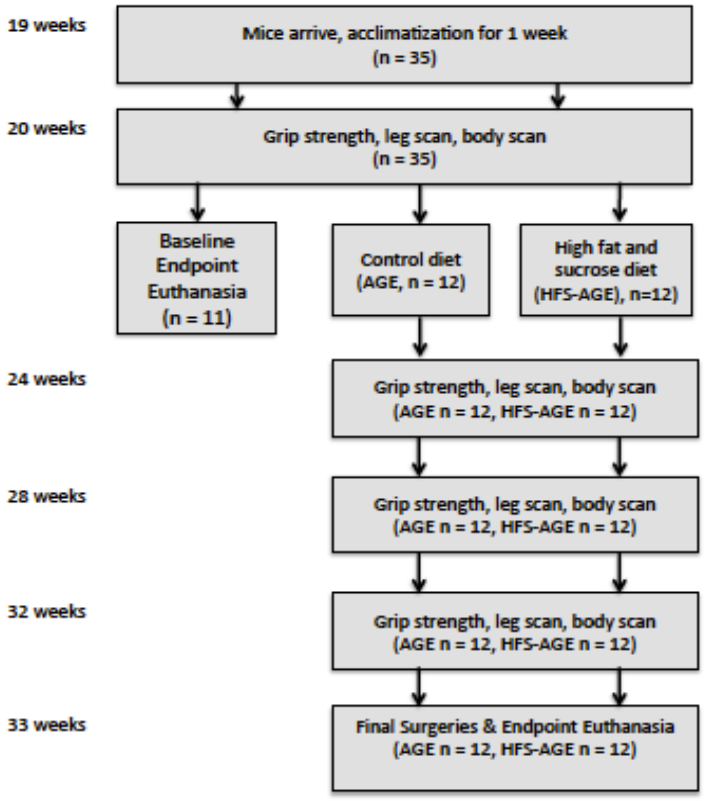

Figure 4.1. *Flow chart of study design.* Leg scans and body scans completed using a µCT (Bruker SkyScan 1176, Kontich, Belgium). Grip strength testing included all four limbs and the front limbs only using a grid and T-bar, respectively, attached to a grip strength meter (Bioseb, Pinellas Park, FL). Calcein green and alizarin red injected for bone histology to measure mineral apposition rate. CRN is an abbreviation for the Cairns Family Health and Biosciences building.

Experimental Diets

Harlan Teklad Diet assisted in creating diets that were consistent with previous high fat studies [72, 81, 82, 116] and were matched as closely as possible for protein, minerals, and vitamins on an energy basis. To be able to study the effects of dietary fat content on the rate of decline of bone with aging, it was important to keep levels of key micronutrients, especially calcium, phosphate, and vitamin D, consistent per energy so that only the effect of the high fat and sucrose levels were being studied. By design, the HFS contains a higher level of energy by weight. Thus, if micronutrients are not adjusted per unit of energy, the level of micronutrients per kcal is lower in mice fed the HFS compared to control diet. The majority of studies in the literature do not do this adjustment so it is uncertain whether reported adverse effects on bone health are due to the higher level of fat and sucrose in the diet or the lower level of micronutrients known to be critical for supporting bone health or possibly both. The level (45% kcal) and source (lard) of fat used in this study is similar to that commonly used in other studies that have examined the effects of a diet-induced obesity on either bone [72, 81, 82] or muscle [116] individually. Since vitamin D is fat-soluble and positively affects bone, it was important to match the diets for vitamin D content. Since lard is known to contain vitamin D, the lard used in the modified AIN-93M HFS was tested for vitamin D content, but none was detected by a third party lab (Covance). As a result, the standard AIN-93M vitamin mix was used for both the control and HFS diets. Although, there is no specific requirement level for alpha-linolenic acid in mice, soybean oil was included in the diets so that mice received a sufficient amount of alpha-linoleic acid and linoleic acid. Specific composition and ingredients of the control and HFS are listed in Table 4.1.

Table 4.1. Study diet composition and ingredients.

	Control Diet (AIN-93M)	**Modified AIN93M Diet**
Protein (% kcal)	13.7	13.8
Carbohydrate (% kcal)	75.9	40.8
Fat (% kcal)	10.3	45.3
Energy (Kcal/g)	**3.6**	**4.6**
Ingredient	**g/kg**	**g/kg**
Casein	140.0	180.0
L-Cystine	1.8	2.3
Corn Starch	465.7	154.2
Maltodextrin	155.0	115.0
Sucrose	100.0	200.0
Lard	--	200.0
Soybean Oil	40.0	30.0
Cellulose	50.0	58.0
Mineral Mix, AIN-93M-MX (94049)	35.0	44.8
Vitamin Mix, AIN-93M-VX (94047)	10.0	12.8
Choline Bitrate	2.5	3.0
TBHQ, antioxidant	0.008	0.008

Body Weight and Food Intake

Body weight was recorded three times a week on the same day for all animals using a pan balance. Food intake was measured three times a week (food provided-food remaining) and was replaced with fresh food three times a week. From these food intake measurements, the total amount of food consumed per day was calculated (g/day), from which food intake per day was normalized to body weight (food g/day/body weight g) for each mouse. In addition to food intake, energy intake (kcal/day) was also calculated by multiplying the food intake per day by the energy density (kcal/g) of the diets (AGE diet 3.6 kcal/g and HFS-AGE 4.6 kcal/g), from which energy intake was normalized to body weight (kcal/day/body weight g) for each mouse.

Surgical Procedures

Endpoint surgeries for the removal of tissues were conducted under isoflurane anesthetic once a surgical plane had been established (i.e., lack of pedal withdrawal reflex with a toe pinch). The left leg soleus and EDL muscles were removed tendon to tendon with silk sutures 4-0 suture (Surgical Specialties Corporation, Reading, PA) tied at the tendons for muscle contractile testing [114, 116], while the right leg muscles were freeze-clamped immediately for future analysis. The abdominal cavity was opened to sever the aorta and vena cava to remove the heart for euthanasia via exsanguination (SOP-EUTH04, Methods of euthanasia for various animals).

***In Vivo* Scans Using Micro Computed Tomography**

In vivo body scans (body composition: fat, lean, and bone mass) and hindlimb scans (bone structure) were completed using the Bruker SkyScan 1176 μCT (Kontich, Belgium). Mice were anaesthetized in an induction chamber with isoflurane at a constant flow rate of 3-5% and transitioned to a nose cone for maintenance of the anesthetic (SOP-HEAL25), Use of isoflurane in rodent surgeries using a vaporizer). For body scans of the abdominal region mice were laid supine and the entire lumbar vertebra was included in the scanning field using the thoracic vertebra as landmarks, identified by the ribs, and the top of the sacrum. Body scans were conducted with a standard resolution using a 1 mm aluminum filter at 40 kilovolts and 200 microamps, with a 430 millisecond exposure time and a rotation step of 0.8°. For leg scans the mice were positioned in right lateral recumbency with the right hind leg extended and secured to the scan bed with styrofoam and dental wax. The entire tibia was included in the scanning field using the ankle and knee joint as landmarks. Leg scans were conducted with a high resolution using a 1 mm

aluminum filter at 40 kilovolts and 200 microamps, with a 430 millisecond exposure time and a rotation step of 0.7°. These *in vivo* measures were repeated on the control and HFS groups throughout the study at 20, 24, 28, and 32 weeks of age to measure longitudinal progression of aging and aging plus a HFS on body composition, bone structure, and BMD.

After completion of all the *in vivo* scans images were processed and analyzed using the same parameters for all samples for either the leg scans or body scans. Reconstruction parameters (Table 4.2) were set in NRecon (software version 1.6.9.10, Bruker, Kontich, Belgium) and image reorientation was performed using Dataviewer software (software version 1.5.1.3, Bruker, Kontich, Belgium) to orientate samples as vertical as possible. Following which, regions of interest were selected and analyzed using CTan software (software version 1.14.4.1+, Bruker, Kontich, Belgium). The tibia region of interest was set using the end of the growth with an offset of 30 slices and region of interest of 60 slices, while the body scan region of interest was landmarked by the beginning and end of the third lumbar vertebra. The tibia was analyzed by setting up a task list to automatically separate trabecular from cortical bone using a task list (Table 4.3), while body scans were analyzed by setting ranges for fat (1-35), fat free (36-84), and bone tissues (85-255). During the study phantoms were scanned once per scan period (i.e. 20, 24 weeks) to calibrate the μCT for BMD.

Table 4.2. Reconstruction parameters for *in vivo* scans of proximal tibia and body composition.

	In vivo leg scans	*In vivo* body scans
Beam hardening	40%	30%
Ring artifact	8	8
Smoothing	4	8
Dynamic threshold	0.0 – 0.110	0.0 – 0.056

Table 4.3. Task list for *in vivo* analysis of proximal tibia

Thresholding	low 90, high 255
Despeckle	sweep, all except largest, image, 3D space
ROI shrink wrap	shrink wrap, 2D space
Bitwise operations	image = NOT image
Bitwise operations	image = image & ROI
Morphological operations	opening, round image, 2D space, radius=2
Despeckle	sweep, all except largest, image, 3D space
Morphological operations	closing, round, image, 2D space, radius=10
Morphological operations	opening, round image, 2D space, radius=10
Morphological operations	erosion, round image, 2D space, radius=3
Morphological operations	dilation, round image, 2D space, radius=2
Bitwise operations	ROI = ROI sub image
Reload	image
Save bitmaps	image inside ROI, BMP, copy dataset to log files
Save bitmaps	ROI, BMP, convert to monochrome
Thresholding	low 90, high 255, copy dataset to log file
ROI shrink wrap	shrink wrap, 2D space
Structure	2-D analysis
BMD	histogram

Grip Strength Testing

Grip strength testing was used as a functional *in vivo* measure of muscle strength using a Bioseb Grip Test 3 system. The grip strength of all four limbs and front limbs only was measured by either using a grid for all four paws or a T-bar for the front paws only. Once mice had a grip they were gently pulled backwards horizontally until the grip was released. The grid and T-bars were attached to a grip strength meter (Bioseb, Pinellas Park, FL) that measured the force produced. Each grip strength test for all four limbs and front limbs was performed in triplicate. Outliers were excluded if they were two standard deviations above or below the average and results were reported as the group average of the averaged three grip strength tests for each mouse.

Muscle Contractile Function Tests

Muscle contractile experiments were conducted on *In Vitro* Muscle Testing Systems from Aurora Scientific Inc. (Aurora, Ontario) using the soleus and EDL muscles excised during the surgical procedures. The soleus was chosen as a representative slow twitch muscle (approximately 30% type I fibres and 49% type IIa fibres) and EDL was chosen as a representative fast twitch muscle (approximately 24% type IIx and 56% type IIb fibres) [110]. These systems allow for the control of muscle length, shortening and lengthening speed, and temperature. The excised muscles were suspended by the sutures tied at the proximal and distal tendons of the muscle in a vertical organ bath containing Tyrodes solution (Table 4.4) continually being circulated with 95% O_2 and 5% CO_2, maintained at a temperature of 25°C. Tyrodes solution is an isotonic physiological saline solution that simulates the *in vivo* environment, providing the muscle with all the essential substrates and ions to survive during the contractile experiments and maintaining normal osmolarity. The viability of a muscle following excision is of great importance, by using fusiform muscles such as mouse soleus and EDL the muscle diameter is small enough to receive sufficient oxygenation and substrate delivery through diffusion at 25^{o}C, even to support muscle contraction [134].

Once muscles were set up in the vertical organ baths, muscle resting length was arbitrarily set to 12 mm with a resting tension between 3-5 mN, followed by a slip tetanus protocol (100Hz for 400ms) to prevent slippage of the sutures at the tendon-suture junction. Muscles were then allowed to equilibrate, with individual muscle twitches (1 Hz for 100 ms) stimulated at 3-minute intervals for either the 30-minute equilibration protocol or until the twitch force had stabilized (i.e., no change in the magnitude of the twitch force). Following equilibration, the muscle length at which the maximal active

twitch force (P_t) was produced, known as the optimal length (L_o), was calculated. This was accomplished by stimulating the muscle to produce single twitches (1 Hz for 100ms) at various lengths. Force traces were analyzed to determine the Pt, calculated by subtracting passive force (i.e., resting tension) from total force, and using that resting tension to determine optimal length for the muscle being tested. Muscle length was measured using digital vernier calipers (Electron Microscopy Sciences, Hatfield, PA) with the adjusted resting tension at which P_t was measured. This muscle length was then set as the new L_o in the software, which was used as the reference length for the experimental protocol. Following these standard procedures, the muscles were ready for the experimental protocol.

Two slightly different systems were used for the soleus and EDL, due to the duration of the contractile protocols all soleus were analyzed on one system and all EDL analyzed on the other. This was not an issue because soleus and EDL were not being compared. For soleus parallel platinum electrodes controlled by a 701C biphase stimulator stimulated soleus to contract. Data was collected using a 305C servomotor acquired through a 604A analog-to-digital interface controlled by a 305C dual-mode level system. The ASI600a software (version 3.210) was used for data acquisition and basic analysis. For EDL, parallel platinum electrodes controlled by a 701B biphase stimulator stimulated the EDL to contract. Data was collected using a 300C-LR servomotor acquired through a 604A analog-to-digital interface controlled by a 300C-LR dual-mode level system. The ASI600a software (version 1.60) was used for data acquisition and basic analysis and data was exported to Excel for both the soleus and EDL for further analysis (Microsoft Canada Co., Mississauga, ON).

Aside from slight differences in the systems, the experimental protocol only varied by the maximum stimulation, because soleus is a slow twitch muscle it requires a lower stimulation frequency compared with EDL, since it is a fast twitch muscle and requires a high stimulation frequency. Soleus was stimulated at 120 Hz and EDL was stimulated at 150 Hz. Muscle contractile measures for both soleus and EDL included isometric twitch peak force, isometric tetanus peak force, force-frequency curve, maximum shortening speed, half relaxation time, rate of force development (+df/dt), and rate of relaxation (-df/dt).

Table 4.4. Composition of Tyrodes solution.

Compound	**Grams/L**
Sodium Chloride	7.07
Potassium Chloride	0.37
Sodium Bicarbonate	2.02
D-Glucose	0.99
Sodium Hydrogen Phosphate	0.05
Magnesium Chloride	0.05
EDTA	0.03
Calcium Chloride	0.20

Muscle CSA

Muscle CSA was calculated for both soleus and EDL using the following calculation,

$$CSA = (m / l * d * (L_f/L_o))$$

Where m is for muscle mass (mg), l is for muscle length (mm), d is for mammalian skeletal muscle density (1.06 mg/mm^3) [135], and L_f/L_o is the fibre length-to-muscle length ratio (soleus 0.71 and EDL 0.44) [114].

Muscle Function Analysis

Muscle viability was determined based on tetanus peak force cut offs for the soleus (<150 mN) and EDL (<200 mN), if muscles produced less than the cut off they were not considered viable. Resting tension was subtracted from peak twitch or tetanus

peak force to calculate peak force and normalized to muscle CSA (mN/mm^2). Rate of force production and rate of force relaxation data was smoothed using a moving average of 17 time points to account for oscillations in the force traces and the maximum was determined from this smoothed data. Both peak twitch and tetanus half relaxation time were calculated by subtracting the time of half the peak force (peak force/2) from the time of peak force. As for the slack test, the ASI600a software was used to view tetanus traces, the time for force redevelopment was recorded at 3 mN for the soleus and 10 mN for the EDL. The recorded time points for each change in L_0 (10%, 12.5%, 15%, 17.5%, 20%) were plotted to calculate the y-intercept (slope= $\%L_0/ms$), which was converted to muscle lengths per second (y-intercept/100) and divided by the fibre length factor (soleus 0.71, EDL 0.44) [114]. The force frequency curve was plotted by subtracting the resting tension from the peak force for each frequency then normalized to the peak force produced for the force frequency curve (% maximum force).

Ratio of Outcomes of Bone and Muscle

Bone and muscle outcomes were chosen to represent the structure and/or function of these tissues. To represent trabecular structure proximal tibia BV/TV was selected since it is a responsive to alterations in diet, while vBMD was selected as a measure of bone quantity and has previously been used as an outcome to calculate bone to muscle ratios [9]. As for muscle, peak tetanus force was selected as the representative functional measure, while CSA was selected as a measure muscle quantity. Ratios included BMD:CSA, BMD:peak tetanus, BV/TV:CSA, and BV/TV:peak tetanus.

Muscle Immunohistochemistry

Upon completion of the contractile experiments both soleus and EDL were set in an embedding compound (Cryomatrix, Pittsburgh, PA) for muscle fibre typing with specific myosin heavy chain (MHC) antibodies. Muscles were orientated longitudinally in Cryomatrix, frozen in 2-methylbutane and stored at -80°C until further analysis.

Soleus and EDL were sliced at -20°C into 10 μm sections using a cryotome (77200187 Issue 5; ThermoShandon, Runcorn, UK) and placed on a microscope slide that had been vectabonded (Vectabond Reagent for Tissue Section Adhesion, SP-1800; Vector Laboratories, Burlingame, CA). Slides were then stained for myofibrillar ATPase to determine muscle fibre type. Staining began by blocking muscle sections with 10% goat serum (G9023; Sigma-Aldrich, St. Louis, MO) in 1x phosphate buffer saline (1 tablet dissolved in 200 mL distilled water; P4417; Sigma-Aldrich, St. Louis, MO) (100 μL/slide) for 1 hour at room temperature, followed by a primary antibody concoction of MHCI (1:50 dilution; BA-F8-s; Developmental Studies Hybridoma Bank, University of Iowa, Iowa City, IA), MHCIIa (1:600 dilution; SC-71-s; Developmental Studies Hybridoma Bank, University of Iowa, Iowa City, IA), and MHCIIb (1:100 dilution, BF-F3-s; Developmental Studies Hybridoma Bank, University of Iowa, Iowa City, IA) appropriately diluted in 10% goat serum blocking solution (100 μL/slide) for 3 hours at room temperature. Slides were then washed in 1x phosphate buffer saline three times for 5 minutes and the secondary antibody concoction, Alexa Fluor 350 anti-mouse IgG2b (1:500 dilution, A-21140; Life Technologies, Eugene, OR), Alexa Fluor 488 anti-mouse IgG1 (1:500 dilution, A-21121; Life Technologies, Eugene, OR), and Alexa Fluor 555 anti-mouse IgM (1:500 dilution, A-21426; Life Technologies, Eugene, OR), was appropriately diluted in 10% goat serum blocking solution (100 μL/slide) for 1 hour at

room temperature in the dark. Again slides were washed in 1x phosphate buffer saline three times for 5 minutes prior to applying ProLong Gold antifade reagent (P10144; Molecular Probes, Eugene, OR) and a #1 coverslip (12-542B; Fischer Scientific, Waltham, MA) [110].

Muscle sections were viewed at 20x magnification using a Zeiss Axio Observer Research Microscope (491912-0003-000; Zeiss, Oberkochen, Germany) attached to a digital camera (ORCA-Flash4.0 V2 Digital CMOS camera; C11440-22CU; Hamamatsu Photonics K.K., Japan) and ZenPro software (Zen 2 blue edition; version 2.0.0.0; Zeiss, Oberkochen, Germany) to tile and stitch images together. ImageJ software was used to calculate the number and area of each fibre type, which was determined manually depending on the fibre stain.

Statistical Analysis

Body weight and food intake were analyzed with a repeated measures one-way ANOVA. Grip strength (front limbs and four limbs), body composition (percent lean mass, percent fat mass, and percent bone mass), tibia structure (BV/TV, Tb.Th, Tb.N, Tb.Sp, and BMD), were analyzed with a repeated measures two-way ANOVA with group and age as factors. Muscle function tests for soleus and EDL (CSA, peak twitch, peak tetanus, rate of force development, rate of relaxation, half relaxation time, maximum unloaded shortening velocity, and force frequency) were analyzed with a one-way ANOVA. Statistical significance was accepted at $p < 0.05$.

Chapter 5: Results

Body Weight & Food Intake

At 20 weeks of age, when mice were randomly assigned to the BSL, AGE, or HFS-AGE groups, there were no differences in body weight among groups. Following the 13-week intervention, the HFS-AGE group weighed 30% more than the AGE group ($p<0.0001$) (Figure 5.1). There was an interaction for energy intake (kcal/day), with the HFS-AGE group having a higher energy intake compared to the AGE group ($p<0.0001$) (Figure 5.2.A.). However, when energy intake was normalized to body weight (kcal/body weight/day) there was an overall interaction ($p<0.0001$) but no main effect for group (Figure 5.2.B).

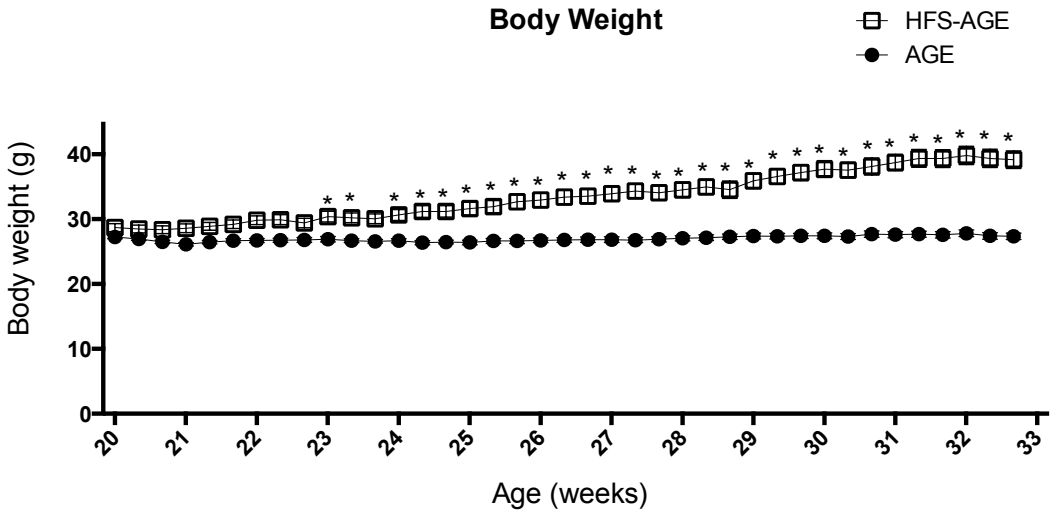

Figure 5.1. Body weights of AGE (n=12) compared to HFS-AGE (n=11) mice from 20 weeks of age to 33 weeks of age. Data are reported as mean±SE. *, signifies significant differences between AGE and HFS-AGE groups at a specific time point. There was an overall interaction ($p<0.0001$) with a main effect by group ($p<0.0001$) and over time for the HFS-AGE group ($p<0.0001$) but not the AGE group.

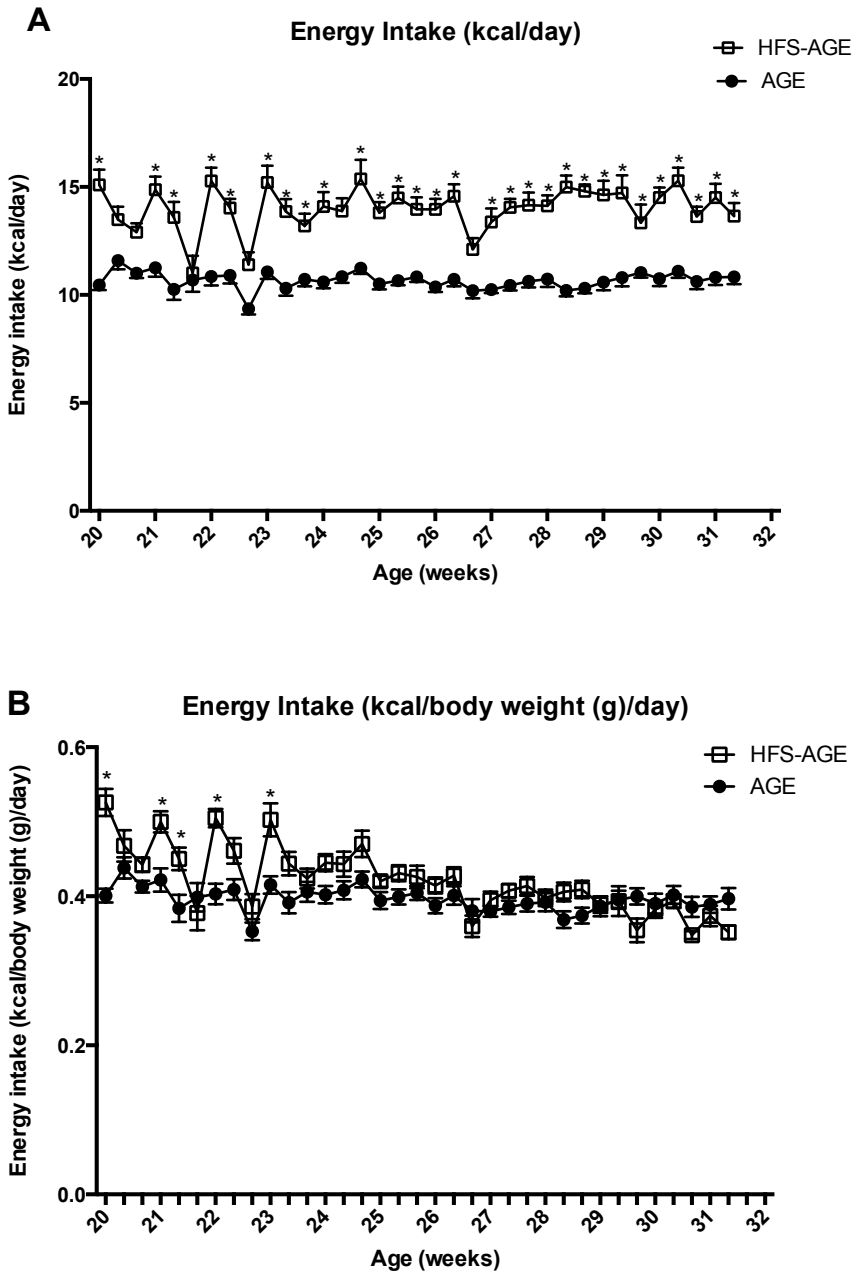

Figure 5.2. Energy intake (kcal/day) and energy intake normalized to body weight (kcal/body weight/day) for AGE (n=12) compared to HFS-AGE (n=11) groups from 20 weeks of age to 33 weeks of age. Data are reported as mean±SE *, signifies significant differences between AGE and HFS-AGE groups at a specific time point. (A) There was an interaction for energy intake with the HFS-AGE group having a higher energy intake than the AGE group ($p<0.0001$). (B) There was an overall interaction for energy intake normalized to body weight ($p<0.0001$), but no main effect for group.

Body Composition

From 20 weeks to 33 weeks of age both AGE and HFS-AGE had declines in lean mass ($p<0.0001$), however HFS-AGE had a greater decrease (46%) compared to AGE (13%) ($p<0.0001$) (Figure 5.3.A). Fat mass increased in both AGE and HFS-AGE ($p<0.0001$), with HFS-AGE group having a greater increase (79%) compared to AGE (51%) ($p<0.0001$) (Figure 5.3.B). There was an overall interaction for bone mass, with differences between groups at 28 weeks ($p<0.0001$) and 33 weeks ($p<0.0001$) as a result of an increase in AGE and decrease in HFS-AGE (Figure 5.3.C).

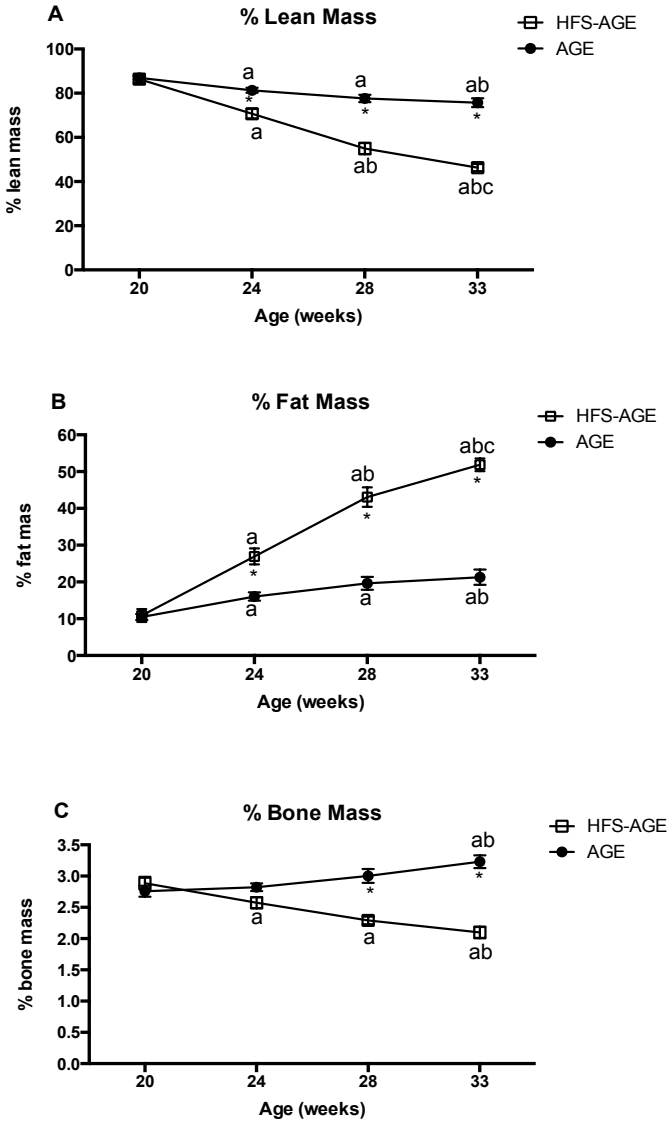

Figure 5.3. % lean mass, fat mass, and bone mass were measured at the mid-truncal region for AGE (n=12) and HFS-AGE (n=11), with the third lumbar vertebra as a landmark for exact positioning using μCT. Data are reported as mean±SE *, signifies significant differences between AGE and HFS-AGE groups for each time point, while letters signify significant differences between time points within a group (a, compared to 20 weeks; b, compared to 24 weeks; c, compared to 28 weeks). (A) Relative lean mass had an interaction ($p<0.0001$) with a 13% decline in the AGE group compared to the 46% decline in the HFS-AGE group and an overall decrease in lean mass over time for both groups. (B) Relative fat mass had an interaction ($p<0.0001$). The AGE group had a 51% increase in fat mass compared to the 79% increase in fat mass for the HFS-AGE group and an overall increase in lean mass over time for both groups. (C) % bone mass had an interaction ($p<0.0001$) with differences between groups at 28 weeks ($p<0.0001$) and 33 weeks ($p<0.0001$). There was an increase in % bone mass over time for the AGE group, while there was a decline over time for the HFS-AGE group.

Structure and BMD of Proximal Tibia

Proximal tibia structure was compromised with aging, and feeding a HFD did not alter this relationship. BV/TV declined from 20-week of age (BSL) to 24-weeks of age, followed by a maintenance period to the study end point at 33-weeks of age. Over the 13-week intervention, the decrease in BV/TV was similar for AGE (34% decrease) and HFS-AGE (45% decrease) ($p<0.0001$) (Figure 5.4.A). Tb.Th similarly declined in both groups (9% for AGE, 8% for HFS-AGE) over the 13-week intervention ($p<0.05$) (Figure 5.4.B). Tb.N also declined over this time period (29% for AGE, 41% for HFS-AGE) ($p<0.05$), however unlike BV/TV and Tb.Th, HFS-AGE did not have a maintenance period from 24-weeks to 33-weeks of age but declined ($p<0.05$) (Figure 5.4.C). Tb.Sp increased in both AGE and HFS-AGE from 20-weeks to 24-weeks of age ($p<0.05$), however AGE had a decrease in Tb.Sp from 24-weeks to 33-weeks ($p<0.05$), resulting in an overall non-significant alteration in Tb.Sp from 20-weeks to 33-weeks of age. In contrast, HFS-AGE had no changes in Tb.Sp from 24-weeks to 33-weeks age, resulting in a total overall increase of 19% ($p<0.05$) (Figure 5.4.D). While BMD of proximal tibia had an overall interaction ($p<0.05$) and main effect for time ($p<0.001$), there was no main effect between AGE and HFS-AGE. BMD continually declined from 20-weeks to 33-weeks of age with a similar total overall decrease in both AGE (17% decrease) and HFS-AGE (23% decrease) with no differences between groups (Figure 5.5). Overall, aging negatively impacted bone structure as a result of a decrease in Tb.N and an increase in Tb.Sp that contributed to the decline in BV/TV as well as a decline in BMD. Feeding a HFS did not alter the effect of AGE alone, as there were no differences between the AGE and HFS-AGE groups for any of the proximal tibia measures.

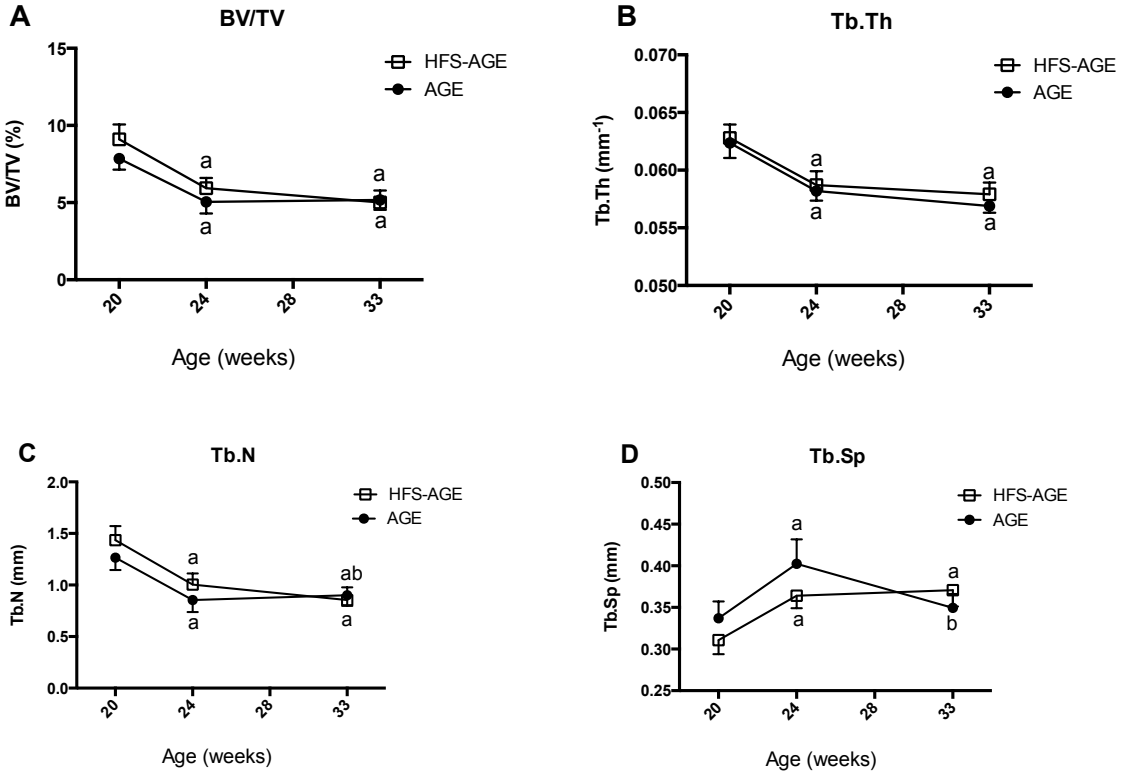

Figure 5.4. Proximal tibia bone structure was measured using μCT for the AGE (n=12) and HFS-AGE (n=11) groups. Data are reported as mean±SE, letters signify significant differences between time points within a group (a, compared to 20 weeks; b, compared to 24 weeks). (A) BV/TV had no interaction or main effect between AGE and HFS-AGE groups, but there was a main effect for time ($p<0.0001$). (B) Tb.Th had no interaction or main effect between AGE and HFS-AGE groups, but there was a main effect for time ($p<0.0001$). (C) Tb.N had an interaction ($p<0.05$) with no main effect for group, but a main effect for time ($p<0.0001$). (D) Tb.Sp had an interaction ($p<0.05$) with no main effect for group, but a main effect for time ($p<0.0001$).

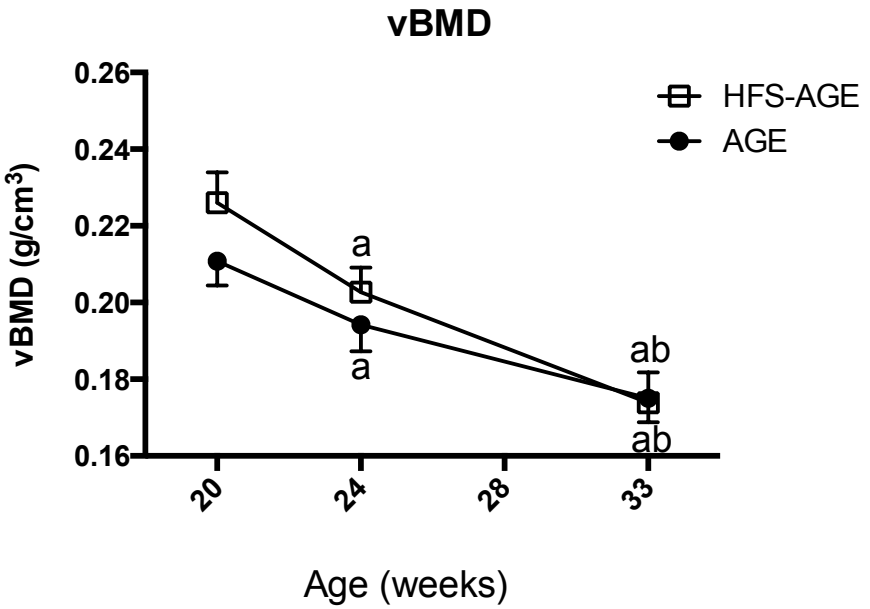

Figure 5.5. Proximal tibia vBMD was measured using μCT for the AGE (n=12) and HFS-AGE (n=11) groups. Data are reported as mean±SE, letters signify significant differences between time points within a group (a, compared to 20 weeks; b, compared to 24 weeks). vBMD had an interaction ($p<0.05$)) with no main effect for group, but a decrease in BMD over time ($p<0.0001$).

Grip Strength of Four Limbs and Front Limbs

Four limb and front limb grip strength testing (Figure 5.6) showed no interaction or main effect between AGE and HFS-AGE. There was a main effect for time for the front limb grip strength in both AGE and HFS-AGE, with an overall decline in grip strength from 20 weeks to 33 weeks ($p<0.05$). There was also a main effect for time for front limb grip strength with only an increase in front limb grip strength from 20 weeks to 28 weeks in AGE ($p<0.05$).

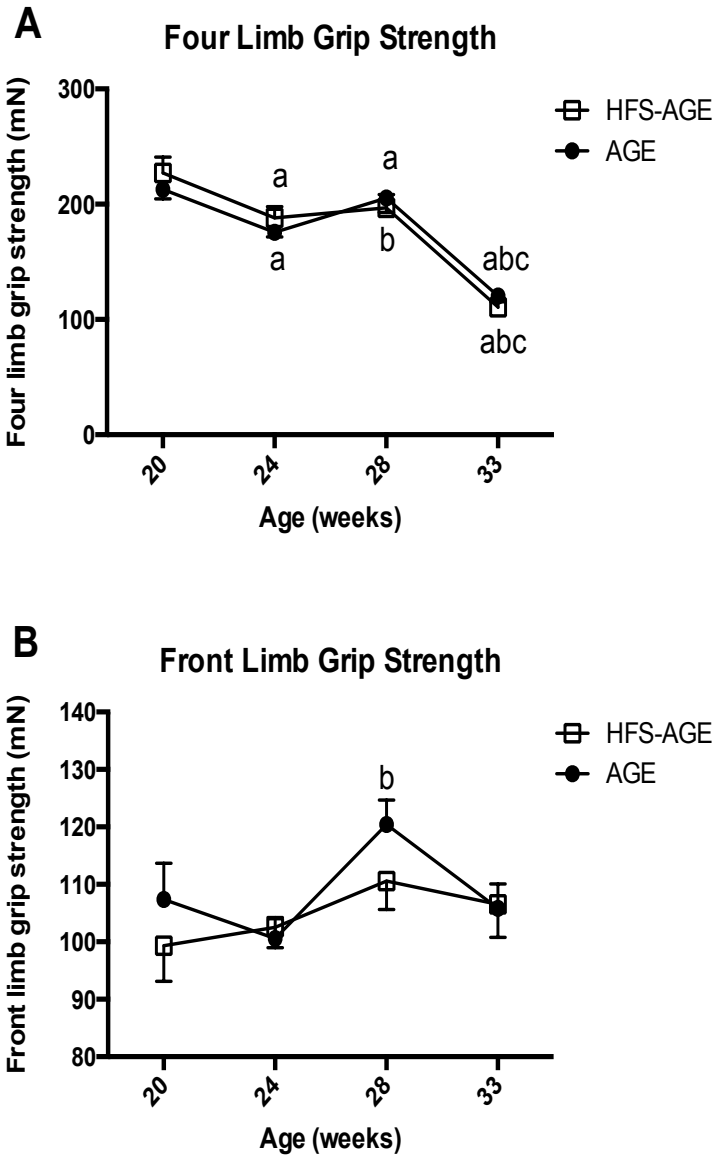

Figure 5.6. Mouse grip strength was measured in triplicate for all four limbs and front limbs for the AGE (n=12) and HFS-AGE (n=12) groups. Data are reported as the group mean±SE of the mean of the triplicate grip strength measure for each mouse, letters signify significant differences between time points within a group (a, compared to 20 weeks; b, compared to 24 weeks; c, compared to 28 weeks). (A) Four limb grip strength testing had no interaction or main effect for group, but a main effect for time ($p<0.01$). (B) Front limb grip strength testing had no interaction or main effect for group, but a main effect for time ($p<0.05$).

Muscle Contractile Function

Soleus

The soleus CSA of HFS-AGE was 22% greater than AGE (p=0.0008) with no difference among any of the other groups (Figure 5.7). However, these alterations in muscle CSA did not equate to alterations in muscle function, as there were no differences among groups for peak twitch force (Figure 5.8.A) or peak tetanus force (Figure 5.8.B). There were no differences in twitch or tetanus rate of force development among groups (Figure 5.9). As for rate of relaxation, there were differences in tetanus rate of relaxation between BSL and AGE ($p<0.001$) and BSL and HFS-AGE ($p<0.01$) (Figure 5.10). In contrast to rate of relaxation, the twitch half relaxation time had differences between BSL and AGE ($p<0.001$) and BSL and HFS-AGE ($p=0.02$), but there were no differences in tetanus half relaxation time (Figure 5.11). There was no effect of aging or aging superimposed with a HFS on maximum unloaded shortening velocity (Figure 5.12). Similarly, there was no shift in the force frequency curve with age or diet (Figure 5.13).

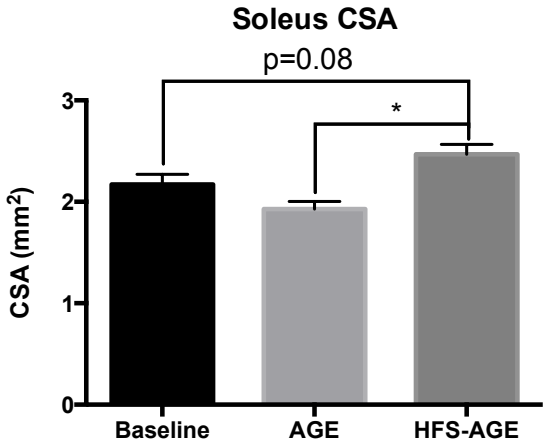

Figure. 5.7. Soleus CSA was measured for the BSL (n= 11), AGE (n=11), and HFS-AGE (n=11) groups. Data are reported as mean±SE *, signifies significant differences among groups. The HFS-AGE group had a greater CSA than the AGE group (p=0.0008) with no difference among the other groups.

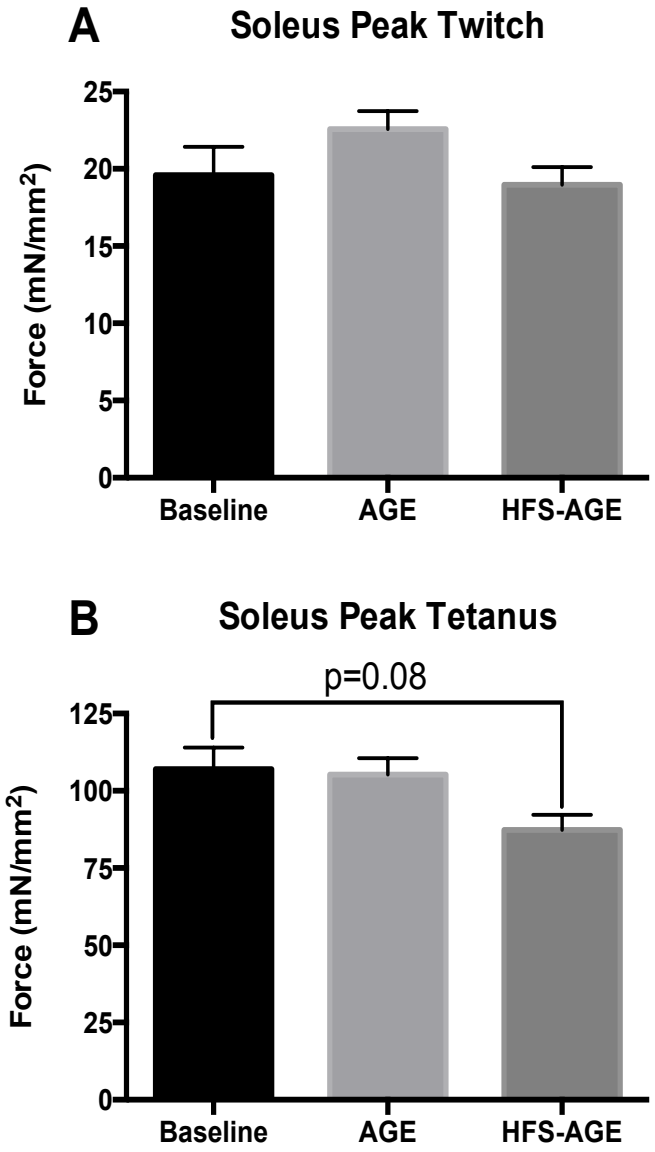

Figure. 5.8. Soleus twitch and tetanus force normalized to CSA was measured for the BSL (n= 10), AGE (n=10), and HFS-AGE (n=9) groups. Data are reported as mean±SE. (A) There were no differences among groups for peak twitch. (B) There were no differences among groups for peak tetanus.

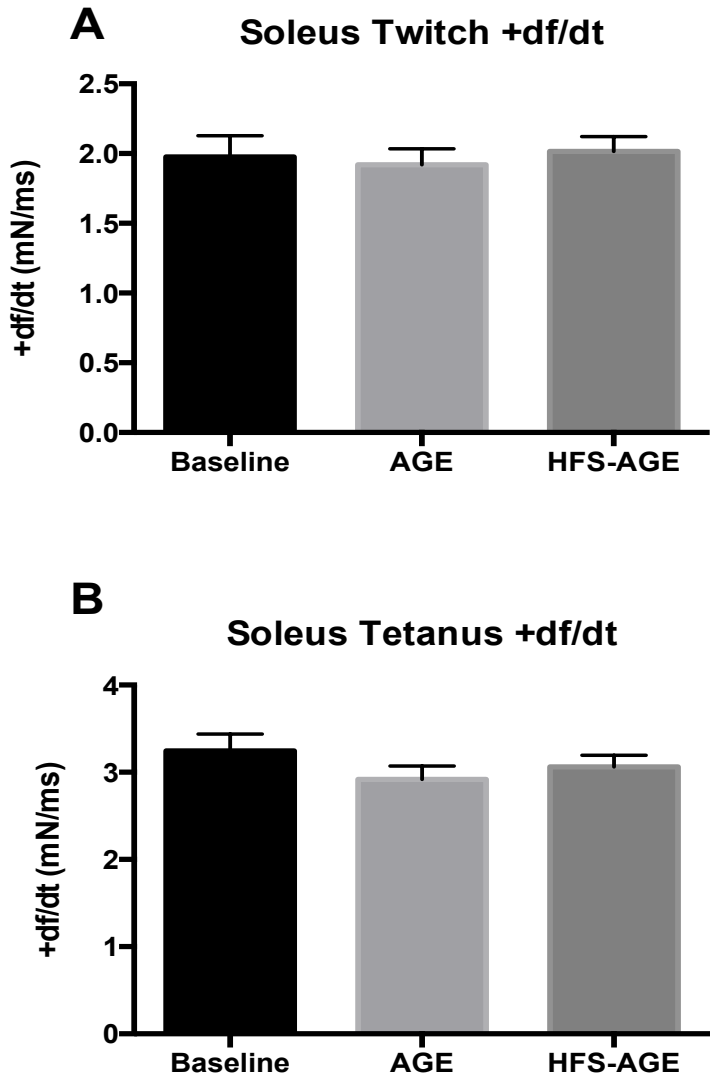

Figure. 5.9. Soleus rate of force development was measured for the BSL (n= 10), AGE (n=10), and HFS-AGE (n=9) groups. Data are reported as mean±SE. (A) There were no differences among groups for twitch force development. (B) There were no differences among groups for tetanus force development.

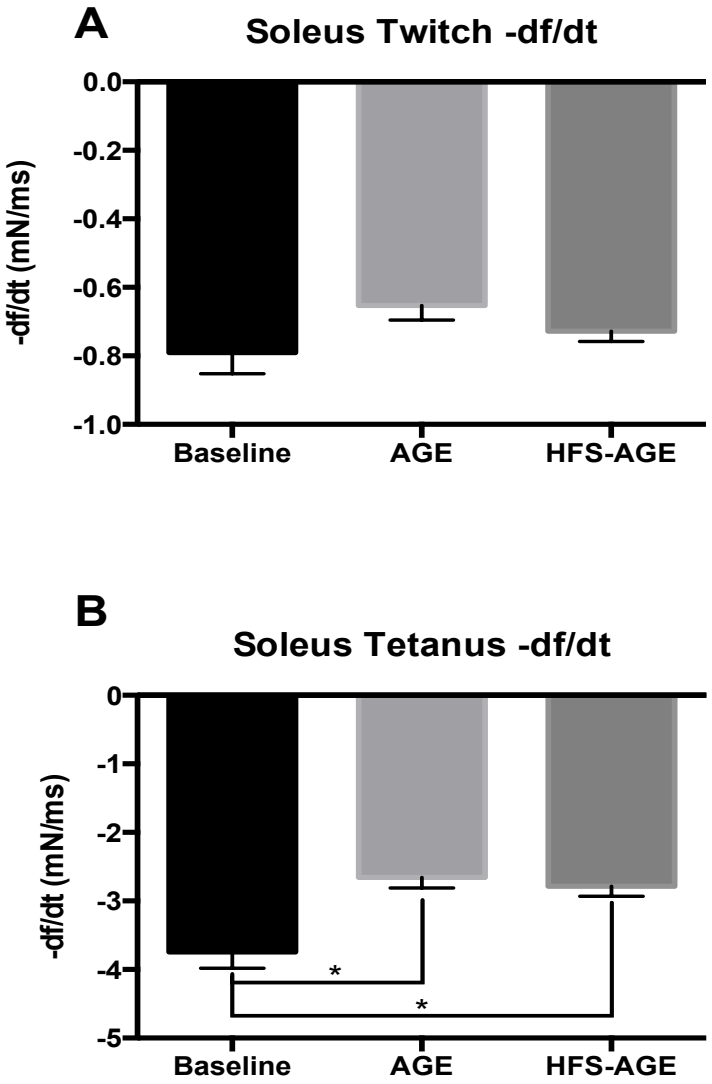

Figure 5.10. Soleus rate of muscle relaxation was measured for the BSL (n= 10), AGE (n=10), and HFS-AGE (n=9) groups. Data are reported as mean±SE *, signifies significant differences among groups. (A) There were no differences among groups for twitch rate of relaxation. (B) Rate of relaxation decreased compared to the BSL group for both AGE ($p<0.001$) and HFS-AGE ($p<0.01$), but there was no difference between the AGE and HFS-AGE groups.

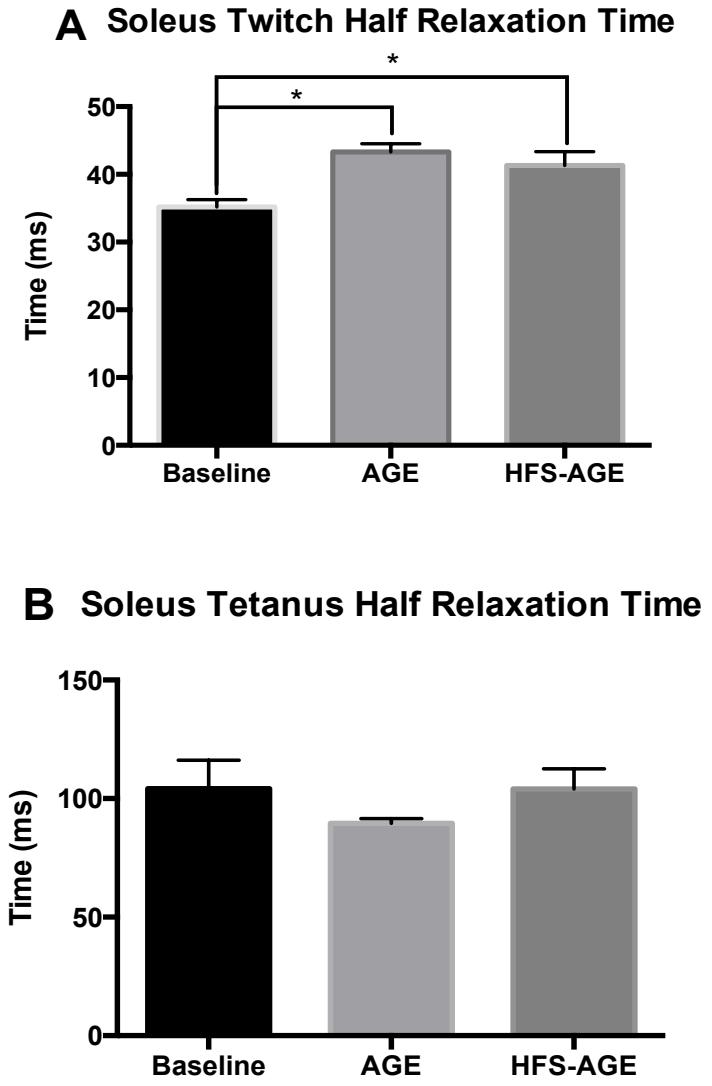

Figure. 5.11. Soleus half relaxation time was measured for the BSL (n= 10), AGE (n=10), and HFS-AGE (n=9) groups. Data are reported as mean±SE *, signifies significant differences among groups. (A) There were differences between BSL and AGE ($p<0.001$) and BSL and HFS-AGE ($p=0.02$), but no difference between AGE and HFS-AGE. (B) There were no differences among groups for tetanus half relaxation time.

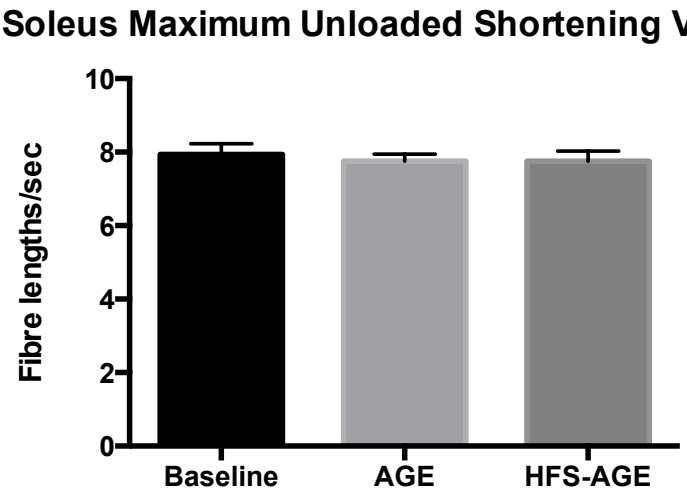

Figure. 5.12. Soleus maximum unloaded shortening velocity was measured for the BSL (n= 10), AGE (n=10), and HFS-AGE (n=9) groups. There were no differences among groups.

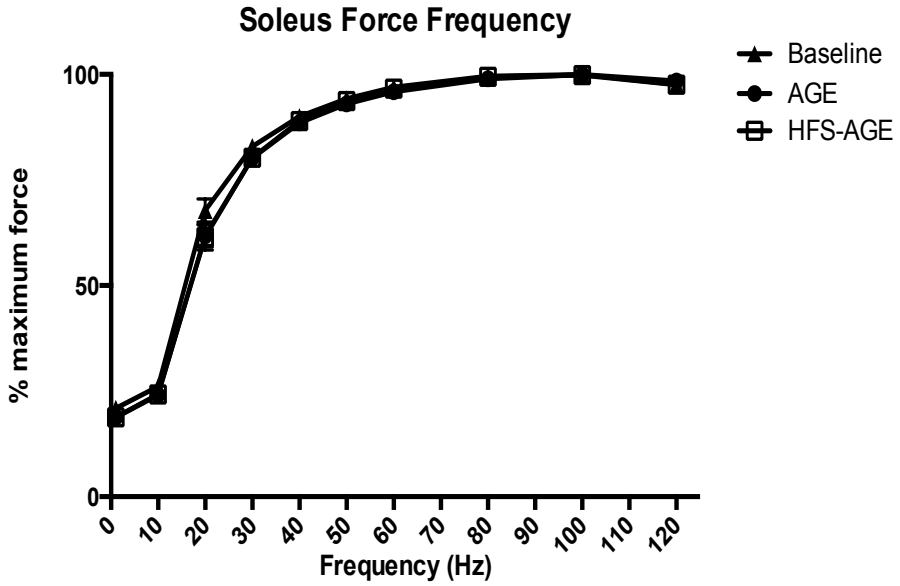

Figure. 5.13. Soleus force frequency was measured for the BSL (n= 10), AGE (n=10), and HFS-AGE (n=9) groups. There was no interaction or main effect for group.

EDL

EDL CSA of AGE had a 13% decrease compared to BSL, whereas there were no differences between AGE and HFS-AGE or BSL and HFS-AGE (Figure 5.14). Peak twitch normalized to CSA increased from BSL for AGE ($p<0.0001$) and HFS-AGE ($p<0.0001$), 43% and 53%, respectively, however there was no difference in peak tetanus normalized to CSA among groups (Figure 5.15). Twitch rate of force production increased by 44% for AGE ($p=0.0004$) and 53% for HFS-AGE ($p<0.0001$) compared to BSL, however there were no differences among groups for tetanic rate of force production (Figure 5.16). Similarly, twitch rate of relaxation increased by 54% for AGE ($p=0.002$) and 49% for HFS-AGE ($p=0.004$) compared to BSL, whereas tetanic rate of relaxation between groups decreased by 74% for AGE ($p=0.008$) and 74% for HFS-AGE ($p=0.01$) compared to BSL (Figure 5.17). Alterations in rate of relaxation with AGE and HFS-AGE did not carry over to half relaxation time (Figure 5.18) or maximum unloaded shortening velocity (Figure 5.19) for either twitch or tetanus among groups. However, for the force frequency curve there was an interaction ($p<0.0001$) and main effect for group ($p=0.0002$). Both AGE and HFS-AGE produced greater force than BSL at 20, 30, 40, 50, 60, 70, and 80 Hz (Figure 5.20).

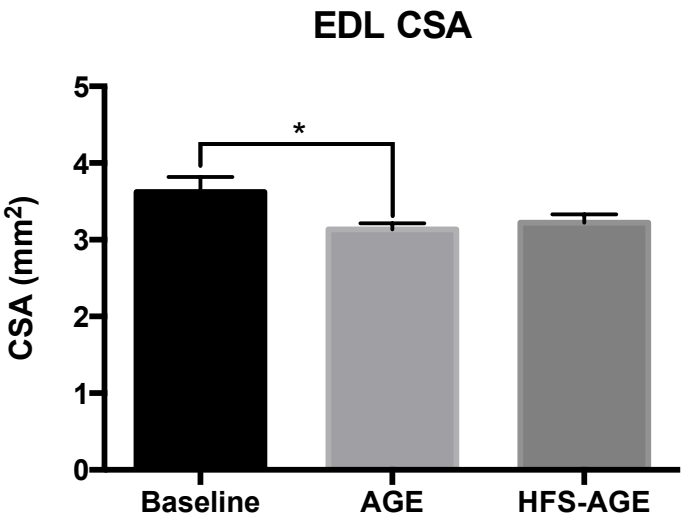

Figure. 5.14. EDL CSA was measured for the BSL (n= 11), AGE (n=11), and HFS-AGE (n=11) groups. Data are reported as mean±SE *, signifies significant differences between groups. The AGE group EDL CSA was lower than the BSL group ($p<0.05$), and no differences between AGE and HFS-AGE or BSL and HFS-AGE groups.

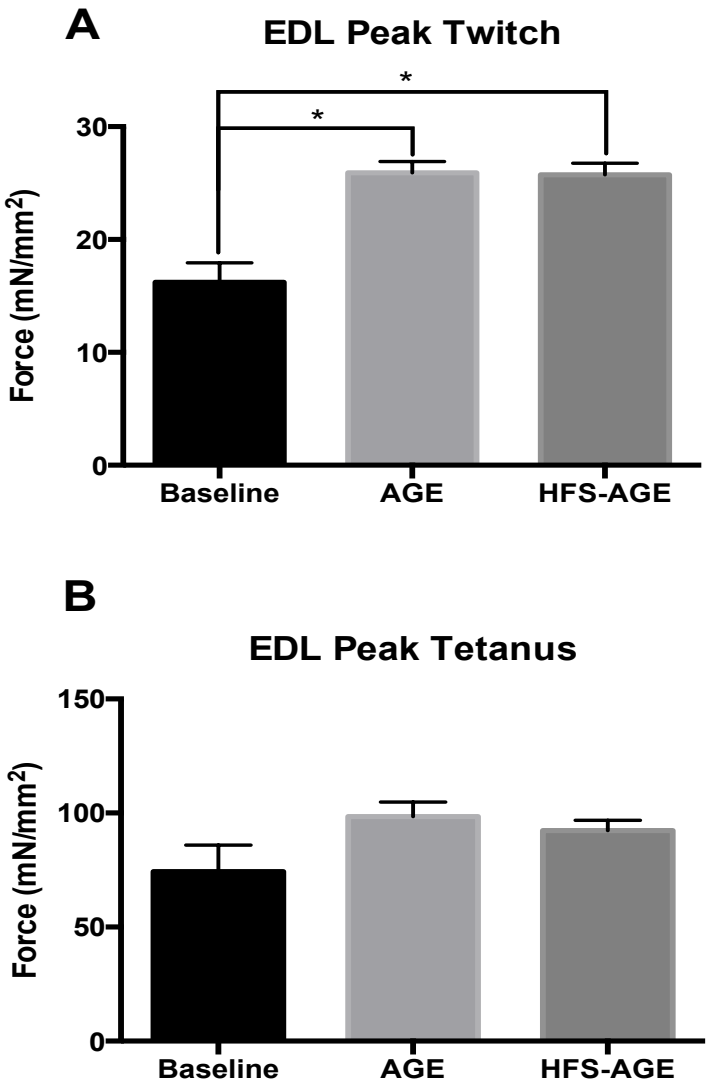

Figure 5.15. EDL peak twitch and tetanus normalized to CSA was measured for the BSL (n= 7), AGE (n=9), and HFS-AGE (n=9) groups. Data are reported as mean±SE *, signifies significant differences between groups. (A) There were differences for peak twitch force between BSL and AGE ($p<0.0001$) and BSL and HFS-AGE ($p<0.0001$). (B) There were no differences among groups for peak tetanus.

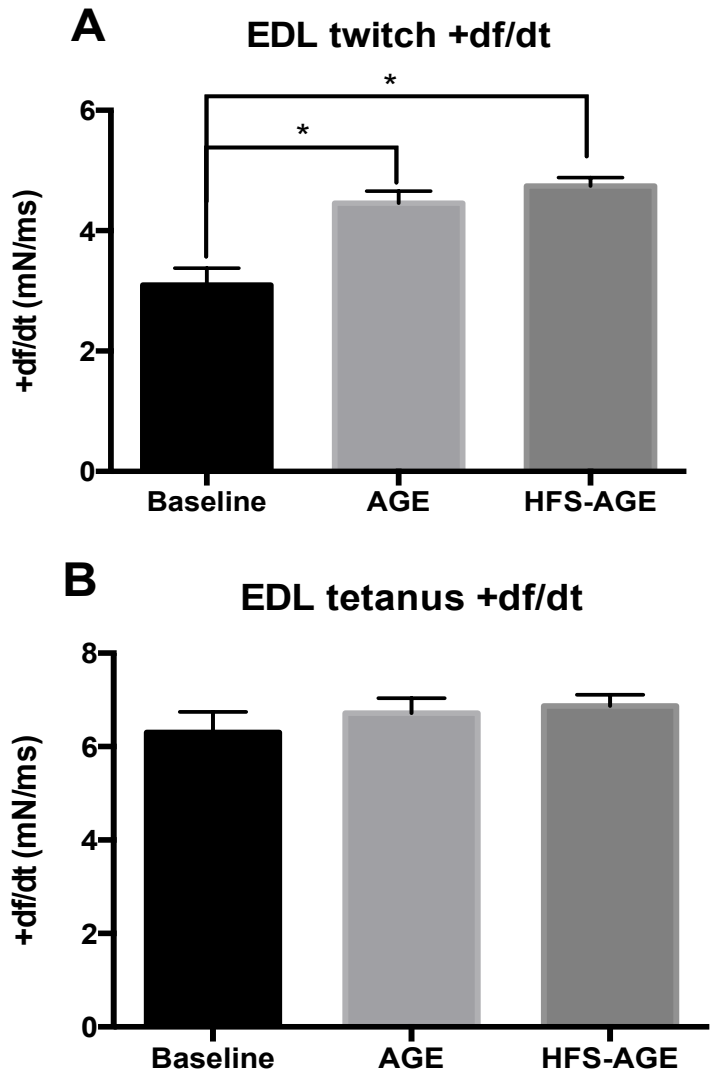

Figure 5.16. EDL rate of force production was measured for the BSL (n= 7), AGE (n=9), and HFS-AGE (n=9) groups. Data are reported as mean±SE *, signifies significant differences between groups. (A) The AGE compared to BSL had a greater rate of force production ($p=0.0004$) and HFS-AGE compared to BSL had a greater rate of force production ($p<0.0001$). (B) There were no differences among any groups for tetanus rate of force production.

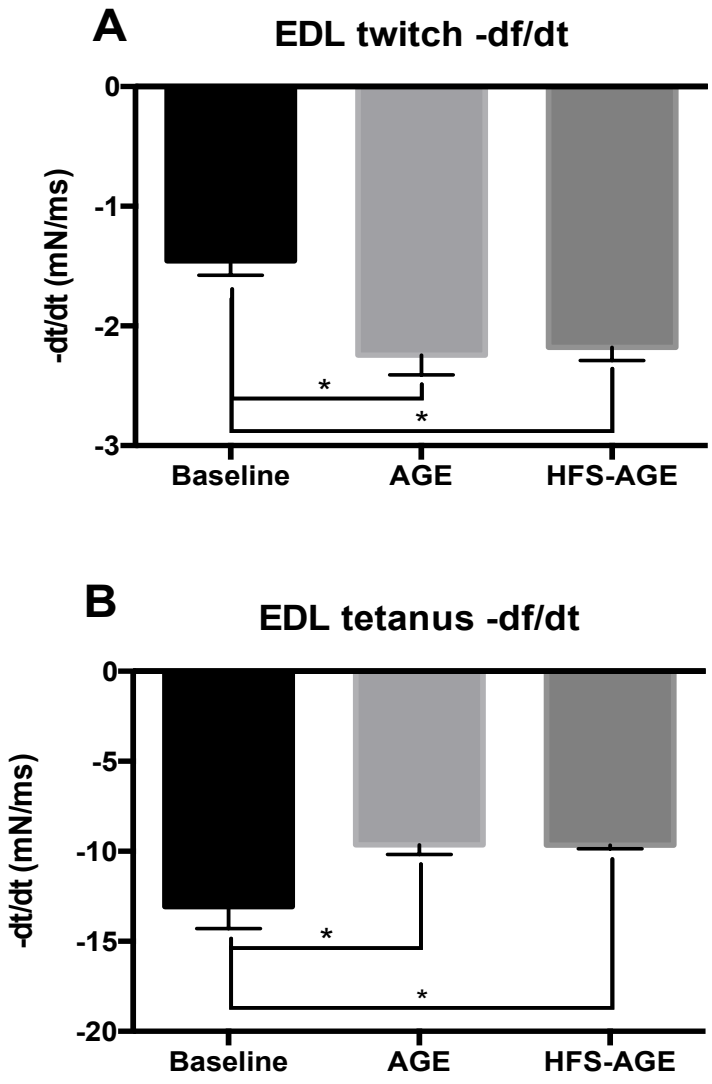

Figure 5.17. EDL rate of relaxation was measured for the BSL (n= 7), AGE (n=9), and HFS-AGE (n=9) groups. Data are reported as mean±SE *, signifies significant differences between groups. (A) There were differences for twitch rate of relaxation between BSL and AGE (p=0.002) and BSL and HFS-AGE (p=0.004). (B) There were differences for tetanus rate of relaxation between BSL and AGE (p=0.008) and BSL and HFS-AGE (p=0.01).

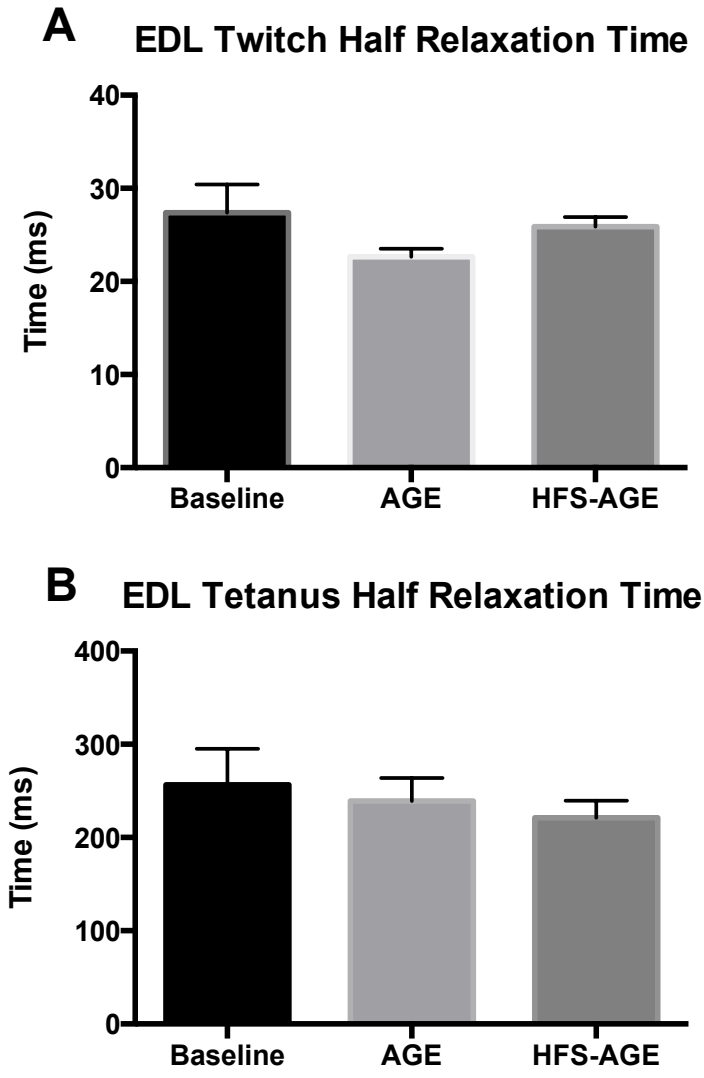

Figure 5.18. EDL half relaxation time was measured for the BSL (n= 7), AGE (n=9), and HFS-AGE (n=9) groups. Data are reported as mean±SE. (A) There were no differences among groups for twitch half relaxation time. (B) There were no differences among groups for tetanus half relaxation time.

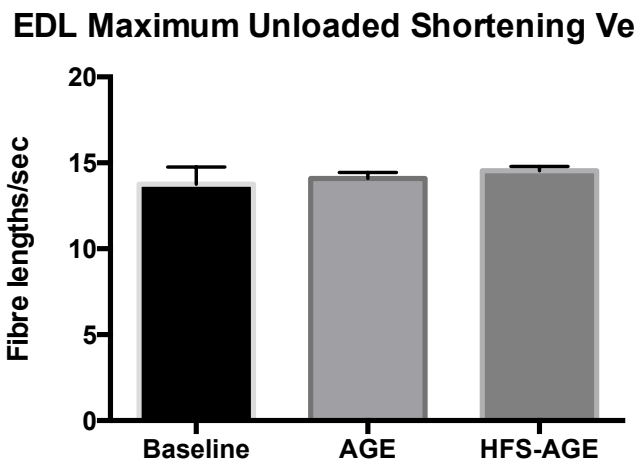

Figure 5.19. EDL maximum unloaded shortening velocity was measured for the BSL (n= 10), AGE (n=9), and HFS-AGE (n=9) groups. There were no differences among groups.

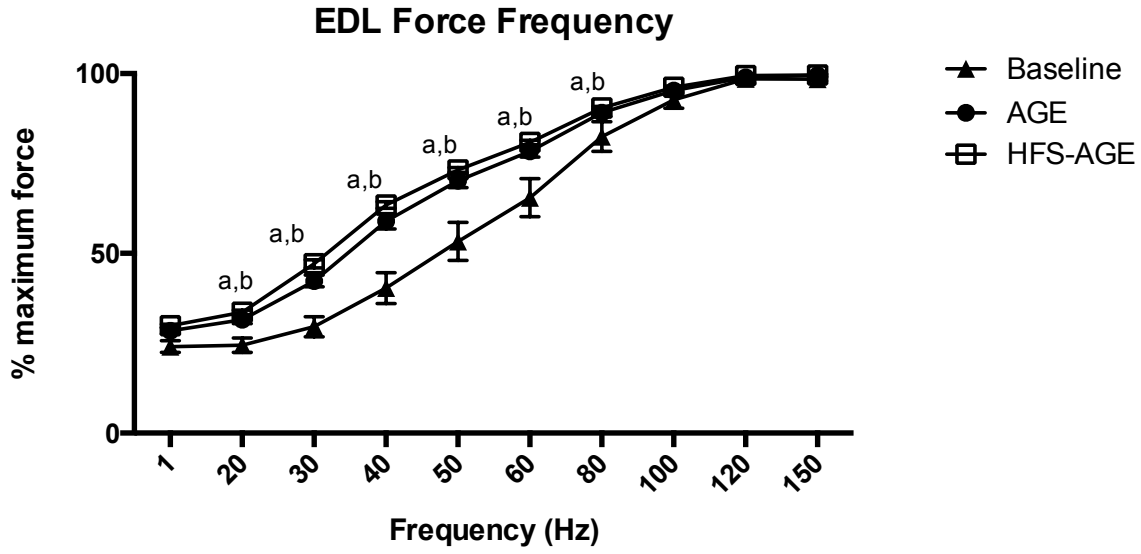

Figure 5.20. EDL force frequency was measured for the BSL (n= 7), AGE (n=9), and HFS-AGE (n=9) groups. Data are reported as mean±SE, a, represents significant differences between BSL and AGE, and b, represents significant differences between BSL and HFS-AGE. There was an interaction ($p<0.0001$) and main effect for group ($p=0.0002$).

Muscle Fiber Typing

Soleus

Soleus type I fibres for HFS-AGE group were 32% larger compared to AGE ($p<0.0001$) and 14% larger compared to BSL ($p=0.0002$), while AGE had a 20% decrease compared to the BSL group ($p<0.0001$) (Figure 5.21.A). This trend continued for soleus type IIa fibres with HFS-AGE group being 30% larger compared to AGE ($p<0.0001$) and 16% larger compared to BSL ($p=0.001$), while AGE had a 17% decrease compared to the BSL ($p=0.004$) (Figure 5.21.B). As for soleus type IIa-b hybrid fibres, HFS-AGE had a 25% larger CSA compared to AGE ($p<0.0001$) and an 18% larger CSA compared to BSL ($p<0.0001$) (Figure 5.21.C). Similarly, soleus type IIb fibres for HFS-AGE had a 51% larger CSA compared to AGE ($p<0.0001$) and a 37% larger compared to BSL ($p<0.0001$) (Figure 5.21.D). However, there was no alteration in the relative composition of the soleus muscle (Figure 5.22).

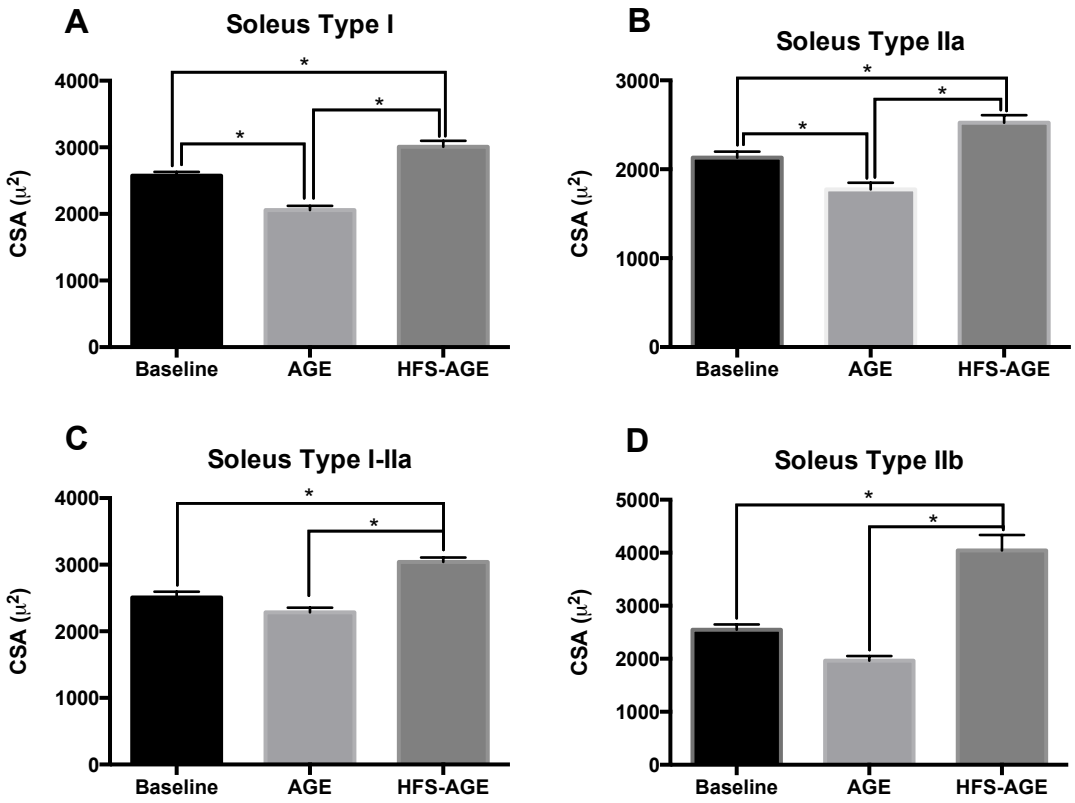

Figure 5.21. Soleus muscle fibre type CSA was measured for BSL (n=6), AGE (n=6), and HFS-AGE (n=6). Data are reported as mean±SE *, signifies significant differences among groups. (A) The type I fibres of the AGE group decreased from BSL ($p<0.0001$), while the HFS-AGE group had an increase in CSA compared to BSL ($p=0.0002$), with a difference between the AGE and HFS-AGE groups ($p<0.0001$). (B) The type IIa fibres of the AGE group decreased from BSL ($p=0.004$), while the HFS-AGE group had an increase in CSA compared to BSL ($p=0.001$), with a difference between the AGE and HFS-AGE groups ($p<0.0001$). (C) The hybrid type IIa-IIb fibres of the HFS-AGE group had an increase in CSA compared to the BSL group ($p<0.0001$) and the AGE group ($p<0.0001$). (D) The type IIb fibres of the HFS-AGE group had an increase in CSA compared to the BSL group ($p<0.0001$) and the AGE group ($p<0.0001$).

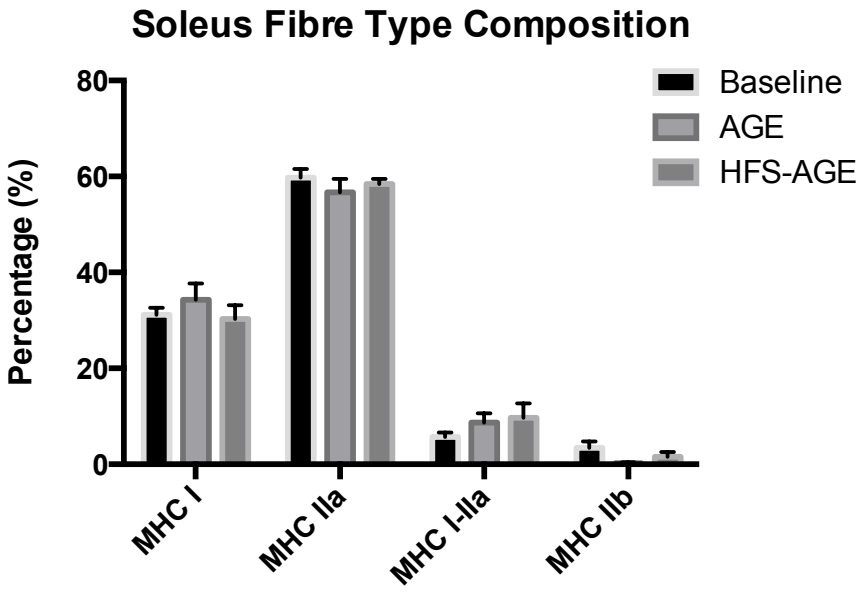

Figure 5.22. Soleus muscle fibre type composition was measured for the BSL (n=6), AGE (n=6), and HFS-AGE (n=6). There were no alterations in fibre the soleus fibre type composition.

EDL

EDL type IIa fibres for HFS-AGE were 23% smaller compared to AGE ($p<0.0001$) and 14% smaller compared to BSL group ($p=0.006$) (Figure 5.23.A). For EDL type IIa-IIx hybrid fibres, AGE had 24% larger fibres compared to BSL group ($p=0.01$) (Figure 5.23.B), whereas type IIx fibres in both AGE ($p=0.0005$) and HFS-AGE ($p=0.004$) were larger compared to BSL (18% and 16%, respectively) (Figure 5.23.C). The CSA of type IIx-IIb hybrid fibres were smaller for HFS-AGE compared to AGE (19% decrease, $p=0.02$) and BSL (28% decrease, $p<0.0001$) (Figure 5.23.D). The type IIb fibres followed the same trend with HFS-AGE having smaller fibres compared to AGE (11%, $p=0.04$) and BSL (14%, $p=0.004$) (Figure 5.23.E). For EDL fibre composition there was an increase in type IIx-IIb hybrid fibers ($p=0.02$) and decreased in type IIb fibres ($p=0.01$) for AGE compared to the BSL (Figure 5.24).

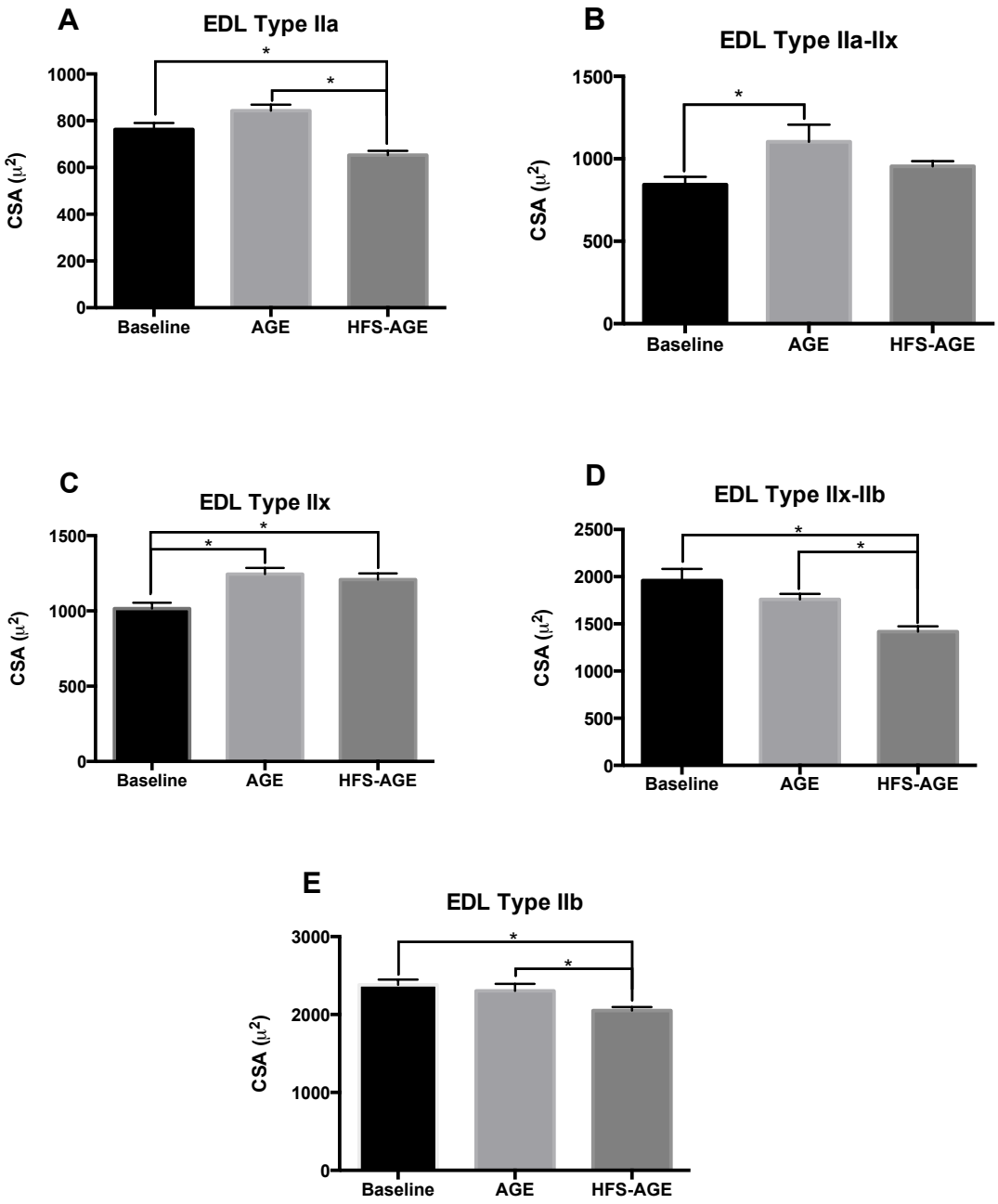

Figure 5.23. EDL muscle fibre type CSA was measured for the BSL (n=6), AGE (n=6), and HFS-AGE (n=6). Data are reported as mean±SE *, signifies significant differences among groups for each fibre type. (A) The type IIa fibres of the HFS-AGE group was smaller than both the BSL (p=0.006) and AGE groups (p<0.0001). (B) The type IIa-IIx hybrid fibres of the AGE group were larger than both the BSL groups (p<0.0001). (C) The type IIx fibres of both the AGE and HFS-AGE group were larger than the BSL group (p=0.0005 and p=0.004, respectively). (D) The type IIx-IIb hybrid fibres of the HFS-AGE group were smaller than both the BSL (p<0.0001) and AGE groups (p=0.02). (E) The type IIx fibres of the HFS-AGE group were smaller than both the BSL (p=0.004) and AGE groups (p=0.04).

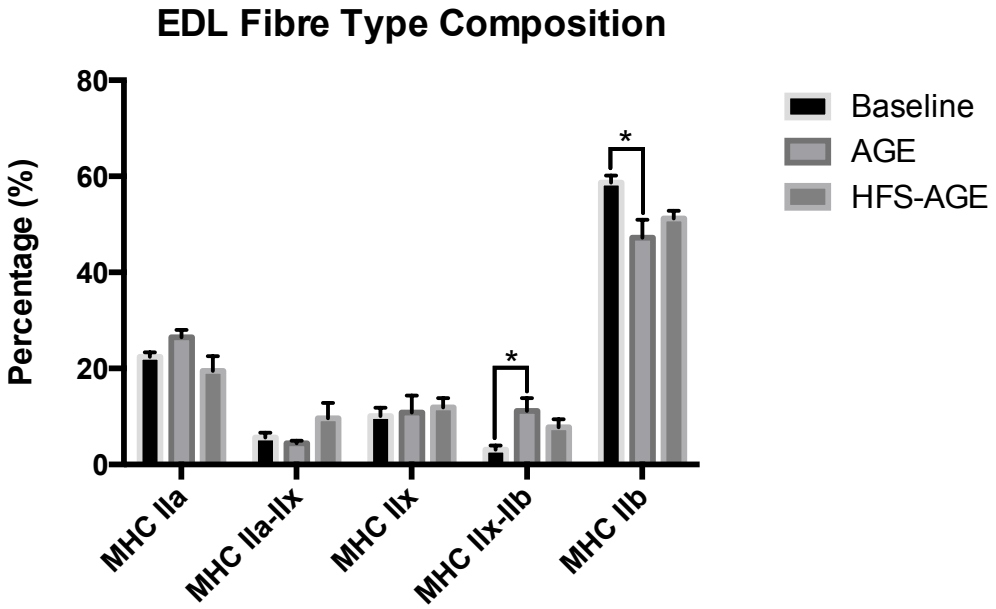

Figure 5.24. EDL muscle fibre type composition was measured for the BSL (n=6), AGE (n=6), and HFS-AGE (n=6). Data are reported as mean±SE *, signifies significant differences among groups for each fibre type. There was an increase the proportion of the type IIx-IIb hybrid fibres for the AGE group compared to BSL (p=0.02) and for the type IIb fibres for the AGE group compared to BSL (p=0.01).

Ratios of Outcomes of Bone and Muscle

Bone to Muscle Ratios Determined from Proximal Tibia and Soleus Measures

The proximal tibia BV/TV to soleus peak tetanus decreased by 36% in AGE ($p<0.05$) and 32% in HFS-AGE ($p<0.05$) compared to BSL (Figure 5.25.A). The proximal tibia BV/TV to soleus CSA ratio decreased by 41% for AGE ($p<0.01$) and 45% for HFS-AGE ($p<0.001$) compared to the BSL (Figure 5.25.B). There were no differences among groups for proximal tibia BMD to soleus peak tetanus (Figure 5.25.C). Finally, for the ratio of proximal tibia BMD to soleus CSA there was a decrease (28%) in HFS-AGE compared to BSL ($p<0.01$) and no difference compared to AGE ($p=0.07$) (Figure 5.25.D).

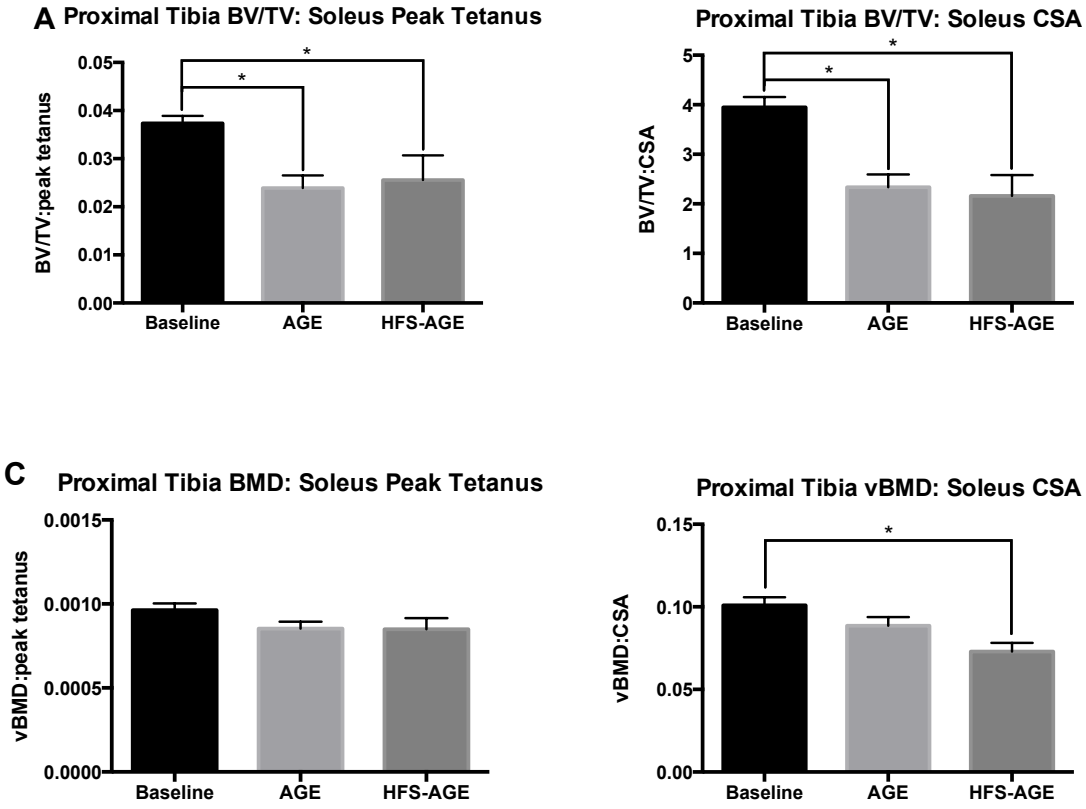

Figure 5.25. The ratio of the BV/TV and BMD of proximal tibia to the peak tetanus and CSA of soleus was analyzed, BSL (n= 10), AGE (n=10), and HFS-AGE (n=9. Data are reported as mean±SE *, signifies significant differences between groups. (A) The BV/TV to soleus peak tetanus ratio decreased for the both the AGE ($p=0.02$) and HFS-AGE ($p<0.05$) groups compared to the BSL group. (B) The BV/TV to soleus CSA ratio decreased for the both the AGE ($p<0.01$) and HFS-AGE ($p<0.001$) groups compared to the BSL group. (C) There were no differences between groups for the BMD to soleus peak tetanus ratio. (D) The HFS-AGE group had a lower BMD:CSA ratio compared to the BSL ($p<0.01$).

Bone to Muscle Ratios Determined from Proximal Tibia and EDL Measures

The ratio of proximal tibia BV/TV to the EDL peak tetanus decreased for AGE (46%, $p<0.01$) and HFS-AGE (41%, $p<0.05$) compared to BSL (Figure 5.26.A). The proximal tibia BV/TV to EDL CSA decreased for AGE (39%, $p<0.05$) compared to BSL (Figure 5.26.B). There was a decrease in the proximal tibia BMD to EDL peak tetanus ratio for

AGE compared to BSL ($p<0.05$) (Figure 5.26.C). As for the ratio of proximal tibia BMD to EDL CSA, there were no differences among groups (Figure 5.26.D).

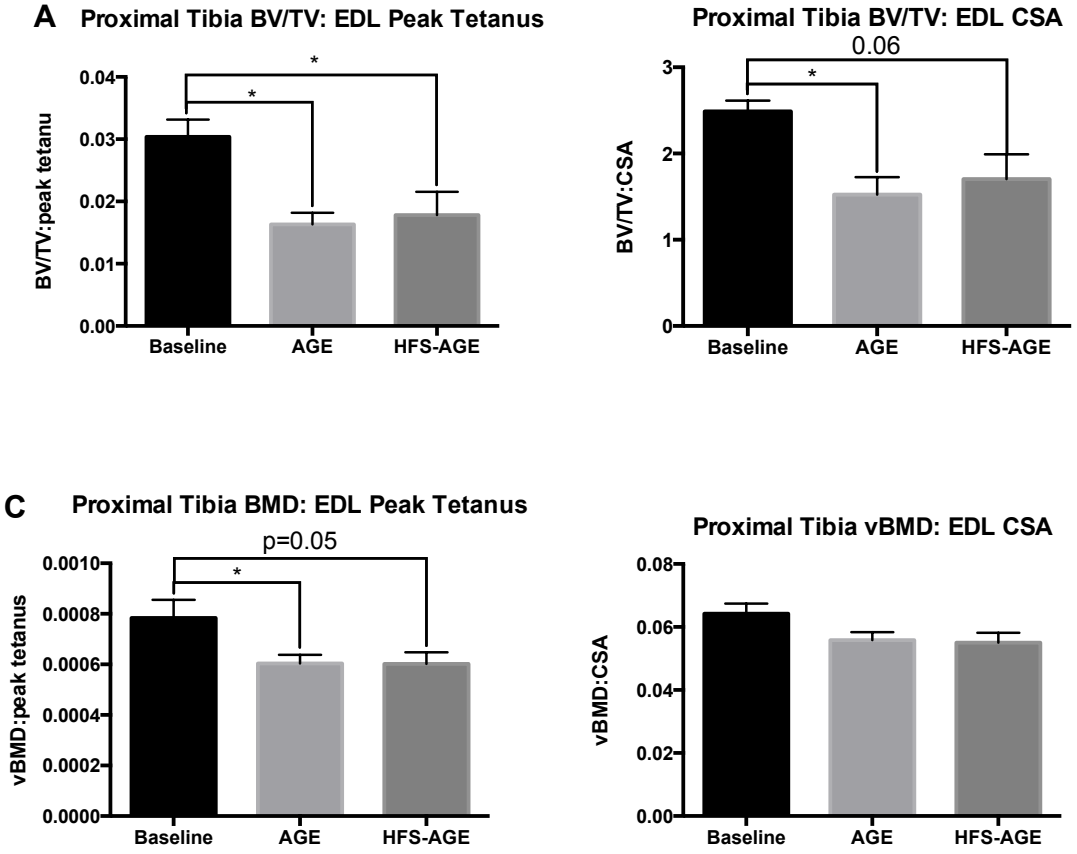

Figure 5.26. The ratio of the BV/TV and BMD of proximal tibia to the peak tetanus and CSA of EDL were calculated, BSL (n= 7), AGE (n=9), and HFS-AGE (n=9). Data are reported as mean±SE *, signifies significant differences between groups. (A) The BV/TV to EDL peak tetanus ratio decreased for the AGE ($p<0.01$) group compared to the BSL group. (B) The BV/TV to EDL CSA ratio decreased for the both the AGE ($p=0.02$) and HFS-AGE ($p=0.03$) groups compared to the BSL group. (C) The BMD to EDL peak tetanus ratio decreased for the AGE ($p<0.05$) compared to BSL group. (D) There were no differences among groups for BMD to EDL CSA.

Chapter 6: Discussion

Summary of Main Findings

The present study takes a novel approach to studying aging male C57BL/6J mice beginning a HFS during middle aged (20 weeks of age) and combining both bone (trabecular structure, BMD) and muscle (grip strength, muscle contractile function, fibre typing) measures to analyze the effects of aging superimposed with a HFS. This comprehensive set of measures allowed novel ratios of bone and muscle to be analyzed. In addition, careful attention to diet composition was an important aspect to this study. One of the main findings of this study was that bone, measured as trabecular architecture and vBMD, had similar declines with aging regardless of diet, and HFS superimposed with aging had no further detrimental effect. Importantly, although soleus muscle of HFS-AGE had a greater structure (CSA), this did not translate to better function (force production). Therefore, although there was greater hypertrophy in soleus from HFS-AGE, this greater muscle size did not have the same contractile function (when normalized to CSA) compared to BSL or AGE, indicating that HFS-AGE potentially had metabolic disturbances resulting in poorer muscle function. Finally, in contrast to human [9] and mouse studies [132] that used different measures from the current study, bone to muscle ratios (regardless of differences in diet) declined with age as a result of a non-coordinate decline between the two tissues, with bone (BV/TV) having a greater rate of decline than muscle (peak tetanus and CSA). However, using BMD for these ratios (as in earlier studies) suggested a more coordinate decline in this ratio as has been previously reported. Previously the majority of bone to muscle ratios with aging have been calculated in humans using areal BMD or bone CSA as the bone measure, with either an increase in this ratio, suggesting a greater decline in muscle than bone, or no change, as reviewed by

[9]. The present study highlights that incorporating measures of trabecular structure, using BV/TV as the bone measure, captures the non-coordinate decline of bone to muscle with aging that may otherwise go undetected by using BMD measures.

Mouse Characteristics

Male C57BL/6J mice were used since they are an accelerated model for studying the effects of aging on bone and muscle and their age-related declines mirror similar alterations in bone and muscle with aging as humans [15, 131]. Using this model allows for longitudinal studies with tightly controlled diets and terminal experiments that are not otherwise possible in humans, such as whole muscle dissection for muscle function and morphology.

HFS-AGE weighed more than AGE at the end of the 13-week diet intervention, which was expected since the HFS was more energy dense (4.6 kcal/g) than the control diet (3.6 kcal/g) resulting in an increased daily energy intake. In addition to this increased body weight, there was a shift in body composition with a decrease in lean mass and increase in fat mass in both groups, as expected this was more prominent in HFS-AGE compared to AGE. Therefore, AGE alone for 13 weeks caused a shift towards increased adiposity and decreased lean mass, even in the absence of a HFS, which mirrors changes in body composition in humans with aging [48]. Previously, alterations in body composition are associated with aging, with a continuous gain in fat mass over the lifespan in male C57BL/6J mice [98, 136]. As for diet-induced obesity, the shift in body composition has been well documented with similar experimental models using 12-week old male C57BL/6J mice (45% kcal fat lard and 173 g/kg sucrose for 11 weeks) [72], 9-month old male C57BL/6J mice (60% kcal fat lard and 68.8 g/kg sucrose for 14 months)

[120], 4-week old male C57BL/6J mice (58% kcal fat coconut oil and 360 g/kg sucrose for 16 weeks) [137], and adult male Wistar rats (45% kcal fat lard and 223 g/kg sucrose for 16 or 24 weeks) [118]. With respect to bone mass, AGE had an increase and HFS-AGE had a decrease in bone mass, but this does not necessarily confirm an alteration in total bone mass since body composition is measured as a relative percentage of total body mass. Therefore, it is suggested that these observed changes in body composition are likely because of a result of a loss in muscle mass and accumulation of fat mass with aging and diet-induced obesity [4]. The increase in absolute fat mass translates to an increase in the percentage fat mass and decrease in percentage lean mass as seen in the present study.

Structure and BMD of Proximal Tibia

Bone structure declined during the 13-week diet intervention for both AGE and HFS-AGE and this was due to decreased Tb.Th and Tb.N and increased Tb.Sp resulting in an overall decline in BV/TV. This indicates that aging is a main contributor to the decline in bone structure since a HFS intervention in middle age had no further effect. For BV/TV, Tb.Th, and Tb.N there was an initial decline followed by a maintenance period, however, for Tb.Sp there was an initial increase for both AGE and HFS-AGE, but a maintenance period for HFS-AGE group and a decrease in Tb.Sp for the AGE group from 24 to 33 weeks. Similarly, for BMD, there was an initial decline in both AGE and HFS-AGE groups, however there was a continued decline till the end of the study for both groups. For all proximal tibia measures there were no differences between AGE and HFS-AGE at any of the time points and both groups followed the same trend over time for all measures with the exception of Tb.Sp. These results were contrary to our hypothesis that AGE

group would have a steady decline in bone throughout the 13-week study, while HFS-AGE group would initially be protected from this age-related bone loss due to the increased body weight with a decline in bone at the end of study.

The decline in bone structure and BMD with aging was unsurprising since it is well established that there is a decline in bone structure and mass with aging [3, 98]. Previously this decline in bone with aging has been shown in male C57BL/6J mice with a continuous decrement from 1.5 to 24 months of age. This decline was a result of a decrease Tb.N and an increase in Tb.Sp resulting in a decrease in BV/TV, however, unlike the current study there was little change in Tb.Th with aging [94]. Similarly, longitudinal assessment of bone structure from 1 to 20 months of age in male C57BL/6J mice highlighted that peak BV/TV occurs between 6-8 weeks of age and there is a steady decline thereafter, characterized by a rapid loss in Tb.N from 2 to 6 months of age [98]. This may explain the rapid loss in proximal tibia from 20 to 24 weeks of age with a slower decline until 33 weeks of age in the present study. Interestingly, some studies report an increase in Tb.Th with aging using adult (5 months) and old (23 months) male rats [97] or measuring male C57BL/6J mice across the lifespan (1 to 20 months of age) [98], however for both studies this increase in Tb.Th was not enough to maintain overall bone structure, since there was still a decline in BV/TV. Therefore, it appears that Tb.Th contributes less to the overall decline in bone structure and it is Tb.N and Tb.Sp that consistently alter BV/TV with aging. Although the relationship between aging and decline in bone has been well established, the effect of aging superimposed with a HFS has not been well investigated. Beginning a HFS diet in mice during middle age is unique

to bone literature with most studies beginning during growth and development [81, 82, 84-86, 88] or young adulthood [72].

The effects of diet-induced obesity on bone is controversial, with some research suggesting that the increased mechanical load as a result of obesity has a positive effect in male C57BL/6J mice [72] or no effect in female C57BL/6J mice [89], while other research suggests a negative effect as a result of increased bone resorption in male C57BL/6J mice [81, 82, 84-88]. This discrepancy in the response of bone to diet-induced obesity may be explained by differences in the age at which diet interventions begin. Young rodent models (4 to 7 weeks of age) that have not yet reached their peak bone mass are adversely affected by diet-induced obesity regardless of the diet duration (1 to 18 months) [81, 82, 84-88]. Discrepancy in age and the effect of diet-induced obesity has specifically been tested with immature bone (5 weeks of age) compared to mature bone (20 weeks of age) being more adversely affected by a diet-induced obesity [85]. However, during young adulthood (12 weeks of age) once bone is fully matured but not yet undergoing age-related bone loss, it is suggested there can be a positive effect of diet-induced obesity on bone [72]. The similar loss of trabecular bone in both AGE and HFS-AGE in the present study suggests that diet-induced obesity has no positive effects inferred by the increased mechanical load and no further negative effects on middle age male C57BL/6J mice. Since the mice were fully matured they were not expected to experience the negative effects associated with diet-induced obesity during growth and development, but since they were older than the mice from the previous study that found positive effects of diet-induced obesity in young adult mice (12 weeks of age) [72] they were not expected to have positive effects on bone either. The increased mechanical load

inferred by increased body weight was not able to overcome the age-related decline in trabecular BMD or bone structure, however it also did not exacerbate the age-related bone loss as hypothesized.

Both with aging and a HFD the cellular activity of bone marrow is altered to favour differentiation of mesenchymal stems into adipocytes instead of osteoblasts [64, 91]. In addition to favouring adipocyte differentiation, osteocytes become dysfunctional with aging, resulting in a progressive inability to sense forces [105], therefore the increased mechanical load as a result of diet-induced obesity may not have the same positive effects seen with adult male C57/BL/6J mice (12 weeks of age) [72]. However, testing a lifelong HFD using male C5BL/6J mice (3 weeks of age) fed a life-time (18 months) high fat westernized diet highlighted greater decline in trabecular bone compared to age matched controls [88] suggesting the a greater detrimental effect of a HFD over the lifespan [88]. Our data suggests that diet-induced obesity does not accelerate the loss of bone with aging during adulthood as exemplified by the same rate of trabecular bone loss in both the AGE and HFS-AGE groups. Previously, it had been hypothesized that diet-induced obesity works in two opposing phases, which includes an initial beneficial phase and a second phase that is detrimental with a lower bone formation rates [72]. This lead to our hypothesis that a HFS superimposed with aging would maintain bone structure and BMD for longer before age-related bone loss occurred, with potentially an increased detrimental effect of a HFS on bone as a result of alterations in cellular activity related to bone remodeling. Based on our results it appears that either the mice were at an age where there was no positive effect of the HFS on bone, but not old enough or on the HFS long enough for an additive detrimental effect with a HFS. Or, since the mice began the

HFS during middle age they may not have accumulated the negative effects associated with a HFS and bone.

Grip Strength

Grip strength was used as a functional *in vivo* measure of muscle strength, however there was no differences between the AGE and HFS-AGE groups at any of the time points. There was a steady decline in four limb grip strength in both AGE and HFS-AGE groups over the duration of intervention. It was difficult to achieve consistent measures for grip strength testing since there were issues with motivation to grip either the T-bar or grid with the mice, as a result measures two standard deviations above or below the mean were removed as outliers. Similar to our results a study comparing male C57BL/6J mice at 4 months, 18 months, and 24 months of age there were no changes in front limb grip strength [138], however, this study did not include aging superimposed with a HFD. In contrast to our front limb results but similar to four limb results, superimposing both aging and a HFD (60% kcal fat lard, 69 g/kg sucrose), using 8-month old male C57BL/6J mice, there was a significant decline in grip strength with a 5-month HFD compared to age matched controls [120]. This discrepancy could be a result of greater difficulties with the mice gripping the T-bar for front limb testing than the grid for four limb testing.

Muscle Contractile Function

This study investigated the effects of a long-term HFS on muscle function superimposed with aging, and it was hypothesized that high fat feeding would exacerbate the decline in muscle function associated with aging. Although it has been well established that there is a decline in muscle mass and strength with aging, the

combination of aging superimposed with a HFS and its effects on muscle function has not been well studied.

Soleus

Soleus muscle size was measured by CSA, which was greater when a HFS was superimposed with aging and there was a trend towards a larger soleus muscle even compared to younger baseline mice. However in contrast to our result, a study using middle aged male C57BL/6J mice (8-months of age) fed either a HFD or control diet for 5 months, resulted in soleus atrophy only for the HFD group [120]. Lee et al, suggested that the soleus was more susceptible to the catabolic effects of a HFD since other muscle of fast/mixed fibre composition had similar rates of atrophy with aging regardless of diet [120]. This discrepancy may be due to differences in starting age, diet composition (e.g. source of fat, sucrose, adjusted vitamins and minerals), diet duration, and the interpretation of atrophy from soleus wet weight. [118]. However, our data suggests a different theory, since soleus is a postural muscle this greater CSA in HFS-AGE may be a result of the increase in body weight that would stress the soleus with ambulatory activity around the cage. This greater soleus CSA of the HFS-AGE was as a result of greater CSA of all the fibre types (I, IIa, I-IIa, IIb), which is in good agreement with previous work that reported greater CSA for soleus type I and IIa fibres with a HFD in 10 week old male C57BL/6J mice on a 60% HFD for 8 weeks [117]. The soleus CSA of the AGE did not differ from BSL, which was unexpected, and this may again be explained by differences in the starting age of our mice. However, immunohistochemistry showed that the AGE group had a decrease in type I and IIa fibres CSA, with no decrease for type I-IIa hybrid or IIb fibres CSA. These differences may be due to the cruder CSA measure compared to

the more sensitive muscle fibre type CSA or these changes in fibre CSA did not translate into a significant loss in whole muscle CSA in the time frame of our study. In contrast, a previous study using 6-month old male C57BL/6J mice reported no age-related decline in soleus fibre CSA, however this was not fibre type specific, and therefore specific fibre changes were likely missed [139].

There was no alteration or shift in fibre type composition for soleus muscle among any of the groups. However, results from previous studies have been mixed, with no alteration in soleus type I or IIa fibres [117] or a significant decrease in type I fibres and no alteration in type IIa fibres with a HFD [121]. There is also a suggested shift in fibre type with aging, results from previous studies are contradictory with some results suggesting a shift towards type I fibres, others suggesting a shift towards type II, and many studies with ambiguous results, leaving the shift in fibre type with aging an unresolved research question [15]. Factors that contribute to the ambiguity in the literature include rodent strain, age, and gender, as well as staining techniques (immunohistochemistry that stains MHC isoforms or H&E staining) and measures of muscle size (mass or CSA).

Although HFS-AGE had a larger CSA, this was not accompanied by increased muscle contractile function. Soleus twitch and tetanus force normalized to CSA was not altered between any of the groups, which is in line with previous results in younger male C57BL/6J mice (10 weeks of age) that found no change in relative force pre- and post-fatigue with a HFD compared to a control group [117]. In addition, a study using both lard and palm oil as a fat source for a HFD (5 weeks) found only a decrease in peak twitch and tetanus force for palm oil, but not for lard in 12 week old male C57BL/6J mice

[116]. This differing effect of lard and palm oil may be due to differences in fatty acid composition with palm oil having greater palmitic acid (a saturated fat) than lard. Even though the mice used in these previous studies were young, the lack of muscle function decline in the middle aged animals used in the present study suggests that soleus muscle function declines at a later age. Although there were no differences among any of the groups for twitch or tetanus rate of force development there was a decreased tetanus rate of relaxation in AGE and HFS-AGE compared to BSL. Interestingly, there was an increase in twitch half relaxation in AGE and HFS-AGE compared to BSL, but no differences among groups for the tetanus half relaxation time, which has previously been shown with no alteration in twitch or tetanus half relaxation time with a HFD using lard as the fat source [116]. The contrast between the rate of relaxation and half relaxation time can be attributed to the differences in the measures, since rate of relaxation takes an average of the whole relaxation phase, while half relaxation is only a snapshot of muscle relaxation. Since Ca^{2+} handling determines relaxation, alterations in relaxation time suggest impaired Ca^{2+} uptake into the sarcoplasmic reticulum [116]. There was no shift in the force-frequency curves, which means that soleus force production was unaltered by aging or HFS across a span of frequencies. Previously, no differences in pre-fatigue force-frequency with a HFD have been reported, but post-fatigue there was a shift in the force-frequency curve resulting in less relative force at the same frequency in fatigued muscle [117]. No alteration in force-frequency with aging alone has also been reported in female mice across the lifespan [140], but in aged (26-27 month) male C57BL/6J mice greater force was produced at submaximal frequencies (10, 20, 30 Hz) compared to young (2-3 month) and middle aged (9-10 month) mice [114]. Finally, there was no

alteration in the maximum shortening velocity among any of the groups, but this was an unloaded shortening velocity therefore it only measured the ability of the fastest fibres to uptake slack. Since there was no major alteration in fibre type composition it is expected that there would be no change in the maximum shortening velocity.

EDL

As expected EDL muscle size measured by CSA decreased with aging, however superimposing a HFD with aging resulted in no alteration in CSA compared to younger baseline mice, suggesting that HFD reduced age related muscle wasting. Previously, middle aged mice (8 months of age) on either a 5 month HFD (60% kcal fat, lard) or control diet displayed similar decreases in muscle weight in mixed gastrocnemius, a mixed fast-twitch muscle, regardless of diet [120], whereas, our results suggest only atrophy of EDL with a control diet but not a HFD. This suggests that, like soleus, EDL of HFS-AGE was loaded more because of the increased body weight, slowing the rate of age-related muscle loss resulting in no differences in the EDL CSA between HFS-AGE and BSL. The only alteration in EDL fibre type composition was an increase in type IIx-IIb hybrid fibres and a decrease in type IIb fibres in AGE compared to BSL, suggesting a potential shift towards more oxidative fibres with aging. Interestingly this shift towards oxidative fibres in gastrocnemius/plantaris muscles, seen as an increase in type IIa fibres and a decrease in type IIb fibres, has been reported in male C57BL/6J mice (10 weeks of age) fed a 8 week HFD (60% kcal fat, lard), but not for their age matched counterparts fed a control diet [117]. Therefore, the effects of diet-induced obesity in aging mice are not only muscle fibre type specific but also potentially also age-specific since the animals

used in this study were mature adults compared to previous studies that have used young animals.

Unexpectedly, the individual fibre type CSA data did not support the alterations in whole muscle EDL CSA for AGE and lack of alteration for HFS-AGE group compared to BSL. The type IIa fibre CSA decreased in HFS-AGE, while AGE maintained its type IIa fibre CSA compared to BSL. Interestingly, the type IIa-IIx hybrid fibre CSA were much larger in AGE compared to both BSL and HFS-AGE while the type IIx fibre CSA increased in both AGE and HFS-AGE compared to BSL. The type IIx-IIb hybrid and type IIb fibres both followed the same pattern with a decrease in CSA in HFS-AGE compared to BSL and AGE. As mentioned above, it has previously been reported that there is no alteration in gastrocnemius muscle wet weight with a HFD, however in contrast to our results this study also found a decrease in gastrocnemius fibre CSA with a HFD but not aging [120]. In a study using young male C57BL/6J mice (10 weeks of age) there was no alteration in any fibre CSA for faster-twitch gastrocnemius/plantaris muscles for either a 8-week HFD or control diet [117]. This discrepancy between muscle CSA or wet weight with fibre specific CSA may be due to overall decreases in fibre number and not fibre CSA, since not every muscle fibre CSA is measured. It is important to note that muscle wet weight and CSA, which is calculated using muscle wet weight, are less accurate measures of alterations in muscle morphology since muscle is composed of many components including contractile proteins, collagen, lipids, and water, whereas fibre CSA is a more direct measure of muscle morphology. Therefore, the decrease in EDL CSA was not as a result of a decrease in fibre CSA and discrepancies with other studies may be due to the comparison of EDL to the

gastrocnemius and plantaris muscles, even though they are both hind limb fast-glycolytic muscles like EDL. Both the gastrocnemius and plantaris muscles have a greater composition of type IIx fibres and less type IIb fibres compared to the EDL [110].

EDL peak twitch force and twitch rate of force development was greater in AGE and HFS-AGE compared to BSL, suggesting improved muscle function with aging or HFS. This is in contrast to previous research that demonstrated EDL peak tetanus force did not improve from young (2-3 months) to adult (9-10 months) male C57BL/6J mice [114]. The discrepancy may be explained by experimenter inexperience at the time of baseline experiments, with EDL peak tetanus <200mN being considered unviable. As for peak tetanus force and tetanus rate of force development there were no differences among any of the groups. As for rate of relaxation both AGE and HFS-AGE had a lower rate of relaxation compared to BSL for both twitch and the tetanus, but no alteration in half relaxation time for twitch or tetanus. In contrast to our results, 12-week old male C57BL/6J mice on a 5-week high fat (45% kcal, lard or palm oil) and sucrose (173 g/kg) resulting in diet-induced obesity did not have any alterations in twitch or tetanus peak force or contraction time, but there was an increase in twitch relaxation time but not tetanus relaxation time with a HFD [116]. The difference in the age of the animals and duration of the diets would explain these differential results, suggesting that the older animals used in this study on the longer duration HFS have greater detriments in muscle function. In addition, it is possible that EDL BSL measures had methodological errors, since there was a lack of experience performing muscle function experiments there were difficulties with EDL *in vitro* testing resulting in low force production (muscle with a peak tetanus <200 mN were removed). Therefore, future work will require ordering

another set of age-matched BSL animals to repeat some of these measures and reconcile these issues.

Although there was no shift in maximum unloaded shortening velocity, there was a leftward shift in the EDL force-frequency curve for AGE and HFS-AGE, meaning that in these groups a greater force is generated at lower frequencies of stimulation. This is consistent with our observation that AGE and HFS-AGE produced greater twitch force, but not tetanus force. An increase in relative force at lower frequencies has been reported post-fatigue, but not pre-fatigue with a 8 week HFD in 10-week old male C57BL/6J mice [117], for aged female C57BL/6J mice (27-28.5 months) [140], and aged (26-27 months) male C57BL/6J mice [114]. Therefore, aging causes a shift in the force-frequency curve pre-fatigue, but it is unknown how aging would shift the force-frequency curve post fatigue.

Ratios of Outcomes of Bone and Muscle

Since aging is associated with both a loss in BMD and strength, referred to as osteoporosis, and a loss in muscle mass and strength, referred to as sarcopenia, it is important to study both these tissues together. The mechanical relationship between bone and muscle, specifically the force exerted from muscle contraction on bone, is suggested to regulate BMD and strength to muscle forces. It is Wolff's law that describes bone plasticity and how bone changes its shape and structure to match mechanical loads [141] and the mechanostat theory states that muscle is a primary source of mechanical loading on bone [12, 130]. The association of muscle CSA of the forearm and radius bone size supports this relationship, which is a non-weight bearing site in humans and the association between muscle CSA and bone size is stronger than that of body weight or fat

mass [9]. Since there is an established mechanical relationship between bone and muscle, it is suggested that there is a ratio of bone to muscle properties including size and strength. These ratios have been investigated in humans using BMD or bone CSA to muscle force, muscle CSA, or lean mass (arm or leg), with many studies finding an increase or no change in this ratio with aging (reviewed in [9]). Similarly, comparing male C57BL/10 mice at 7 week and 24 month of age, there was no alteration in the bone to muscle ratio with aging, measured as tibia mid-diaphysis ultimate load to EDL peak tetanus force normalized to muscle CSA [132]. However, there is limited research studying this relationship in animal models, with other studies examining the effects of estradiol [142] or running and estradiol [143]. Together, these findings suggest no alteration in the bone-to-muscle ratio and have been used as evidence of a coordinate decline in these two tissues with aging.

The ratio of bone-to-muscle measures in this study suggested little to no alterations in this ratio when BMD to either peak tetanus or CSA for both soleus and EDL were used, which fits with previous literature [9, 132]. However, when BV/TV to both peak tetanus or CSA for both soleus and EDL are used, there is a decrease in the bone-to-muscle ratio with aging regardless of diet. Previously, the bone-to-muscle ratio, measured using peak isometric force (EDL) to bone strength (ultimate load of tibia mid-diaphysis), has shown no alteration with aging, comparing 7 week and 24 months old wild-type C57BL/10 male mice [132]. Although this study reported no alteration in the ratio of bone-to-muscle, using bone strength testing only measures the cortical bone and not trabecular bone, and therefore our results highlight the differences in measures used to calculate this ratio, BMD versus BV/TV.

Strengths

The primary goal of this study was to investigate how bone and muscle structure and function are affected by aging superimposed with a HFS. To achieve this goal, mice from the same batch were ordered in to reduce any variations among the animals since there were endpoint surgeries at BSL and following the 13-week intervention. Modeling the HFS from the standard AIN93-M diet ensured that the diets were as similar as possible; the lard used for the HFS diet was also tested for vitamin D content to adjust diets accordingly. In addition, micronutrients (e.g., calcium, phosphate, and vitamin D) were matched for energy since the HFS had a higher energy level by weight, to isolate the effects of diet-induced obesity. Aside from the HFS, the AIN93M diet was used as the control diet instead of standard chow since it is a semi purified diet with consistent composition. Food intake and body weight were tightly tracked by taking these measures three times a week to reduce variations in this measure. The major strength of this study was the combination of analyzing bone and muscle simultaneously with the superimposition of aging and diet-induced obesity, since these tissues have traditionally been studied separately. The longitudinal *in vivo* measurements of bone structure, vBMD, and body composition were measured in the same mouse throughout the study, reducing variation and allowing for direct determination of changes during the life-course studied. As well, using μCT for these measures allowed for very precise bone measures. The combination of grip strength and excised muscle contractile function provided both a functional measure of neuromuscular strength and contractile properties, respectively. Muscle immunohistochemistry provided explanation for alterations in muscle contractile function. This comprehensive set of bone and muscle measures allowed for a thorough

analysis of alterations in bone and muscle with aging and aging superimposed with a HFS.

Limitations

Since the mice used in this study were fully matured, alterations in bone were most likely less substantial compared to that of immature growing mice. As a result, a longer diet intervention or beginning the diet at a younger age may have highlighted differences between aging and aging superimposed with a HFD. Another limitation was an issue with the μCT during scanning, which resulted in the 8-week scans being removed from the data set. As for muscle function testing there were difficulties with the EDL *in vitro* testing system and the experimenter was inexperienced at the time of baseline experiments resulting in greater variability in the measures in this group. In addition, grip strength testing was a new measure within the lab and the measure was very variable as a result of the mice not gripping either the T-bar or grid. Mineral apposition rate was not included in this thesis, which would provide a snapshot of the rate of bone formation and resorption. Future studies should study both sexes to better understand how aging and aging superimposed with diet-induced obesity affects the musculoskeletal system since male and females have different hormonal responses especially with aging.

Conclusions

Hypothesis 1: The aging group will have a steady decline in bone structure and BMD throughout the 13-week study, while the group fed obesogenic diet (HFS-AGE) will initially be protected from the age-related bone loss due to increased body weight, but would have an exacerbated decline in bone structure and BMD at older ages.

Consistent with the hypothesis, aging resulted in a steady decline in bone structure and BMD throughout the 13-week study. However contrary to the hypothesis a HFS superimposed with aging did not protect adult male mice from age-related bone loss at the beginning of the study and also did not result in an exacerbated decline in bone structure or BMD by the end of 13-week diet intervention. Therefore, adult male mice beginning a long-term HFS at 20-weeks of age undergo age-related bone loss at the same rate as age matched controls. At first glance this does not appear consistent with the hypothesized inverted 'U' shape curve, however the mice did not experience any positive effects with the HFS since they were older adults at 20-weeks of age. But, they also did not have an exacerbated decline in bone structure and BMD as expected, perhaps because they were not aged out on the HFS long enough. Therefore, this data expands what is currently known about the inverted 'U' shape hypothesis, as it appears that there is a neutral period during which a HFS does not have either a positive or a negative effect on bone structure and BMD.

Hypothesis 2: The aging group would have a decline in muscle function compared to the baseline group, while the HFS superimposed with aging group would have an exacerbated decline in muscle function associated with aging as a result of disruptions in muscle signaling. Specifically, the soleus force production and EDL relaxation time would be negatively impacted by the HFS.

Soleus and EDL differentially responded to aging and aging superimposed with a HFS. Soleus muscle had hypertrophy with a HFS, which could be an adaptation to the increase in body weight since it is a postural muscle, whereas EDL did not have any hypertrophy but also did not undergo muscle wasting with a HFS during aging. Contrary

to the hypothesis soleus rate of relaxation and half relaxation time but not force generation was negatively impacted with aging and aging superimposed with a HFS, whereas EDL had slower rate of relaxation and improvements in force generation and rate of force production, which is most likely a result of issues during baseline measures.

Hypothesis 3: The ratio of bone to muscle will be constant in the aging group, indicating that these two tissues decline in a coordinate manner. Although the ratio of bone to muscle will also remain constant in the high fat diet superimposed on aging group, this would be a result of both the bone and muscle structure and function being negatively affected to a similar extent by a high fat diet in aging animals.

The present study found that bone and muscle do not decline at the same rate with aging regardless of diet in adult male C57BL/6J mice, which was a result of a greater decline in bone structure than muscle function or size. This was supported by the ratios of BV/TV to both peak tetanus or muscle CSA, however relationship did not hold when BMD was used as the bone measure, reinforcing that BV/TV is a more sensitive measure that captures alteration in bone that would otherwise potentially be missed just using BMD.

Significance

The two greatest aspects affecting musculoskeletal health are aging and the obesity epidemic, which makes it an integral area of research to understand the effects of this dichotomy. This study was a comprehensive investigation of bone (bone structure, and BMD) and muscle (functional contractile strength, contractile properties, and fibre type) to study the ratio of change between bone and muscle quality and quantity with aging superimposed with a HFS. Our data suggests that bone declines at a greater rate

than muscle regardless of diet or the lack of alteration in the mechanical influence of muscle contraction on bone. Based on our results and the literature this indicates that the timing of diet intervention is integral, with less positive effects observed during growth and development, positive effects during young adulthood, and a lack alteration in the rate of decline bone during later adulthood in male C57BL/6J mice as observed in the present study.

Future Directions

Further analysis will be completed for bone histology to measure the mineral apposition rate. This analysis will provide information on the rate of bone formation and resorption as an indirect measure of osteoblast and osteoclast activity at the end of the 13 weeks. Future studies should continue to explore the relationship between bone and muscle across the lifespan with obesogenic diet interventions. This is important for expanding research investigating critical time points for nutrition and how the musculoskeletal system is affected. Since muscle and bone is integrally linked it is critical to study these tissues in conjunction

To explore this relationship a life-long HFS into senescence should be used, terminating animals in varying life stages (e.g. 6 weeks, 20 weeks, 34 weeks, 48 weeks, and 62 weeks). Using magnetic resonance imaging both bone and muscle can be measured longitudinally to track bone structure, muscle CSA, and body composition, along with BMD using dual energy X-ray absorptiometry at 2-week increments. Mineral apposition rate would also be measured by injecting calcein and alizarin markers 7 and 2 days prior to euthanasia. Muscle function testing measures would include peak twitch force, peak tetanus force, rate of force development, rate of relaxation, half relaxation

time, and force-velocity curve (which was missing from the current investigation). Fibre type would also be analyzed to track alterations in fibre composition and fibre CSA. Again a focus would be on the ratio of bone-to-muscle using both BV/TV and BMD as bone measures and peak tetanus and CSA as muscle measures. This study would help to better understand the hypothesized inverted 'U' associated with a HFS on bone and incorporate muscle function to associate mechanical load with alterations in bone. A follow up study to extending a HFS over the lifespan would be to begin a high fat diet at different stages of life (e.g. 6 weeks, 20 weeks, 34 weeks, 48 weeks) with measures mentioned above. The combination of these two studies would address the discrepancies in the literature. Future work should also investigate how animal models mimic aging and aging superimposed with HFS in humans in both bone and muscle to better interpret findings from previous research.

References

1. Zheltoukhova, K., L. O'Dea, and B. Stephen, *Taking the strain: The impact of musculoskeletal disorders on work and home lifeq.* The Work Foundation part of Lancaster University, 2012: p. 1-60.
2. *The burden of musculoskeletal conditions.* World Health Organization, 2003.
3. Boskey, A.L. and R. Coleman, *Aging and Bone.* Critical Reviews in Oral Biology and Medicine, 2010. **89**(12): p. 1333-1348.
4. Goodpaster, B.H., et al., *The loss of skeletal muscle strength, mass and quality in older adults:The health, aging and body composition study.* J Gerontol A Biol Sci Med Sci, 2006. **61**(10): p. 1059-1064.
5. *Life with arthritis in Canada: A personal and public health challenge*, P.H.A.o. Canada, Editor. 2010.
6. Cordain, L., et al., *Origins and evolution of the Western diet- health implications for the 21st century.* Am J Clin Nutr, 2005. **81**: p. 341-354.
7. *Obesity in Canada.* Public Health Agency of Canada & Canadian Insitute for Health Information, 2011.
8. Bonewald, L.F., et al., *Forum on bone and skeletal muscle interactions: summary of the proceedings of an ASBMR workshop.* J Bone Miner Res, 2013. **28**(9): p. 1857-65.
9. Novotny, S.A., G.L. Warren, and M.W. Hamrick, *Aging and the muscle-bone relationship.* Physiology, 2015. **30**(1): p. 8-16.
10. Hamrick, M.W., *The skeletal muscle secretome: an emerging player in muscle-bone crosstalk.* Bonekey Rep, 2012. **1**: p. 60.
11. Hamrick, M.W., *A role for myokines in muscle-bone interactions.* Exerc Sport Sci Rev, 2011. **39**(1): p. 43-7.
12. Frost, H.M., *Bone "mass" and the "mechanostat": A proposal.* The Anatomical Record, 1987. **219**(1): p. 1-9.
13. *Canada's population estimates- Age and sex, July 1, 2015.* Statistics Canada, 2015: p. 1-6.
14. Chan, K.G. and G. Duque, *Age-related bone loss: Old bones, new facts.* Gerontology, 2002. **48**: p. 62-71.
15. Ballak, S.B., et al., *Aging related changes in determinants of muscle force generating capacity: a comparison of muscle aging in men and male rodents.* Ageing Res Rev, 2014. **14**: p. 43-55.
16. Faulkner, J.A., S.V. Brooks, and Z. Eileen, *Chapter 9: Skeletal muscle weakness and fatigue in old age: Underlying mechanisms*, in *Special Focus on the Biology of Aging*. 1991, Springer: Berlin Heidelberg. p. 147-166.
17. Cao, J.J., *Effects of obesity on bone metabolism.* J Orthop Surg Res, 2011. **6**: p. 30.
18. Compston, J., *Obesity and bone.* Curr Osteoporos Rep, 2013. **11**(1): p. 30-5.
19. Reid, I.R., *Fat and bone.* Arch Biochem Biophys, 2010. **503**(1): p. 20-7.
20. Bosma, M., et al., *Re-evaluating lipotoxic triggers in skeletal muscle: relating intramyocellular lipid metabolism to insulin sensitivity.* Prog Lipid Res, 2012. **51**(1): p. 36-49.
21. Seeman, E. and P.D. Delmas, *Bone quality - The material and structural basis of bone strength and fragility.* The New England Journal of Medicine, 2006: p. 2250-2261.

22. Currey, J.D., *Chapter 1- The structure of bone tissue*, in *Bones: Structures and Mechanics*. 2002, Princeton University Press: Princeton, NJ.
23. Bouxsein, M.L., et al., *Guidelines for assessment of bone microstructure in rodents using micro-computed tomography.* J Bone Miner Res, 2010. **25**(7): p. 1468-86.
24. Felsenberg, D. and S. Boonen, *The bone quality framework: determinants of bone strength and their interrelationships, and implications for osteoporosis management.* Clin Ther, 2005. **27**(1): p. 1-11.
25. Buckwalter, J.A., et al., *Bone Biology.* The journal of Bone and Joint Surgery, 1995. **77**: p. 1256-1275.
26. Heaney, R.P., et al., *Peak bone mass.* Osteoporos International, 2000. **11**: p. 985-1009.
27. Dodington, D.W. and W.E. Ward, *Chapter 5: Osteoporosis* in *Diet, Exercise, and Chronic Disease: The Biological Basis of Prevention*. 2014, CRC Press: Boca Raton, FL.
28. Collins, S., et al., *Genetic vulnerability to diet-induced obesity in the C57BL/6J mouse: physiological and molecular characteristics.* Physiol Behav, 2004. **81**(2): p. 243-8.
29. Ward, W.E., et al., *Chapter 21: Functional foods and bone health: Where are we at?*, in *Functional Food Product Developmeent*. 2010, Wiley-Blackwell: Oxford, UK.
30. Ilich, J.Z. and J.E. Kerstetter, *Nutrition in Bone Health Revisited: A Story Beyond Calcium.* Journal of the American College of Nutrition, 2000. **19**(6): p. 715-737.
31. Watkins, B.A., Lippman, H. E., Bouteiller, L. L., Li, Y., Seifert, M. F., *Bioactive fatty acid: role in bone biology and bone cell function.* Progress in Lipid Research, 2001. **40**: p. 125-148.
32. Ahmadieh, H. and A. Arabi, *Vitamins and bone health: beyond calcium and vitamin D.* Nutr Rev, 2011. **69**(10): p. 584-98.
33. Palacios, C., *The role of nutrients in bone health, from A to Z.* Crit Rev Food Sci Nutr, 2006. **46**(8): p. 621-8.
34. Bonjour, J.-P., *Dietary Protein: An Essential Nutrient For Bone Health.* Journal of the American College of Nutrition, 2005. **24**(sup6): p. 526S-536S.
35. Rizzoli, R. and J.P. Bonjour, *Dietary protein and bone health.* J Bone Miner Res, 2004. **19**(4): p. 527-31.
36. Bonjour, J., *Review: Calcium and phosphate: A duet of ions playing for bone health.* Journal of the American College of Nutrition, 2011. **30**(5): p. 438S-448S.
37. Peterson, C.A., J.A.C. Eureli, and J.W. Erdman, *Alterations in calcium intake on peak bone mass in the female rat.* Journal of Bone and Mineral Research, 1995. **10**(1): p. 81-95.
38. Vatanparast, H., et al., *Positive effects of vegetable and fruit consumption and calcium intake on bone mineral accrual in boys during growth from childhood to adolescence: the University of Saskatchewan Pediatric Bone Mineral Accrual Study.* American Journal of Nutrition, 2005. **82**: p. 700-706.
39. Zhu, K., et al., *Growth and bone mineral accretion during puberty in Chinese girls: a five-year longitudinal study.* J Bone Miner Res, 2008. **23**(2): p. 167-72.

40. Schapira, G., et al., *Calcium and vitamin D enriched diets increase and preserve vertebral mineral content in aging laboratory rats.* Bone, 1995. **16**(5): p. 575-582.
41. Dawson-Hughes, B., Harris, S. S., E.A. Krall, and G. Dallal, *Effect of calcium and vitamin D supplementation on bone density in men and women 65 years of age or older.* The New England Journal of Medicine, 1997. **337**: p. 670-676.
42. Tang, B.M.P., et al., *Use of calcium or calcium in combination with vitamin D supplementation to prevent fractures and bone loss in people aged 50 years and older: a meta-analysis.* The Lancet, 2007. **370**(9588): p. 657-666.
43. Mozar, A., et al., *High extracellular inorganic phosphate concentration inhibits RANK-RANKL signaling in osteoclast-like cells.* J Cell Physiol, 2008. **215**(1): p. 47-54.
44. Kanatani, M., et al., *Effect of high phosphate concentration on osteoclast differentiation as well as bone-resorbing activity.* J Cell Physiol, 2003. **196**(1): p. 180-9.
45. Marie, P.J., *The calcium-sensing receptor in bone cells: a potential therapeutic target in osteoporosis.* Bone, 2010. **46**(3): p. 571-6.
46. Bikle, D.D., *Vitamin D and bone.* Curr Osteoporos Rep, 2012. **10**(2): p. 151-9.
47. Lips, P., *Vitamin D deficiency and secondary hyperparathyroidism in the elderly-consequences for bone loss and fractures and therapeutic implications.* Endocrine Reviews, 2001. **22**(4): p. 477-501.
48. Visser, M. and T.B. Harris, *Body Composition and Aging.* 2012: p. 275-292.
49. Wortsman, J., et al., *Decreased bioavailability of vitamin D in obesity.* American Journal of Clinical Nutrition, 2000. **72**: p. 690-693.
50. Bell, N.H., et al., *Evidence for alteration of vitamin D endocrine system in obese subjects.* Journal of Clincal Investigation, 1985. **76**: p. 370-373.
51. Liel, Y., et al., *Low circulating vitamin D in obesity.* Calcified Tissue Inernational, 1988. **43**: p. 199-201.
52. Compston, J.E., et al., *Vitamin D status and bone histomorphometry in gross obesity.* The American Journal of Clinical Nutrittion, 1981. **34**: p. 2359-2363.
53. Bourrin, S., et al., *Dietary protein deficiency induces osteoporosis in aged male rats.* Journal of Bone and Mineral Research, 2000. **15**(8): p. 1555-1563.
54. Schmitz, G. and J. Ecker, *The opposing effects of n-3 and n-6 fatty acids.* Prog Lipid Res, 2008. **47**(2): p. 147-55.
55. Weiler, H.A., et al., *Percent body fat and bone mass in healthy Canadian females 10 to 19 years of age.* Bone, 2000. **27**(2): p. 203-207.
56. Robling, A.G., A.B. Castillo, and C.H. Turner, *Biomechanical and Molecular Regulation of Bone Remodeling.* Annual Review of Biomedical Engineering, 2006. **8**: p. 455-498.
57. Manolagas, S.C. and R.L. Jilka, *Bone marrow, cytokines, and bone remodeling: Emerging insights into the pathophysiology of osteoporosis.* N Engl J Med, 1995. **332**(5): p. 305-311.
58. Nakashima, K., et al., *The Novel Zinc Finger-Containing Transcription Factor Osterix Is Required for Osteoblast Differentiation and Bone Formation.* Cell, 2002. **108**: p. 17-29.
59. Ducy, P., et al., *Osf2/Cbfa1: A Transcriptional Activator of Osteoblast Differentiation.* Cell, 1997. **89**: p. 747-754.

60. Bonewald, L.F., *Mechanosensation and Transduction in Osteocytes.* Bonekey Osteovision, 2006. **3**(10): p. 7-15.
61. Bonewald, L.F., *The amazing osteocyte.* J Bone Miner Res, 2011. **26**(2): p. 229-38.
62. Thomas, T., et al., *Leptin Acts on Human Marrow Stromal Cells to Enhance Differentiation to Osteoblasts and to Inhibit Differentiation to Adipocytes.* The Endocrine Society, 1999. **140**(4): p. 1630- 1638.
63. Akune, T., et al., *PPAR gamma insufficiency enhances osteogensis through osteoblast formation from bone marrow progenitors.* Journal of Clinical Investigation, 2004. **113**(6): p. 846-855.
64. Moerman, E.J., et al., *Aging activates adipogenic and suppresses osteogenic programs in mesenchymal marrow stroma/stem cells: the role of PPAR-γ2 transcription factor and TGF-β:BMP signaling pathways.* Aging Cell, 2004. **3**: p. 379-389.
65. Khosla, S., *Minireview: The OPG:RANKL:RANK System.* Endocrinology, 2001. **142**(12): p. 5050-5055.
66. Felson, D.T., et al., *Effects of weight and BMI on BMD in men and women: The Framingham study.* Journal of Bone and Mineral Research, 1993. **8**(5): p. 567-573.
67. Reid, I.R., et al., *Determinants of total body and regional bone mineral density in normal postmenopausal women: A key role for fat mass.* Journal of Clinical Endocrinology and Metabolism, 1992. **75**(1): p. 45-51.
68. Nielson, C.M., et al., *BMI and fracture risk in older men: the osteoporotic fractures in men study (MrOS).* J Bone Miner Res, 2011. **26**(3): p. 496-502.
69. Nielson, C.M., P. Srikanth, and E.S. Orwoll, *Obesity and fracture in men and women: an epidemiologic perspective.* J Bone Miner Res, 2012. **27**(1): p. 1-10.
70. Johansson, H., et al., *A meta-analysis of the association of fracture risk and body mass index in women.* J Bone Miner Res, 2014. **29**(1): p. 223-33.
71. Zhao, L.J., et al., *Relationship of obesity with osteoporosis.* J Clin Endocrinol Metab, 2007. **92**(5): p. 1640-6.
72. Lecka-Czernik, B., et al., *High bone mass in adult mice with diet-induced obesity results from a combination of initial increase in bone mass followed by attenuation in bone formation; implications for high bone mass and decreased bone quality in obesity.* Mol Cell Endocrinol, 2015. **410**: p. 35-41.
73. Slemenda, C.W., *Body composition and skeletal density- Mechanical loading or something more?* Journal of Clinical Endocrinology and Metabolism, 1995. **80**(6): p. 1761-1763.
74. Miotto, P.M., et al., *High saturated fat diet alters the lipid composition of triacylglycerol and polar lipids in the femur of dam and offspring rats.* Lipids, 2015. **50**(6): p. 605-10.
75. Watkins, B.A., Li, Y., Allen, K. G. D., Hoffman, W. E., Seifert, M. F., *Dietary ratio of n6:n3 PUFA alters the FA composition of bone compartments and biomarkers of bone formation in rats.* The Journal of Nutrition, 2000. **2274-2284**.
76. Lau, B.Y., et al., *Influence of high-fat diet from differential dietary sources on bone mineral density, bone strength, and bone fatty acid composition in rats.* Appl Physiol Nutr Metab, 2010. **35**(5): p. 598-606.

77. Miotto, P.M., et al., *Maternal high fat feeding does not have long-lasting effects on body composition and bone health in female and male Wistar rat offspring at young adulthood.* Molecules, 2013. **18**(12): p. 15094-109.
78. Salari, P., Rezale, A., Larijani, B., Abdollah, M., *A systemic review of the impact of n-3 fatty acids in bone health and osteoporosis.* Med Sci Monit, 2008. **14**(3): p. 37-44.
79. Watkins, B.A., et al., *The endocannabinoid signaling system: a marriage of PUFA and musculoskeletal health.* J Nutr Biochem, 2010. **21**(12): p. 1141-52.
80. Lau, B.Y., et al., *Investigating the role of polyunsaturated fatty acids in bone development using animal models.* Molecules, 2013. **18**(11): p. 14203-27.
81. Cao, J.J., B.R. Gregoire, and H. Gao, *High-fat diet decreases cancellous bone mass but has no effect on cortical bone mass in the tibia in mice.* Bone, 2009. **44**(6): p. 1097-104.
82. Cao, J.J., L. Sun, and H. Gao, *Diet-induced obesity alters bone remodeling leading to decreased femoral trabecular bone mass in mice.* Ann N Y Acad Sci, 2010. **1192**: p. 292-7.
83. Zernicke, R.F., et al., *Long term, high fat sucrose diet alters rat femoral neck and vertebral morphology, bone mineral content, and mechanical properties.* Bone, 1995. **16**(1): p. 25-31.
84. Parhami, F., et al., *Atherogenic high-fat diet reduces bone mineralization in mice.* J Bone Miner Res, 2001. **16**(1): p. 182-8.
85. Inzana, J.A., et al., *Immature mice are more susceptible to the detrimental effects of high fat diet on cancellous bone in the distal femur.* Bone, 2013. **57**(1): p. 174-83.
86. Patsch, J.M., et al., *Increased bone resorption and impaired bone microarchitecture in short-term and extended high-fat diet-induced obesity.* Metabolism, 2011. **60**(2): p. 243-9.
87. Bielohuby, M., et al., *Short-term exposure to low-carbohydrate, high-fat diets induces low bone mineral density and reduces bone formation in rats.* J Bone Miner Res, 2010. **25**(2): p. 275-84.
88. Aslam, M.N., et al., *Bone structure and function in male C57BL/6 mice: Effects of a high-fat Western-style diet with or without trace minerals.* Bone Reports, 2016.
89. Styner, M., et al., *Bone marrow fat accumulation accelerated by high fat diet is suppressed by exercise.* Bone, 2014. **64**: p. 39-46.
90. Zernicke, R.F., Salem, G. J., Schramm, E., *Long term, high-fat sucrose diet alters rat femoral neck and vertebral morphology, bone mineral content, and mechanical properties.* Bone, 1995. **16**(1): p. 25-31.
91. Lecka-Czernik, B. and L.A. Stechschulte, *Bone and fat: a relationship of different shades.* Arch Biochem Biophys, 2014. **561**: p. 124-9.
92. Oh, S.R., et al., *Saturated fatty acids enhance osteoclast survival.* The Journal of Lipid Research, 2009.
93. Schett, G., *Effects of inflammatory and anti-inflammatory cytokines on the bone.* Eur J Clin Invest, 2011. **41**(12): p. 1361-6.
94. Halloran, B.P., et al., *Changes in bone structure and mass with advancing age in the male C57BL/6J mouse.* Journal of Bone and Mineral Research, 2002. **17**(6): p. 1044-1050.

95. Raghavan, M., et al., *Age-specific profiles of tissue-level composition and mechanical properties in murine cortical bone.* Bone, 2012. **50**(4): p. 942-53.
96. Nagaraja, S., A.S. Lin, and R.E. Guldberg, *Age-related changes in trabecular bone microdamage initiation.* Bone, 2007. **40**(4): p. 973-80.
97. Pietschmann, P., et al., *Bone structure and metabolism in a rodent model of male senile osteoporosis.* Exp Gerontol, 2007. **42**(11): p. 1099-108.
98. Glatt, V., et al., *Age-related changes in trabecular architecture differ in female and male C57BL/6J mice.* J Bone Miner Res, 2007. **22**(8): p. 1197-207.
99. Schaffler, M.B., K. Choi, and C. Milgrom, *Aging and matrix microdamage accumulation in human compact bone.* Bone, 1995. **17**(6): p. 521-525.
100. Hirano, T., et al., *Does suppression of bone turnover impair mechanical properties by allowing microdamage accumulation?* Bone, 2000. **27**(1): p. 13-20.
101. Currey, J.D., K. Brear, and P. Zioupos, *The effects of ageing and changes in mineral content in degrading the toughness of human femora.* Journal of Biomechanics, 1996. **29**(2): p. 257-260.
102. Aaron, J.E., N.B. Markins, and K. Sagreiya, *The Microanatomy of Trabecular Bone Loss in Normal Aging Men and Women.* Clinical Orthopaedics and Related Research, 1987. **215**: p. 260-271.
103. *Osteoporosis facts and statistics*, O. Canada, Editor. 2016.
104. Szulc, P. and E. Seeman, *Thinking inside and outside the envelopes of bone: dedicated to PDD.* Osteoporos Int, 2009. **20**(8): p. 1281-8.
105. Chen, J.H., et al., *Boning up on Wolff's Law: mechanical regulation of the cells that make and maintain bone.* J Biomech, 2010. **43**(1): p. 108-18.
106. Frontera, W.R. and J. Ochala, *Skeletal muscle: a brief review of structure and function.* Calcif Tissue Int, 2015. **96**(3): p. 183-95.
107. Saladin, K., *Anatomy and physiology: The unity of form and function.* 2007, Ohio: McGraw-Hill.
108. Bontinelli, B.R., S. Schiaffino, and C. Reggiani, *Force-velocity relations and myosin heavy chain isoform compositions of skinned fibres from rat skeletal muscle.* Journal of Physiology, 1991. **437**: p. 655-672.
109. Armstrong, R.B. and R.O. Phelps, *Muscle fIber type composition of the rat hindlimb.* The American Journal of Anatomy, 1984. **171**: p. 259-272.
110. Bloemberg, D. and J. Quadrilatero, *Rapid determination of myosin heavy chain expression in rat, mouse, and human skeletal muscle using multicolor immunofluorescence analysis.* PLoS One, 2012. **7**(4): p. e35273.
111. Staron, R.S. and D. Pette, *The continuum of pure and hybrid myosin heavy chain-based fibre types in rat skeletal muscle.* Histochemistry, 1993. **100**: p. 149-153.
112. Pette, D. and R.S. Staron, *Mammalian Skeletal Muscle Fiber Type Transitions.* 1997. **170**: p. 143-223.
113. Schiaffino, S. and C. Reggiani, *Fiber types in mammalian skeletal muscles.* Physiology Reviews, 2011. **91**: p. 1447-1531.
114. Brooks, S.V. and J.A. Faulkner, *Contractile properties of skeletal muscles from young, adult, and aged mice.* Journal of Physiology, 1988. **404**: p. 71-82.
115. Graber, T.G., et al., *C57BL/6 life span study: age-related declines in muscle power production and contractile velocity.* Age (Dordr), 2015. **37**(3): p. 9773.

116. Ciapaite, J., et al., *Fiber-type-specific sensitivities and phenotypic adaptations to dietary fat overload differentially impact fast- versus slow-twitch muscle contractile function in C57BL/6J mice.* J Nutr Biochem, 2015. **26**(2): p. 155-64.
117. Shortreed, K.E., et al., *Muscle-specific adaptations, impaired oxidative capacity and maintenance of contractile function characterize diet-induced obese mouse skeletal muscle.* PLoS One, 2009. **4**(10): p. e7293.
118. Masgrau, A., et al., *Time-course changes of muscle protein synthesis associated with obesity-induced lipotoxicity.* J Physiol, 2012. **590**(Pt 20): p. 5199-210.
119. Summers, S.A., *Ceramides in insulin resistance and lipotoxicity.* Prog Lipid Res, 2006. **45**(1): p. 42-72.
120. Lee, S.R., et al., *Effects of chronic high-fat feeding on skeletal muscle mass and function in middle-aged mice.* Aging Clin Exp Res, 2015. **27**(4): p. 403-11.
121. Denies, M.S., et al., *Diet-induced obesity alters skeletal muscle fiber types of male but not female mice.* Physiol Rep, 2014. **2**(1): p. e00204.
122. Morley, J.E., et al., *Sarcopenia.* J Lab Clin Med, 2001. **137**(4): p. 231-43.
123. Balagopal, P., et al., *Effects of aging on in vivo synthesis of skeletal muscle myosin heavy-chain and sarcoplasmic protein in humansl.* American Journal of Physiology, 1997. **273**: p. E790-800.
124. Rowan, S.L., et al., *Denervation causes fiber atrophy and myosin heavy chain co-expression in senescent skeletal muscle.* PLoS One, 2012. **7**(1): p. e29082.
125. Holloszy, J.O., et al., *Skeletal muscle atrophy in old rats: differential changes in the three fiber types.* Mechanisms of Aging and Development, 1991. **60**: p. 199-213.
126. Lynch, G.S., et al., *Force and power output of fast and slow skeletal muscles from mdx mice 6–28 months old.* Journal of Physiology, 2001. **535**(2): p. 591-600.
127. Brooks, S.V. and J.A. Faulkner, *Maximum and Sustained Power of Extensor Digitorum Longus Muscles From Young, Adult, and Old Mice.* Journal of Geontology, 1991. **46**(1): p. B28-33.
128. Edwards, M.H., et al., *Osteoporosis and sarcopenia in older age.* Bone, 2015. **80**: p. 126-30.
129. Burr, D.B., *Muscle Strength, Bone Mass, and Age-Related Bone Loss.* Journal of Bone and Mineral Research, 1997. **12**(10): p. 1547-1551.
130. Frost, H.M., *On Our Age-Related Bone Loss: Insights from a New Paradigm.* Journal of Bone and Mineral Research, 1987. **12**(10): p. 1539-1546.
131. Jilka, R.L., *The relevance of mouse models for investigating age-related bone loss in humans.* J Gerontol A Biol Sci Med Sci, 2013. **68**(10): p. 1209-17.
132. Novotny, S.A., et al., *Bone is functionally impaired in dystrophic mice but less so than skeletal muscle.* Neuromuscul Disord, 2011. **21**(3): p. 183-93.
133. Garriguet, D., *Overview of Canadians' Eating Habits*, S. Canada, Editor. 2004.
134. Barclay, C.J., *Modelling diffusive O(2) supply to isolated preparations of mammalian skeletal and cardiac muscle.* J Muscle Res Cell Motil, 2005. **26**(4-5): p. 225-35.
135. Mendez, J. and A. Keys, *Density and composition of mammalian muscle.* Metabolism, 1960. **9**: p. 184-188.
136. Palmer, A.J., et al., *Age-related changes in body composition of bovine growth hormone transgenic mice.* Endocrinology, 2009. **150**(3): p. 1353-60.

137. Black, B.L., et al., *Differential Effects of Fat and Sucrose on Body Composition in A/J and C57BL/6 Mice.* Metabolism, 1998. **47**(11): p. 1354-1359.
138. Ingram, D.K., et al., *Differential effects of age on motor performance in two mouse strains.* Neurobiology of Aging, 1981. **2**: p. 221-227.
139. Sheard, P.W. and R.D. Anderson, *Age-related loss of muscle fibres is highly variable amongst mouse skeletal muscles.* Biogerontology, 2012. **13**(2): p. 157-67.
140. Moran, A.L., G.L. Warren, and D.A. Lowe, *Soleus and EDL muscle contractility across the lifespan of female C57BL/6 mice.* Exp Gerontol, 2005. **40**(12): p. 966-75.
141. Cowin, S.C., *Wolff's law of trabecular arhitecture at remodelling equilibrium.* Journal of Biomechanical Engineering, 1986. **108**: p. 83-88.
142. Warren, G.L., et al., *Estradiol effect on anterior crural muscles-tibial bone relationship and suceptibility to injury.* American Physiological Society, 1996. **80**(5): p. 1660-1665.
143. Warren, G.L., et al., *Voluntary run training but not estradiol deficiency alters the tibial bone-soleus muscle functional relationship in mice.* Am J Physiol Regul Integr Comp Physiol, 2007. **293**(5): p. R2015-26.

Appendix I:
Project Outcomes

Outcome	Description
µCT Body Composition	Measure of relative lean mass, fat mass, and bone mass
µCT Bone Measures	
BV/TV	Ratio of segmented bone volume to total volume of the region of interest (%)
Tb.Th	Mean thickness of the trabecular struts (mm)
Tb.N	Measure of the average number of trabecular struts per unit length (mm^2)
Tb.Sp	Mean distance between trabecular struts (mm)
BMD	Measure of the density of bone within the region of interest (g/cm^3)
***In vivo* Grip Strength**	Measure of neuromuscular function and functional measure of muscle strength by determining the maximal peak force produced by a mouse (front limb or all four limb)
Muscle Function	
Cross-sectional Area (CSA)	Measure of muscle CSA (mm^2)
Peak twitch force	Measure of the maximum force from a twitch (mN)
Peak tetanus force	Measure of maximum force from a tetanus (mN)
+df/dt	Rate of force production (mN/ms)
-df/dt	Rate of relaxation (mN/ms)
Half relaxation time	Time of half the tetanus maximal force (ms)
Maximum unloaded shortening velocity	Velocity calculated from the time it takes the muscle redevelop tension after a set change in muscle length (fibre lengths/s)
Force frequency curve	Plotting the maximum force through a range of frequencies
Fibre typing	Staining muscle cross-sections for the different myosin heavy chains (type I, IIa, IIx, and IIb)
Bone to muscle ratios	Measure of bone (proximal tibia BV/TV or BMD) to muscle (soleus and EDL peak tetanus and CSA)

Appendix II:
Micro-computed Tomography

Setting up the Micro-computed Tomography (μCT) System

1. Open SkyScan program and turn on the X-ray, allow X-ray to warm up for 10-15 minutes
2. Complete flatfield
    - Options → scanner setup (might have to click crtl+alt+shift+s to unlock), select scanning parameters:

Body scanning parameters: 40 kilovolts and 200 microamps, with a 430 millisecond exposure time and a rotation step of 0.8°

Leg scanning parameters: 40 kilovolts and 200 microamps, with a 430 millisecond exposure time and a rotation step of 0.7°

3. Scout Scan
    - Scout scan to view

Reconstruction

1. Open NRecon program
2. Open image file and set up reconstruction parameters (see chart below)
3. To batch reconstruct files choose 'add to batch' following setup
4. Once all bone have been setup and added to batch choose 'start reconstruction'

Reconstruction parameters for in vivo leg and body scans using NRecon program.

	In vivo leg scans	*In vivo* body scans
Beam hardening	40%	30%
Ring artifact	8	8
Smoothing	4	8
Dynamic threshold	0.0 – 0.110	0.0 – 0.056

Reorientation

1. Open Dataviewer program
2. Reorientate each sample by holding 'ctrl' key while using mouse to move bone in the x, y, z image planes
3. Reorientate the bone as straight as possible in the x and y planes
4. Save the transaxial plane as dataset

Region of Interest

1. Open CTan program
2. Open reoriented file
3. Set region of interest at either end of slice selection
    - For proximal tibia set an offset of 30 slices from the end of the growth plate with a 60 slice region of interest
    - For body scans identify the very beginning and end of the third lumbar vertebra

4. Save the region of interest

Analysis

1. Open CTan program
2. Open ROI file
3. Run analysis with task list

In vivo leg scan proximal tibia analysis task list.

Task List	**Parameters**
Thresholding	low 90, high 255
Despeckle	sweep, all except largest, image, 3D space
ROI shrink wrap	shrink wrap, 2D space
Bitwise operations	image = NOT image
Bitwise operations	image = image & ROI
Morphological operations	opening, round image, 2D space, radius=2
Despeckle	sweep, all except largest, image, 3D space
Morphological operations	closing, round, image, 2D space, radius=10
Morphological operations	opening, round image, 2D space, radius=10
Morphological operations	erosion, round image, 2D space, radius=3
Morphological operations	dilation, round image, 2D space, radius=2
Bitwise operations	ROI = ROI sub image
Reload	image
Save bitmaps	image inside ROI, BMP, copy dataset to log files
Save bitmaps	ROI, BMP, convert to monochrome
Thresholding	low 90, high 255, copy dataset to log file
ROI shrink wrap	shrink wrap, 2D space
Structure	2-D analysis
BMD	histogram

Appendix III:
Muscle Contractile Experiments

Setting Up the In Vitro Apparatus

1. After turning on the computer, open the single channel data collection program
2. Open 'Set Up', 'Protocol' and 'Scope' windows
3. Switch ASI stimulator and servomotor/force transducer control units ON
4. Zero the force in signal by clicking 'Record Fin' in 'Set Up' window periodically until the value stabilizes around a given number (usually 27-32 mV)
5. Pour Tyrode's solution into bath
6. Turn Circulator ON
7. Turn oxygen using master valve on gas cylinder, and adjust air flow into vertical organ bath using fine black adjustment knobs to obtain a steady stream of bubbles

Surgical Procedures

1. Place mouse in chamber for anesthetic induction at 5% isoflurane
2. Once mouse is under transfer to nose cone and maintain isoflurane between 2-5%
3. Begin procedures once the pedal reflex is absent
4. Remove skin to expose hind limb musculature
5. Isolate TA tendon, and remove TA
6. Stop bleeding associated with removal of TA using Kimwipe
7. Isolate EDL and tie non-absorbable silk sutures to the proximal and distal tendons of the EDL
8. Place muscle in intermediate bath before mounting muscle in vertical organ bath
9. Isolate Achilles tendon and cut through calcaneus bone being careful not to cut the tendon
10. Isolate the soleus and tie non-absorbable silk sutures to the proximal and distal tendons of the soleus
11. Place muscle in intermediate bath before mounting muscle in vertical organ bath

Mounting Isolated Muscles

1. Zero Fin
2. Open bottom clamp
3. Loop top suture onto servomotor lever arm
4. Straighten bottom suture and insert into bottom clamp
5. Tighten bottom clamp
6. Adjust muscle length using adjustment knob until muscle is taut (3-5 mN) and lock in place

Muscle Function Experimental Setup

1. Input reference length (soleus 12mm and EDL 11 mm)
2. Load equilibration sequence in Sequencer view of Protocol window
3. Enable Slip Tetanus protocol to check for suture slippage
4. Enable Equilibration protocol
5. Following Equilibration protocol or until muscle consistently produces same force, enable Optimal Length protocol
6. Determine the resting tension at which the largest active force is produced (i.e., total tension – passive tension)
7. Set muscle length to resting tension that best represents Lo
8. 7. Use digital venire calipers to measure the new length, input as Reference Length and record Lin
9. Begin experimental protocol

Appendix IV:
Muscle Histology Mounting

Muscle Mounting

1. Prepare cork sections (1X1) large enough to fit muscle sample and label both sides
2. With liquid nitrogen in liquid nitrogen container, cool the 2-methyl butane in the metal bowl (-155°C)
3. Listen for first and second sizzle of 2-methyl butane; the inner area of the metal bowl should become white and slushy
4. Place blob of Cryomatrix embedding compound in the center of the cork and dip into the cooled 2-metyl butane until it begins to freeze along perimeter, continue process to build 'tower' with perimeter frozen and center unfrozen
5. Orient muscle section in the center of the Cryomatrix embedding compound as vertical as possible with muscle fibres perpendicular to the cork
6. Add extra Cryomatrix embedding compound to ensure the muscle is completely covered
7. In one swift motion invert the set sample and drop into the cooled 2-methyl butane for 30-90 seconds
8. Wrap sample in tin foil (labeled on both sides) and store sample at -80°C until slicing.

Protocol: Muscle Slicing

1. Cool cryostat to -22°C
2. Equilibrate muscle samples in cryostat for approximately 20 minutes
3. Slice samples at 10µm thickness
4. Adjust blade and glass antiroll plate as needed
5. Slice 4-6 transverse sections per microscope
6. Store slides at -80°C until staining

Appendix V:
Muscle Immunofluorescence Fiber Typing

Procedure:

1. Air dry slides for 10 minutes at room temperature.
2. Incubate sections for 1 hour in blocking solution: 10% goat serum in 1 x PBS (100µL/slide) at room temperature on shaker.
3. Blot dry slides avoiding muscle sections.
4. Incubate sections in 1˚ antibodies appropriately diluted in blocking solution for 1 hour (100µL/slide) at room temperature on shaker. Give the stock antibody tubes a quick shake/inversion before pipetting out of them to make 1˚ antibody cocktail.
   - MHCl (BA-F8) @ 1:50 – IgG2b: blue
   - MHClla (SC-71) @ 1:600 – IgG1: green
   - MHCllb (BF-F3) @ 1:100 – IgM: red
5. Wash slides 3 x 5 minutes in a Columbia jar with 1 x PBS.
6. Blot dry slides avoiding muscle sections.
7. Incubate sections in appropriate 2˚ antibodies diluted 1:500 in blocking solution for 1 hour at room temperature in the dark on shaker. Ensure as little light as possible makes contact with the 2˚ antibodies and sections from this point
8. Wash slides 3 x 5 minutes in a Columbia jar with PBS.
9. Apply 15µL of Prolong to each slide and mount with a number 1 coverslip. The coverslip can be pressed gently to remove bubbles, but do not apply pressure direction above sections, they will squish.
10. Tack the corners of the coverslip down with nail polish and place in a labeled, lightproof slide box.
11. Slides should be imaged no longer than 2 days after staining, next day imaging seems to work best once Prolong gold has set.

Appendix VI:
Grip Strength Testing

Grip strength testing allows for the measure of neuromuscular function by determining the maximal peak force developed by a rodent (mouse or rat). In vivo grip strength testing is a functional measure of muscle strength and is a quick, repeatable measure.

Procedure

1. While the Bioseb Grip Strength Meter is turned off, set up the desired attachment (T-bar or grid) depending on the grip strength measure (e.g. front limb or all four limbs)
2. Once the system is set up, turn it on and tare the instrument by pressing the 'zero' key.
3. Hold the mouse by the base of the tail above the T-bar or grid depending on the measure
4. Move the mouse down until the front limbs or all four limbs grab the T-bar or grid
5. While the mouse is grasping, lower its position to a horizontal position and gently pull following the axis of the sensor until the grip is released
6. Record the maximum force displayed on the screen.

Notes

- Repeat all measures in triplicate.
- Gently pull mice or rats in one smooth motion with no abrupt movements. The goal is to get a constant velocity movement to insure repeatable measures.

Appendix VII:
Bone to Muscle Outcome Ratio Calculations

Bone to muscle outcome ratios were calculated using BV/TV as a representative measure of trabecular structure and vBMD as a measure of bone quantity for this study, and soleus and EDL peak tetanus force was selected as a representative measure of muscle contractile function. In addition, CSA was used as a measure of muscle quantity. Ratios included vBMD:CSA, vBMD:peak tetanus, BV/TV:CSA, and BV/TV:peak tetanus.

The AGE and HFS-AGE bone measures (BV/TV or vBMD) were divided by muscle measures (peak tetanus or CSA) within each animal. Since BSL had no measure for trabecular bone, the average from baseline measures (BV/TV and vBMD) from AGE and HFS-AGE was used respectively (variation between animals for bone measures prior to interventions was extremely low with no significant difference between groups)

Sample Calculation

	BV/TV	vBMD	Soleus peak tetanus	Soleus CSA
C6-blank	7.28%	0.199 g/cm^3	208 mN	2.03 mm^2

Ratio = BV/TV / peak tetanus
= 7.28/ 208
= 0.035

Ratio = BV/TV / CSA
= 7.28/ 2.03
= 3.59

Ratio = vBMD / peak tetanus
= 0.199/ 208
= 9.6×10^{-4}

Ratio = vBMD / CSA
= 0.199/2.03
= 0.098